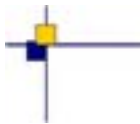


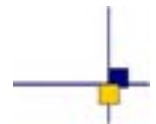


CalVal In-Situ altimetry / Argo TS profiles



Validation of altimeter data by comparison with in-situ T/S Argo profiles

for Jason-1, Envisat and Jason-2
2011-2015 SALP contract No 104685



Reference : CLS.DOS/NT/13-256

Nomenclature : SALP-RP-MA-EA-22281-CLS

Issue : 1rev 0

Date : April 1, 2014

Chronology Issues :		
Issue :	Date :	Reason for change :
1.0	December 2013	Creation

People involved in this issue:				
	AUTHORS	COMPANY	DATE	INITIALS
WRITTEN BY	J.F. Legeais	CLS		
CHECKED BY	S. D'Alessio	CLS		
APPROVED BY	JP. Dumont	CLS		
	M. Ablain	CLS		
APPLICATION AUTHORISED BY				

Analyse documentaire :	
Context :	
Key words :	Altimetry, Argo Temperature and Salinity profiles, In-Situ calibration, MSL
hypertext links :	

Distribution :		
Company	Means of distribution	Names
CLS/DOS	electronic copy	G. DIBARBOURE V. ROSMORDUC
CNES	electronic copy	thierry.guinle@cnes.fr nicolas.picot@cnes.fr aqgp_rs@cnes.fr dominique.chermain@cnes.fr delphine.vergnoux@cnes.fr

List of tables and figures

List of Tables

1	<i>Corrections applied for altimetric SSH calculation</i>	41
---	---	----

List of Figures

1	<i>Spatial distribution of the floats that have delivered data within the last 30 days before the mentioned date (Argo Information Center).</i>	3
2	<i>Spatial (left) and temporal (right) distribution of temperature and salinity Argo profiles from 2002 to 2013.</i>	4
3	<i>Monitoring of the percentage of the ocean covered by Argo profiling floats ($\pm 60^\circ$ and without inland seas).</i>	4
4	<i>Regional trends of the mass contribution to the sea level derived from GRGS V2 dataset of the GRACE measurements.</i>	6
5	<i>Histogram of valid SLA (DUACS merged maps) - DHA differences (number of profiles according to the observed sea level differences in meters, left) and map of the invalid SLA - DHA differences (right).</i>	8
6	<i>Dispersion between DUACS merged maps of altimeter SLA and the steric DHA from Argo plus the mass contribution from GRACE.</i>	9
7	<i>Left: Taylor diagram of the Argo + GRACE time series compared with Jason-2 SLA (gray reference dot), including the GRACE NASA Tellus RL04 (black circle) and RL05 (blue triangle). Right: monitoring of the mass contributions to the sea level from GRACE: global mean (blue) and averaging kernel (green) of the NASA Tellus RL05 dataset and global mean of the GRGS V2 dataset.</i>	11
8	<i>Left: global mean of altimeter and Argo+GRACE (GRGS V2) sea levels. Right: periodogram of the annual signal of the altimetry - Argo - GRACE measurements.</i>	11
9	<i>Sensitivity of the Taylor distance between Jason-1 measurements and Argo+GRACE data according to the length of the time series (from 2 to 9 years). The trend and periodic signals are not removed.</i>	15
10	<i>Global mean differences between Jason-1 altimeter measurements and Argo dynamic heights (without the mass contribution) with (left) and without (right) annual and semi-annual signals. Along-track altimeter data are box-averaged before collocating with each Argo in-situ profile with 1x1 (blue curves) and 1x3 (red curves) boxes.</i>	16
11	<i>Histogram of the variance differences between altimetry and Argo data using successively 1x1 and 1x3 degrees boxes for averaging along-track Jason-1 altimeter measurements before collocating with each Argo profile. Positive values traduce a more homogeneous altimeter sea level with in-situ data when using 1x3 boxes.</i>	17
12	<i>Number per box of altimeter (AVISO DUACS merged product) - Argo differences over the period 2004-2012 with various subsampling of the list of Argo floats: all (top left), 1/2 (top right), 1/4 from the 1st (bottom left) and 1/4 from the third (bottom right).</i>	18
13	<i>Global mean differences (with different subsampling of the list of Argo floats) between altimetry (AVISO DUACS merged product) and Argo measurements (left) and between altimetry and Argo+GRACE (GRGS V2) data (right).</i>	19

.....

14	<i>Left: mean of Argo + GRACE (GRGS V2) sea level measurements with different sub-sampling of the Argo floats (bottom curves) and mean of the corresponding colocated DUACS merged altimeter data. Right: Taylor diagram (correlation and standard deviation) of these time series: the gray dot is the altimeter DUACS merged sea level product and statistics obtained with Argo+mass values are represented for different sampling of the Argo floats: all (red square), half (green circle), 1/4 (blue and cyan triangles). Trends and periodic signals are included.</i>	20
15	<i>Left: 3-months filtered mean differences between altimetry and Argo+mass (GRGS V2) for Jason-1 (red), Envisat (blue) and Jason-2 (green) missions with the GIA effects included. Right: idem after removing the trend.</i>	22
16	<i>Regional mean differences between Jason-1 sea level and Argo (left) or Argo+mass (GRGS V2) (right).</i>	23
17	<i>Left: regional differences between Jason-1 and Envisat of the mean differences between altimetry and Argo+mass (GRGS V2) over 2004.5-2012.5. Right: regional differences between Jason-1 and Jason-2 of the mean differences between altimetry and Argo data over 2008.5-2012.</i>	24
18	<i>Trends of the differences between Jason-1 SLA and Argo data separating the North and South hemispheres ($lat \geq 20^\circ$) with (left) and without (right) under-weighting of the DORIS stations in the SAA. The hemispheric trend differences are of 0.0 mm/yr and 0.6 mm/yr respectively.</i>	26
19	<i>Difference of maps of sea level trends from Envisat derived with the GFZ and GDR-D orbit solutions.</i>	27
20	<i>Trends of the differences between Envisat SLA and Argo data separating the Western ($180^\circ - 0^\circ$) and Eastern hemispheres ($0^\circ - 180^\circ$) with the GFZ (left) and GDR-D (right) orbit solution. The hemispheric trend differences are of 0.8 mm/yr with both solutions.</i>	27
21	<i>Regional sea level trend differences for the TOPEX sea level measurements computed with the GPD versus the radiometer wet troposphere correction over TOPEX cycles 370 to 481.</i>	28
22	<i>Trends of the differences between TOPEX SLA and Argo data separating the Indian ocean and the North Pacific ocean with the GPD (left) and the radiometer (right) wet troposphere correction.</i>	29
23	<i>Histogram of the variance differences between altimetry and Argo data (left) and tide gauges (right) using successively the GPD and the radiometer wet troposphere correction for the TOPEX mission. Negative values traduce a more homogeneous altimeter sea level with in-situ data when using the GPD correction.</i>	29
24	<i>Global mean differences between altimetry (AVISO 2014 in red and AVISO 2010 in blue) and Argo measurements with (left) and without (right) annual and semi-annual signals.</i>	30
25	<i>Top: Regional mean differences between AVISO 2014 and 2010 (colocated with Argo profiles) over 2004-2012. Bottom: trends of the differences between altimetry and Argo data separating the Western ($180^\circ - 0^\circ$) and Eastern hemispheres ($0^\circ - 180^\circ$) with the AVISO 2010 (left) and AVISO 2014 (right) versions.</i>	31
26	<i>Global mean differences between altimetry (AVISO 2014 in red and AVISO 2010 in blue) and summed Argo + mass (GRACE GRGS V2) measurements (left) and periodogram of the annual signal of the differences (right).</i>	32

- 27 *Time series of altimetry (AVISO 2014 in red and AVISO 2010 in blue) and summed Argo + mass (GRACE GRGS V2) measurements (left) and associated Taylor diagram (correlation and standard deviation) of these time series: the gray dot is the Argo+mass reference value and statistics obtained with AVISO 2014 (AVISO 2010) are represented by triangles (circles), separating different temporal scales: detrended (black), annual cycle (green), high frequencies ($\leq 1y.$, red) and low frequencies ($\geq 1y.$, blue).* 33
- 28 *Top: histogram of the variance differences for all time series of each Argo floats: $Var(AVISO\ 2014 - Argo) - Var(AVISO\ 2010 - Argo)$. Bottom: time series of altimetry (AVISO 2014 in red and AVISO 2010 in blue) and summed Argo + mass (GRACE GRGS V2) measurements restricted to the Antarctic Circumpolar Current (left) and associated Taylor diagram (correlation and standard deviation) of these time series (right): the gray dot is the Argo+mass reference value and statistics obtained in the ACC with detrended AVISO 2014 (AVISO 2010) are represented by a triangle (circle).* 34

List of items to be defined or to be confirmed

Applicable documents / reference documents

Contents

1. Introduction	1
2. Presentation of the databases	3
2.1. Altimeter measurements	3
2.2. Argo in-situ measurements	3
2.3. GRACE measurements of the mass contribution	5
3. Method of comparison: evolution and reduction of the uncertainty	7
3.1. Description of the processing sequence	7
3.1.1. Overview	7
3.1.2. Comparison of similar physical contents	7
3.1.3. Colocation of in-situ and altimeter data	8
3.1.4. Validation of compared altimeter and in-situ measurements	8
3.1.5. Computation of global statistics	9
3.2. Evolution of the method of in-situ comparison	10
3.2.1. New version of the processing sequence for an automatic use	10
3.2.2. New reference period	10
3.2.3. The mass contribution from GRACE: use of a new dataset	10
3.2.4. Impact of the Glacial Isostatic Adjustment (GIA)	12
3.3. Improved estimation of the uncertainty	13
3.3.1. Estimation of the uncertainty of sea level trends	13
3.3.2. New diagnostic: Spatial distribution of statistics of the differences	13
3.3.3. New diagnostic: the Taylor diagram	13
3.4. Sensitivity analyses	15
3.4.1. The Taylor distance	15
3.4.2. Impact of the altimeter data processing	16
3.4.3. Impact of the Argo subsampling	18
3.4.4. Argo steric dynamic heights: impact of the reference depth on the comparison with altimetry	21
4. Analyses of the altimeter sea level differences with the external reference	22
4.1. Global altimeter drifts and inter annual variability	22
4.2. Regional mean differences	23
5. Evaluation of new altimeter standards	25
5.1. Overview	25
5.2. Uncertainty of the method for the detection of trends difference	26
5.2.1. Impact of the weighting of DORIS stations in the South Atlantic Anomaly region on the Jason-1 orbit solution	26
5.2.2. Comparison of GFZ and GDR-D orbit solutions for Envisat	27
5.3. Assessment of the GPD wet troposphere correction on TP	28
5.4. Quality assessment of the DUACS DT 2014 reprocessing	30
5.5. Assessment of the ESA Sea Level Climate Change Initiative product	35
6. Conclusions and futures	36
7. References	38

8. Annexes	40
8.1. Annex: Corrections applied for altimeter SSH computation	40
8.2. A contribution to the sea level closure budget: global steric sea level estimation from Argo	42
8.3. Evaluation of the Sea Level CCI dataset with respect to in-situ data	63

1. Introduction

The calibration and validation of the altimeter sea level is usually performed by internal assessment of the mission and via inter comparison with other altimeter missions. The comparison with in-situ measurements is fundamental since it provides an external and independant reference. This document is the synthesis report for 2013 concerning altimeter and in-situ validation activities which aims at comparing altimeter data with temperature and salinity (T/S) profiles provided by lagrangian floats of the ARGO network. This activity is supported by CNES in the frame of the SALP contract for all altimeter missions and by ESA for Envisat mission. The method uses results of a study made at CLS in the frame of an IFREMER / Coriolis contract. In 2013, some studies have been performed in the context of the ESA Sea Level Climate Change Initiative (CCI) and of the Euro-Argo Improvements for the GMES Marine Services (E-AIMS) projects.

Three objectives are achieved with the comparison of altimetry with the in-situ T/S profiles:

- To detect potential anomalies (jumps or drifts) in altimeter sea level measurements which can not be detected by comparison with other altimetric missions.
- To evaluate the quality of altimetric measurements and the improvement provided by new altimeter standards in the computation of sea level anomalies (geophysical corrections, new orbit solutions, retracking,...).
- To detect potential anomalies in in-situ data and estimate their quality.

Argo T/S profiles constitute a complementary dataset to tide gauges measurements. Indeed, although the temporal sampling is reduced (10-day profiles for a single float and hourly measurements for tide gauges), the spatial coverage of the Argo network is much larger since the global open ocean is almost completely sampled. Several results obtained through this activity are made robust thanks to the cross comparisons with several types of in-situ datasets (T/S profiles and tide gauges), which increases the quality assessment of altimeter measurements. In addition, the comparison with external and independant data enables us to contribute to the improvement of the error characterization of altimetry measurements, and especially at climate scales (Ablain et al., 2012, [1]).

Following the objectives described in the previous annual report (see [7]), major efforts have been performed in 2013 to better understand the physical content of the observed sea level differences, to better estimate the error of the method and to reduce the uncertainty associated with the results.

1. Concerning the data, Argo T/S profiles provide the steric Dynamic Height Anomaly (DHA) above a reference level associated with the thermohaline expansion of the water column. The associated physical content is thus different than the altimeter observations of the total height of the water column. An improvement of the method has been achieved by including the mass contribution to the sea level derived from the Gravity Recovery And Climate Experiment (GRACE) in order to compare homogeneous physical contents. In 2013, following a detailed analysis of this mass contribution, a new dataset of GRACE measurements has been used in order to better close the sea level budget and thus better estimate the absolute altimeter MSL drift.
2. Concerning the method of comparison, the processing sequence has been strongly improved, the length of the reference period of the sea level anomalies has been increased. Some new tools have been developed to contribute to the estimation of the uncertainty of the results and

sensitivity analyses have been performed in order to better understand the observed signals and improve our confidence in the results.

3. The impact estimation of new altimeter standards is analyzed by comparison with the external in-situ reference. The studies concern several orbit solutions, a new wet troposphere correction for TOPEX/Poseidon mission, the assessment of the ESA CCI sea level dataset and of the reprocessed SSALTO/DUACS 2014 merged product.

2. Presentation of the databases

2.1. Altimeter measurements

In this study, along-track (level 2) altimeter SSH are used from several satellite altimeters, where standards are updated compared with the Geophysical Data Record (GDR) altimeter products. Details of the SSH computation and time period for each altimeter are presented in annex 8.1. and available in the MSL part of the Archiving, Validation and Interpretation of Satellite Oceanographic website (AVISO, <http://www.aviso.oceanobs.com/en/news/ocean-indicators/mean-sea-level/processing-corrections/index.html>). As the comparison with in-situ data is performed since 2004, we focus the analyses on the Envisat, Jason-1, Jason-2 and TOPEX-Poseidon space missions. Sea Level Anomalies (SLA) of all altimeter missions are computed with a reference to the Mean Sea Surface (MSS) CNES/CLS 2011 model (Schaeffer et al., 2012, [11]). Concerning Envisat mission, the reprocessed (V2.1) altimeter data are used (which includes the GDR-C orbit solution). Grids of merged altimeter products (L4) can also be compared with in-situ data.

2.2. Argo in-situ measurements

The lagrangian profiling floats of the Argo program are used as a reference in this study. They provide a global monitoring of ocean temperature and salinity (T/S) data between the surface and around 2 000 dbar for most of them with a 10-day sampling and a lifetime of a few years. The objective of a global network of 3 000 operating floats has been achieved in 2007 and figure 1 displays the spatial distribution of the floats that have delivered data within the last 30 days before the mentioned date.

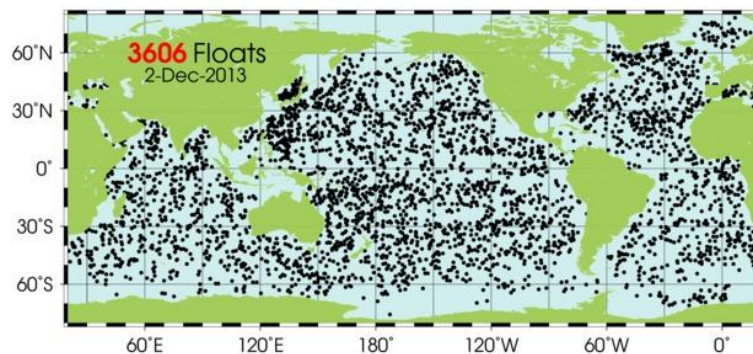


Figure 1: *Spatial distribution of the floats that have delivered data within the last 30 days before the mentioned date (Argo Information Center).*

Delayed mode and real time quality controlled (Guinehut et al., 2009: [3]) T/S profiles from the Coriolis Global Data Assembly Center (www.coriolis.eu.org) are used. Note that the delayed mode data concerns only two thirds of the dataset. Figure 2 shows spatial and temporal distribution of Argo measurements over the period 2002 - March 2013. The database has intentionally not been updated later in 2013 in order to perform all studies of this year with the same in-situ reference.

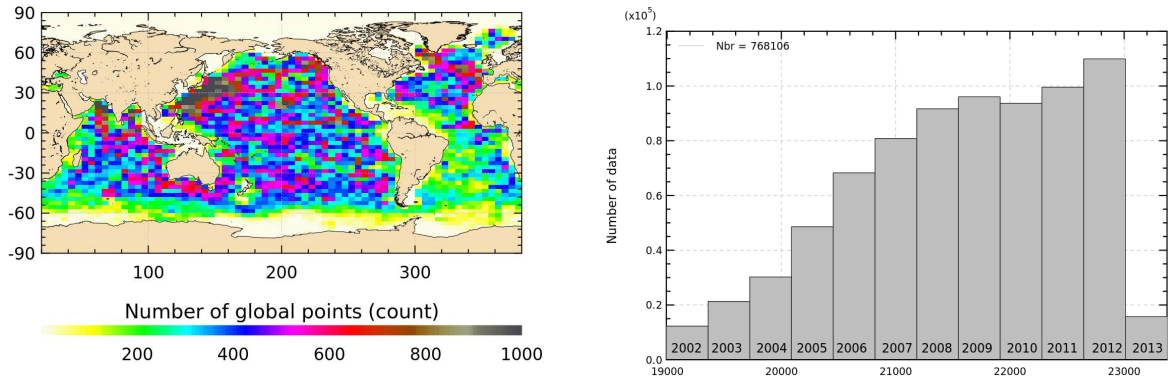


Figure 2: *Spatial (left) and temporal (right) distribution of temperature and salinity Argo profiles from 2002 to 2013.*

The vast amount of T/S profiles are available over almost the global open ocean (figure 2, left). Best sampled areas (Kurushio current, parts of the North Indian and North Atlantic oceans) have 1000 profiles per box of 3°x5°. About 500 profiles per box are found in large parts of the global ocean, except in the South West Atlantic ocean and in the southern part of the Antarctic Circumpolar current where about 200 profiles per box are found. The number of available profiles has regularly increased since 2002 (figure 2, right) and reaches 100 000 per year since 2009 (all studies have been performed with the in-situ database as March 2013). Nevertheless, spatial distribution has not always been high enough in some areas to produce statistically valid analyses. As discussed by Roemmich and Gilson, 2009 ([10]), figure 3 indicates that considering a threshold of two thirds of the open ocean surface covered by Argo floats ($\pm 60^\circ$), analyses should be performed with in-situ data from about mid 2004 onwards, which is done in this report. This constitutes a great asset for latest altimeter missions (Jason-1, Envisat et Jason-2). It leads to a global in-situ dataset of more than 900 000 T/S profiles distributed over almost the global open ocean.

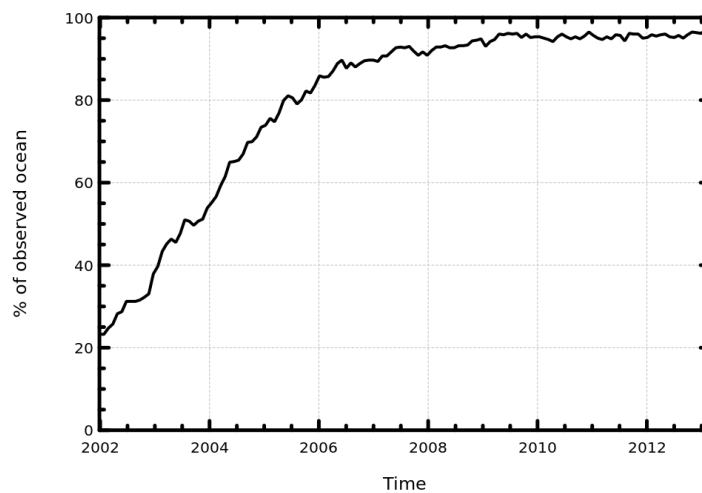


Figure 3: *Monitoring of the percentage of the ocean covered by Argo profiling floats ($\pm 60^\circ$ and without inland seas).*

The associated steric Dynamic Height Anomalies (DHA) are computed using a reference level and a contemporaneous mean dynamic height (also called synthetic climatology). The reference level chosen for the studies is 900 dbar (about 900m deep) but in 2013, a sensitivity analysis of this level of integration has been performed (see the dedicated part of this report) in order to estimate the impact on the spatial sampling of the network and on the steric content of the sampled water column.

The large number of available T/S profiles constitutes an independent dataset well adapted for comparison with altimeter data over the open ocean where tide gauges distribution is not sufficient. To perform these studies, a processing sequence has been developed (in the frame of the SALP project) which aims at being regularly operated to validate all altimeter missions. As further discussed, major updates of this tool have been performed in 2013 in order to make it more efficient and also to provide an easy use of the tool in the calibration and validation systematic analyses.

2.3. GRACE measurements of the mass contribution

The physical contents of the altimeter and steric in-situ dynamic heights are different and in particular, a phase offset is observed between the two global averages due to the seasonal distribution of the mass contribution which is missing in the Argo dataset (Chen et al, 98, [2]). This mass contribution is derived from GRACE data in order to compare with altimetry. Until last year, ocean data based on spherical harmonics from the University of Texas, Center for Space Research (CSR) (NASA Tellus website) were used in our comparison of altimetry versus Argo + GRACE measurements. In 2013, the use of the GRACE Release 05 dataset has shown a strong deterioration of the performances of these comparisons (correlation and std dev. of the differences between altimetry and Argo+GRACE) compared with the release 04 dataset. After discussions directly with the data provider (Don Chambers) and with users (LEGOS), it appears that this dataset (whatever the release used) is not adapted for our method of comparison.

Indeed, the difference of performances between the two releases was related with the leakage correction used to reduce the effect of much larger land and ice sheets that leak into the ocean both from the Gaussian filter and the destriping algorithm.

According to Chambers D. (personal communication): for RL04, a Gaussian smoother was applied to mapped GRACE data over the land and zeros was applied over the ocean. Then, it was subtracted from the ocean maps. The noise was clearly reduced in the residuals, but there were apparent residual errors that appeared from the destriping, which also leaks signals into the ocean. For RL05, the application of a destriping filter to the mapped GRACE data was tested over land in addition to the Gaussian smoother. This had a significant impact in reducing the residuals over the tropical ocean and improving correlation with local Ocean Bottom Pressure (OBP) variation from the JPL_ECCO model. Thus, this leakage correction has been chosen for the RL05 maps.

Whatever the release used, while comparing altimetry with Argo and the mass contribution, a global average of the GRACE maps is performed, which is not a good way to estimate the global mean mass variations from GRACE. Instead, according to the data provider, users should use an averaging kernel convolved with the original gravity coefficients, which does not require smoothing or destriping. The GRACE mapped data which are made available on the NASA Tellus web-site, are intended to be used to study more local ocean bottom pressure variations, not global ones, because of this problem. This is explained in the appendix of Johnson and Chambers 2013 ([4]).

Thus, we have chosen to use another dataset of the GRACE mass contribution to the sea level

which is provided by the GRGS research group (<http://grgs.obs-mip.fr/grace>, V2). It consists of 10-days maps (monthly maps for the NASA dataset) of equivalent sea level from 2003 to August 2012. An update over a longer period should be soon available. Altimeter data is thus also compared with Argo measurements only since the mass component is not available for recent days. The GRGS GRACE data are not corrected from the post glacial rebound (Glacial Isostatic Adjustment) correction. This point will be discussed in the next section. No filtering is applied and the map of the mass trend (in equivalent sea level) thus clearly show the North - South stripes of the GRACE data (see figure 4) but these effects are considered to vanish when performing global average of the maps, which is allowed since they are not filtered. This will be illustrated in the section showing the results of the sea level differences. Note that the major areas of ice melting (Greenland, Patagonia and Antarctic peninsula) are clearly observed on figure 4.

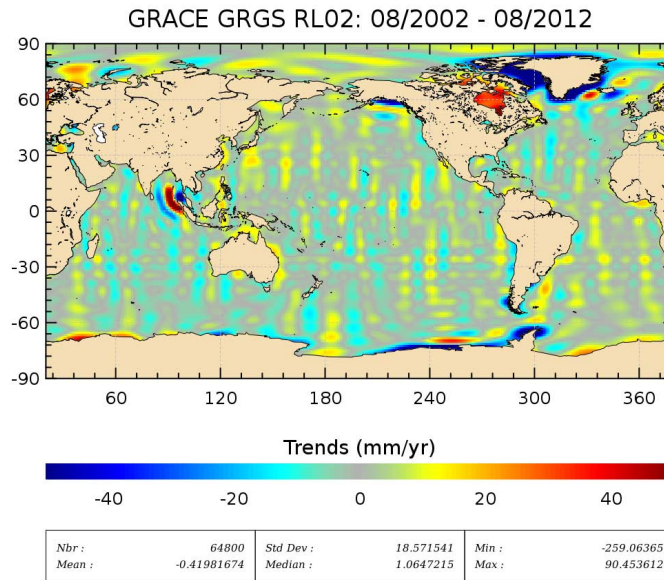


Figure 4: *Regional trends of the mass contribution to the sea level derived from GRGS V2 dataset of the GRACE measurements.*

Concerning our activity, the impact of using this new dataset is discussed in the following section. This leads to a reduced uncertainty of the estimation of the absolute drift of the altimeter sea level.

3. Method of comparison: evolution and reduction of the uncertainty

In 2013, major efforts have been performed to better estimate the error of the method (sensitivity analyses and new diagnoses) and to reduce the uncertainty associated with the results. In this section, we first present the method of comparison of altimeter SLA with in-situ data and evolutions of the method are then discussed. Some new tools have been developed to contribute to the estimation of the uncertainty of the results and at last, sensitivity analyses have been performed in order to better understand the observed signals and improve our confidence in the results.

3.1. Description of the processing sequence

3.1.1. Overview

Altimeter measurements are compared with in-situ dynamic height anomalies (DHA) derived from the Argo temperature and salinity profiles and with the mass contribution to the sea level derived from GRACE measurements. These are described hereafter:

1. Colocation of altimeter and GRACE data with Argo in-situ profiles
2. Validation of collocated measurements in order to exclude bad data
3. Estimate of statistics

3.1.2. Comparison of similar physical contents

Altimeter measurements are representative of the total elevation of the sea surface (surface to bottom), that includes barotropic and baroclinic components, whereas, DHA from profiling floats are representative of the steric elevation associated with the thermohaline expansion of the water column from the surface to the reference level of integration (i.e. baroclinic component). We combine these data with grids of the mass contribution to the sea level from GRACE to provide an estimation of the total height of the water column so that the same physical content is compared with altimetry. Note that this mass contribution is not systematically used since relative comparison with Argo data may be sufficient to detect the impact of a new altimeter standard for instance. The deep steric contributions are not taken into account in our study.

As discussed in previous annual report of the activity ([7]), in-situ DHA are referenced to a mean of the Argo dynamic heights over a time period different from the reference period of altimeter SLA. In order to compare both types of data with a common temporal reference, altimeter data are computed with the in-situ reference period by removing the mean of altimeter SLA over 2003-2011. The use of a common temporal reference provides more homogeneity between the two types of data and increase their correlation, which thus improves our confidence in the results (see 2011 annual report of the activity, [6]).

3.1.3. Colocation of in-situ and altimeter data

The quality assessment of the altimeter SLA from a single mission is based on the along-track (L2) SLA. As the altimeter sampling is better than the in-situ coverage (a global altimeter coverage of the ocean, for Jason missions, versus a single T/S profile every ten days), grids of 10-day averaged along-track SLA are computed in order to have a sufficient spatial coverage. The quality of gridded merged (L4) products can also be estimated (SSALTO/DUACS maps for instance). Then the colocation of both types of data is made via the interpolation of these grids for each altimeter mission (bi-linearly in space and linearly in time) at the location and time of each in-situ profile. The impact of averaging the altimeter L2 data over 10 days is estimated to be weak considering that the ocean state has not changed significantly within less than 10 days. However, maps of L2 SLA could be derived by optimal interpolation (objective analysis) and the impact of using this updated method has been analyzed (see the following section). Similarly, the 10-days grids of GRACE data (GRGS V2) are also collocated with each Argo profile.

3.1.4. Validation of compared altimeter and in-situ measurements

In order to exclude potential remaining spurious values and improve the correlation between both types of data (and thus increase our confidence in the results), a two steps selection is made in the processing chain over altimeter SLA and in-situ DHA:

- Selection differences between altimeter SLA and in-situ DHA lower than 0.20 m. The choice of this threshold is based on the histogram of SLA differences (figure 5, left). The selection is written as: $|SLA_{alti} - DHA| \leq 0.20m$.
- Selection over a maximal DHA from in-situ data. According to results from global Cal/Val analyses and from analyses of the in-situ dataset, values greater than 1.5 m are not taken into account: $|SLA_{InSitu}| \leq 1.5m$

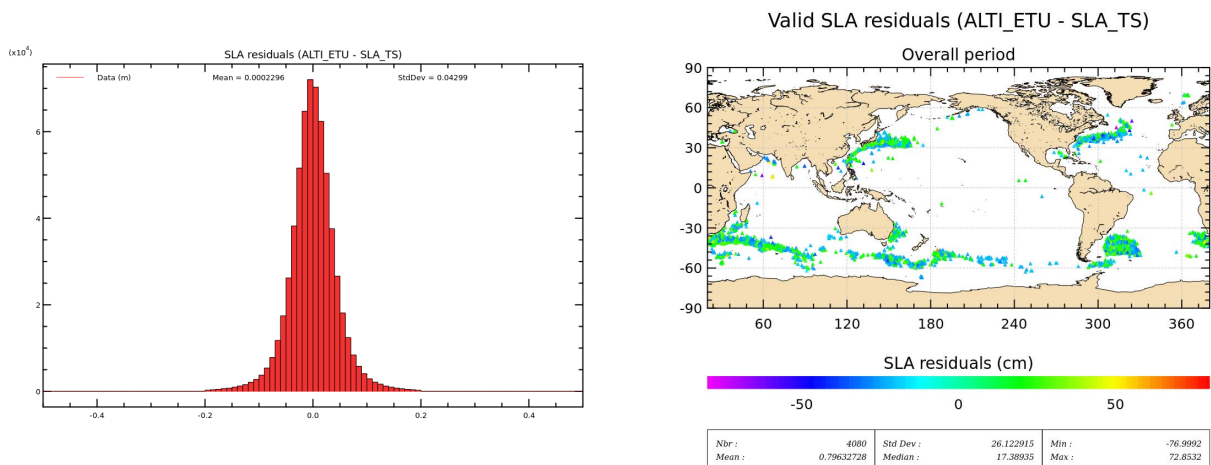


Figure 5: *Histogram of valid SLA (DUACS merged maps) - DHA differences (number of profiles according to the observed sea level differences in meters, left) and map of the invalid SLA - DHA differences (right).*

This selection excludes 1.6% of the total colocated measurements of Jason-1 data and figure 5 (right) indicates that the excluded measurements are mainly located in regions of high ocean variability. They are not associated with erroneous data but their rejection is due to the collocation method itself. Thus, if this validation would not be performed, the uncertainty in these regions would be too high to produce any valid results. The excluded data are totally attributed to the first validation step (threshold on the differences) but the second validation step is kept in case of potential remaining erroneous Argo data. The correlation and rms differences between altimeter SLA and in-situ steric DHA become 0.72 and 6.3 cm respectively whereas they are 0.65 and 7.2 cm when the validation phase is not considered. Thus the results will not be significantly affected by this selection but it strongly increases our confidence in the method.

3.1.5. Computation of global statistics

The processing sequence uses the database of colocated altimetry and Argo profiles to generate statistics of the altimeter sea level differences compared with in-situ measurements for each altimeter mission. Then, various diagnoses are produced from these statistics in order to detect potential anomalies in altimeter data. The global dispersion of the datasets (figure 6) provides information on the correlation and coherence between both types of data and then, deeper analyses can be performed. The evolution of the method of comparison and the integration of new diagnoses are discussed in the following section.

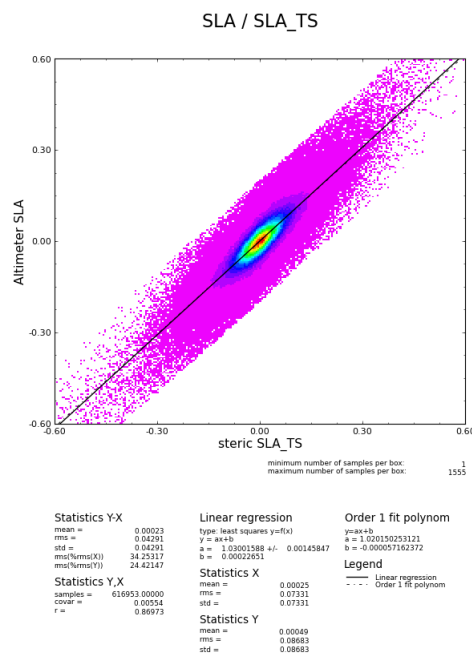


Figure 6: Dispersion between DUACS merged maps of altimeter SLA and the steric DHA from Argo plus the mass contribution from GRACE.

3.2. Evolution of the method of in-situ comparison

3.2.1. New version of the processing sequence for an automatic use

The processing chain which provides the comparison of altimetry with Argo data is relatively time consuming (in spite of previous improvements) and it is not very easy to launch for non expert users. In the context of the analyses of altimeter performances and the impact estimation of new altimeter standards, a list of analyses and diagnoses are systematically and automatically performed (independent of in-situ analyses). As the comparison with Argo data can contribute to this impact estimation, adding in-situ analyses required to develop a new version of the processing chain which could be called by other program in order to provide specific diagnoses. In addition, the time required to process a few years of altimeter data has been considerably reduced (about 2 hours according to the selected diagnoses). This work has been done in 2013 and has required a significant amount of time but it became necessary to allow the development of the activity. The analyses discussed in this report have been produced with this new processing chain.

3.2.2. New reference period

The Argo steric Dynamic Heights are anomalies referenced to a mean of Argo dynamic heights over 2003-2009. This period has been increased to 2003-2011 and is now used for the analyses performed in this report.

Note that altimeter measurements are sea level anomalies referenced to a mean sea surface with an inter annual content associated with the 1993-1999 period. The difference of reference periods have no impact when performing global comparison between altimetry and Argo but it becomes significant when analyzing the regional distribution of the differences. Indeed, observed geographical discrepancies may be attributed to the difference of inter-annual physical content and not to "real" differences between both datasets. Thus, altimeter sea level anomalies are referenced to the in-situ reference period by removing the mean of altimeter measurements over the corresponding period so that homogeneous inter annual contents are compared.

3.2.3. The mass contribution from GRACE: use of a new dataset

The mass contribution to the sea level that is missing in the Argo observations is derived from GRACE data. As discussed in the former section, we used the RL04 dataset from the NASA Tellus provider and the release 05 available in 2013 was expected to be much better. However, figure 7 (left) indicates that the correlation and the standard deviation of the global mean of the (Argo+GRACE) time series compared with altimetry (reference gray dot) are strongly deteriorated with the RL05 (blue triangle) compared with the RL04 (black circle). As previously mentioned, this dataset (whatever the release used) is not adapted for our method of comparison which includes the global mean of the GRACE maps (colocated with Argo profiles).

Indeed, users of the Tellus dataset should perform an averaging kernel convolved with the original gravity coefficients, which does not require smoothing or destriping. Figure 7 (right) indicates that such average (in green) provides very different result from a global average (in blue). A phase offset is observed, which explains the strong deterioration of annual signal estimation and the deteriorated

performances in the Taylor diagram.

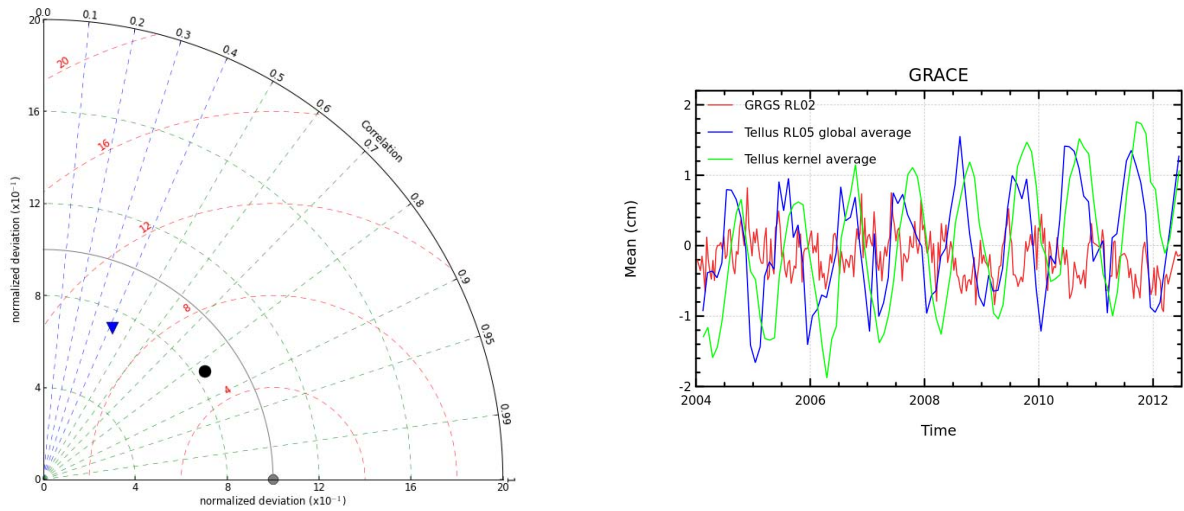


Figure 7: *Left: Taylor diagram of the Argo + GRACE time series compared with Jason-2 SLA (gray reference dot), including the GRACE NASA Tellus RL04 (black circle) and RL05 (blue triangle). Right: monitoring of the mass contributions to the sea level from GRACE: global mean (blue) and averaging kernel (green) of the NASA Tellus RL05 dataset and global mean of the GRGS V2 dataset.*

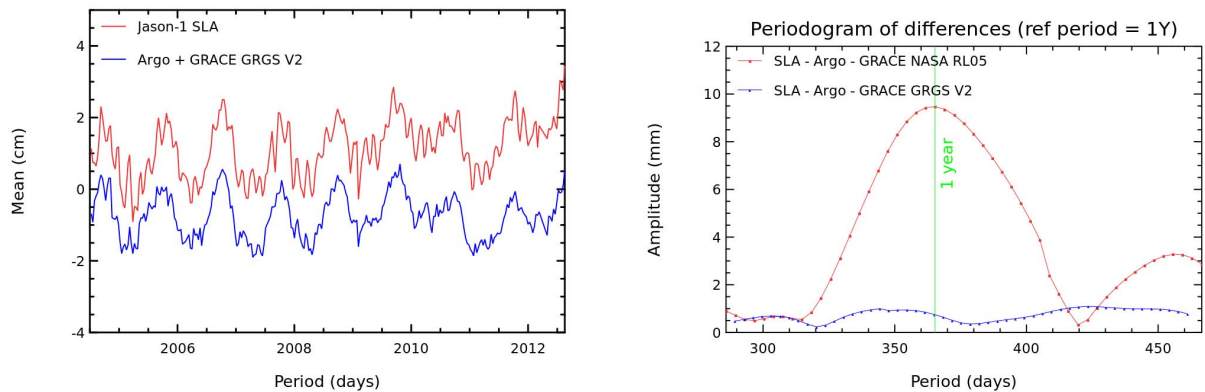


Figure 8: *Left: global mean of altimeter and Argo+GRACE (GRGS V2) sea levels. Right: periodogram of the annual signal of the altimetry - Argo - GRACE measurements.*

Thus, we use the dataset provided by the GRGS/LEGOS (Groupe de Recherche en Geodesie Spatiale) research group (<http://grgs.obs-mip.fr/grace>, V2). As the 10 days-maps are not filtered,

global average is allowed and the physical content of the time series is clearly different from the other dataset (figure 7, right, in red). The observed differences with the NASA dataset (green curve) are related with the differences between upstream processings (spherical harmonic decomposition,...) and downstream processing (filtering or not,...). In particular, the annual signal of the altimeter and Argo+GRACE time series are similar and no obvious phase offset is detected (figure 8, left). The amplitude of the annual signal of the differences used to reach 1 cm with the previous Tellus dataset (figure 8, right, in red) and it has almost disappeared with the GRGS V2 release (in blue). This constitutes a considerable improvement in our method of comparison and the uncertainty on the absolute trend of altimetry should be significantly reduced. However, the error introduced in our method associated with the use of this GRACE dataset still needs to be characterized and the use of the GRGS V3 dataset which should be soon available should help to better determine this level of error.

As (i) the altimeter regional sea level trends are mainly driven by the steric sea level trends (see figure 9 of the document appended in annex 8.2.) and very little correlation is found with the regional trends of the mass contribution and (ii) relatively high uncertainty is associated with the regional mass trends, comparisons of altimetry with Argo only is still performed when relative impacts are discussed (impact of new altimeter standards for instance).

3.2.4. Impact of the Glacial Isostatic Adjustment (GIA)

The Glacial Isostatic Adjustment (GIA), also called the Post Glacial Rebound (PGR) corresponds to the response of the solid envelope of the Earth to the melting of the ice cover from the last deglaciation period (20 000 years ago). The associated impacts are:

- The ocean basin volume changes
- The geoid changes
- Crustal movements

Argo steric measurements are not affected by these impacts but altimeter and GRACE data are (Tamisiea and Mitrova, 2011, [12]). Homogeneous physical contents of the datasets are required for the analyses of the global trends of the differences between altimetry and Argo+GRACE data and a GIA correction has to be included (GIA has no impact on the analysis of inter annual signals since the trend is removed). However, GIA effects have to be taken into account differently for altimetry and for GRACE measurements. Following discussions with users of this correction:

- -0.3 mm/yr is subtracted to altimeter data, which corresponds to the integral of the regional changes of the geoid over the oceans (Peltier's map of the GIA correction). The uncertainty associated with this model is estimated to be around 0.05 mm/yr.
- -0.9 mm/yr is subtracted to GRACE GRGS V2 data, corresponding to the integral of the GIA correction applied on the Tellus/NASA GRACE dataset. The uncertainty associated with this model is estimated to be around 0.3 mm/yr.

Thus, when analyzing the trend of the difference SLA - Argo - GRACE, we compute:

$$\begin{aligned} SLA - (-0.3) - (Argo + GRACE - (-0.9)) \\ = SLA + 0.3 - Argo - GRACE - 0.9 \\ = SLA - Argo - GRACE - 0.6 \end{aligned}$$

3.3. Improved estimation of the uncertainty

3.3.1. Estimation of the uncertainty of sea level trends

The drift of altimeter measurements and the impact estimation of a new altimeter standard are estimated by the trend of the differences with in-situ measurements. In particular, as discussed in the next section (Evaluation of new altimeter standards), the quality of an orbit solution may be analyzed by comparison with Argo data in order to check if there are regional / hemispheric biases in the sea level trends. It thus requires to know if two sea level trends can be statistically distinguished given the level of uncertainty associated with these values.

A new tool has been developed which provides an evaluation of the uncertainty of the trend of a time series thanks to different statistic methods (least squares, Monte-Carlo, Bootstrap, stationarity test of Dickey-Fuller). When applied to the trends of sea level differences between altimetry and Argo measurements, this will contribute to better estimate the uncertainty of the results and thus to increase the confidence associated with the method of comparison. Example is discussed in the following section.

3.3.2. New diagnostic: Spatial distribution of statistics of the differences

In the context of the comparison of altimetry with in-situ measurements, global differences provide many results (mean and standard deviation of the differences, trend, correlation, variance differences, etc) which allow to detect altimeter drift, anomalies and to determine the quality of new altimeter dataset. However, global analyses may not be enough to detect the impact of some evolutions which may be expected at regional scales. Thus, regional analyses of the sea level differences are also performed, be it at large scales (hemispheric differences of the trends for instance) or at smaller scales (map of statistics per boxes). In this situation, maps of the mean and variance of the sea level differences are usually computed but in order to better detect the impact of altimeter standards (which becomes smaller and smaller) and to reduce the uncertainty of the comparisons, new regional diagnoses have been developed in the framework of the new processing sequence (as described above).

Monthly maps of box-averaged altimeter and Argo sea levels and of their difference are computed, which allows the estimation of the spatial distribution of the correlation, the Taylor distance, the ratio of variance and the rms of differences between altimetry and in-situ data. For such analyses, the number of observations per box has to be kept in mind in order to have robust statistics and to avoid erroneous interpretation of the results. No example is provided yet but these diagnoses will be used for the 2014 studies.

3.3.3. New diagnostic: the Taylor diagram

Global analyses of the differences between altimeter and in-situ measurements consists in time series of their mean or variance but also the correlation between all couples of colocated altimeter and Argo profiles with a dispersion diagram (example in figure 6), including all temporal and spatial scales. A well-adapted diagnostic to synthesize the correlation and the standard deviation of altimetry and in-situ data is the Taylor diagram (see figure 7, left) which requires the time series of

the global mean of the sea level (figure 8, left).

The correlation between altimeter and Argo+GRACE time series is mainly associated with the annual signal which could hide some evolution expected at a particular wavelength. Thus, global time series are filtered in order to analyze the Taylor distance associated with the annual signal only, the high frequencies (≤ 1 y.) and the low frequencies (≥ 1 y.). This provides reliable information to estimate if a new altimeter standard or a new dataset makes the altimeter sea level more coherent and homogeneous with the independent reference. An example will be discussed in the following section for the quality assessment of the new 2014 reprocessing of the AVISO SSALTO/DUACS merged altimeter products (figure 27).

3.4. Sensitivity analyses

3.4.1. The Taylor distance

In order to better estimate the uncertainty of the Taylor distance, we analyze its sensitivity to the length of the time series. The 9 years (2004-2012) of the Jason-1 sea level time series is reduced from 2-years long subsamples to the original dataset and the coherence with Argo+mass is estimated for each subsample. Figure 9 shows the dispersion of the associated points. The dispersion is relatively reduced even for small subsamples: the correlation varies from 0.82 to 0.93 and the altimeter standard deviation is from 1.1 to 1.4 times the one of the Argo+mass timeseries. Note that the point associated with the original dataset (black circle) is not in the middle of the cloud dispersion. All wavelengths are included in the signal, and these results are mainly associated with the annual signal. The shortest the timeseries, the more the annual signal prevails and as it is well correlated, the correlation between altimetry and in-situ data increases. In addition, when reducing the length of the timeseries from 9 years to 4 years, the standard deviation decreases, probably because there is less physical content in shorter time series. Such analysis provides an order of magnitude of the uncertainty associated with this diagnosis and will be useful when studying the impact of a new altimeter standard for instance.

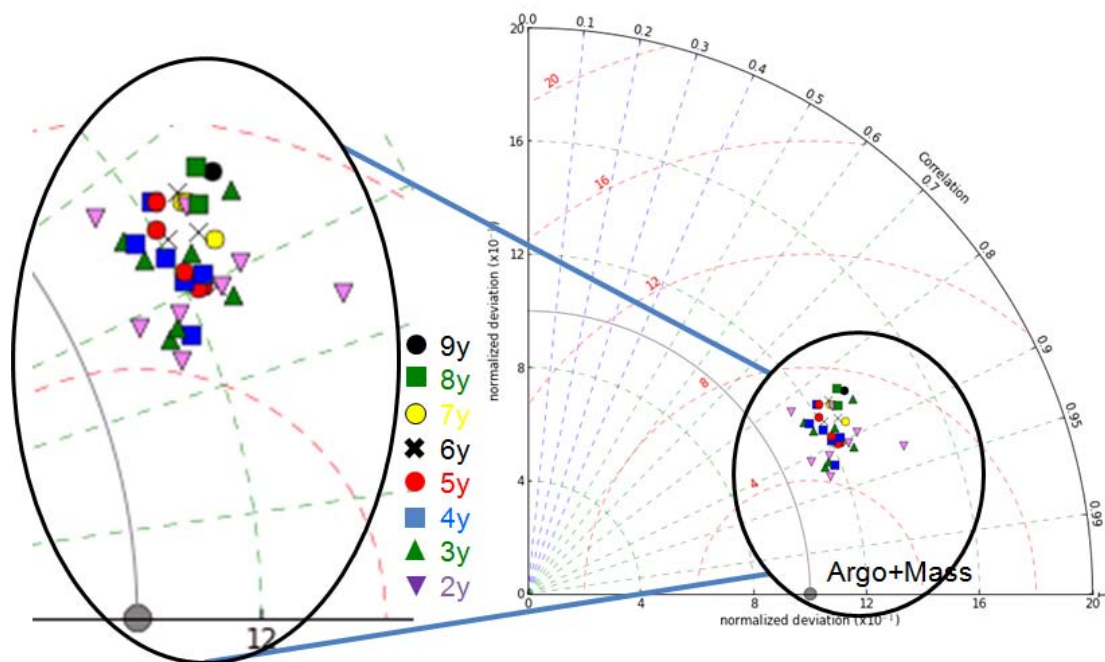


Figure 9: Sensitivity of the Taylor distance between Jason-1 measurements and Argo+GRACE data according to the length of the time series (from 2 to 9 years). The trend and periodic signals are not removed.

3.4.2. Impact of the altimeter data processing

As mentioned at the beginning of this section (Description of the processing sequence), grids of 10-day box-averaged along-track SLA are computed in order to have a sufficient spatial coverage since the altimeter sampling is better than the in-situ coverage. Boxes of 1° latitude \times 3° longitude are used in order to take into account the number of altimeter tracks per cycle and also the rather zonal ocean circulation because of the rotating effect of the Earth (Coriolis force). We want to determine whether box-averaging altimeter data with $1^\circ \times 1^\circ$ has an impact on the results of the comparison.

Figure 10 displays the time series of the differences between altimetry and Argo measurements with (left) and without (right) periodic signals. The amplitude and phase of the annual signal of the differences are not affected, neither the trend of the differences.

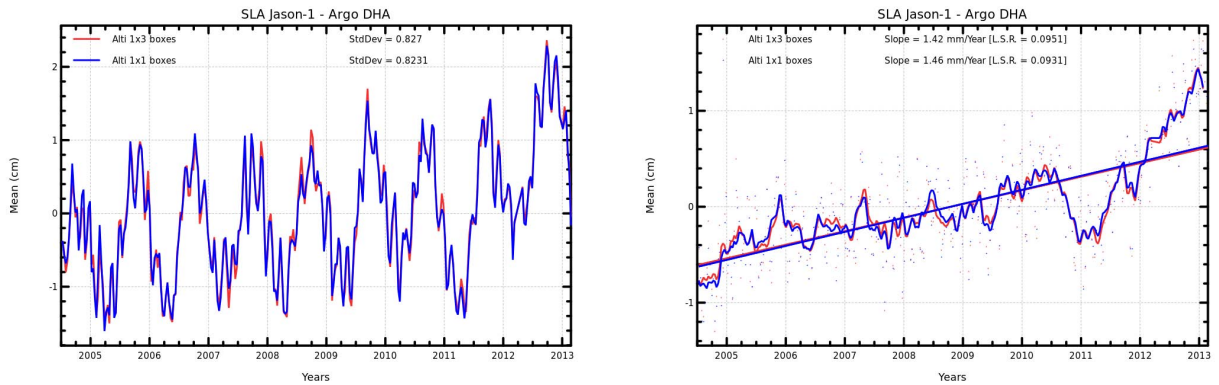


Figure 10: *Global mean differences between Jason-1 altimeter measurements and Argo dynamic heights (without the mass contribution) with (left) and without (right) annual and semi-annual signals. Along-track altimeter data are box-averaged before collocating with each Argo in-situ profile with 1x1 (blue curves) and 1x3 (red curves) boxes.*

In terms of variability, the variance of the differences is computed for the time series of each Argo float, using successively the two different size of box-averaging. Figure 11 shows the histogram of these variances for all Argo floats and the mean of $+1.3 \text{ cm}^2$ indicates that averaging along-track altimeter data with $1^\circ \times 3^\circ$ boxes makes altimeter data more coherent with in-situ Argo observations. Thus, this processing is chosen for the comparisons and all results in this report concerning along-track altimeter data are obtained with this parametrization.

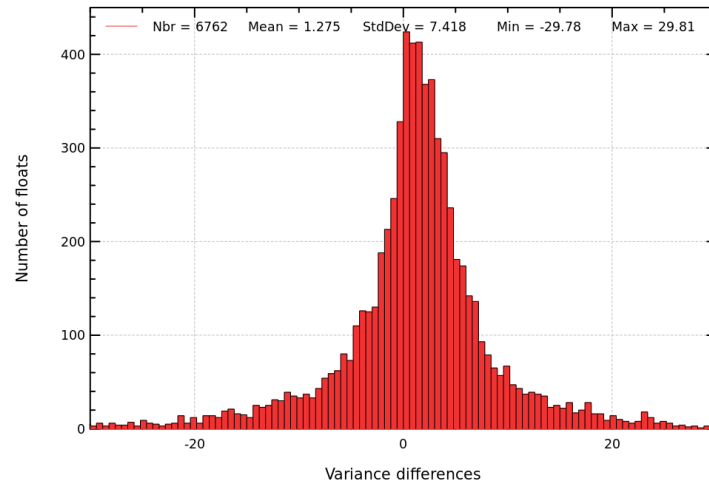


Figure 11: *Histogram of the variance differences between altimetry and Argo data using successively 1x1 and 1x3 degrees boxes for averaging along-track Jason-1 altimeter measurements before collocating with each Argo profile. Positive values traduce a more homogeneous altimeter sea level with in-situ data when using 1x3 boxes.*

3.4.3. Impact of the Argo subsampling

New Argo floats are regularly launched leading to a current in-situ network of almost 9 000 floats over almost the global open ocean. The associated in-situ dynamic heights are used to validate altimeter sea level measurements and we want to determine the sensitivity of these validation studies to the spatial sampling of the Argo floats.

The comparison of AVISO/DUACS merged products with all floats is used as a reference and several comparison are performed using subsamples of the floats list:

- 1 / 2 floats
- 1 / 4 floats, from the first of the list
- 1 / 4 floats, from the third of the list

Figure 12 shows the number of altimetry - Argo differences per box with different subsampling. With half of the dataset (top right), the sampling is significantly reduced homogeneously over the global ocean and with 1/4 of the floats (bottom panels) some areas are not samples at all.

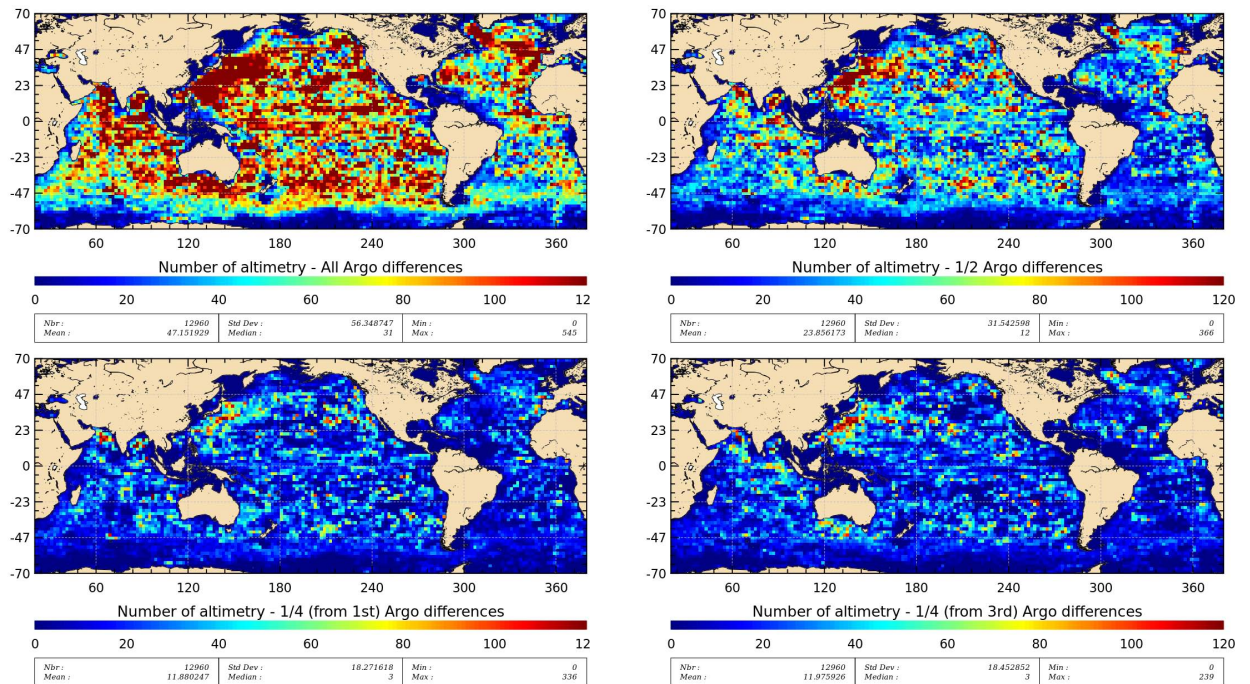


Figure 12: Number per box of altimeter (AVISO DUACS merged product) - Argo differences over the period 2004-2012 with various subsampling of the list of Argo floats: all (top left), 1/2 (top right), 1/4 from the 1st (bottom left) and 1/4 from the third (bottom right).

The global mean differences are computed for each experiment in order to analyze the sensitivity of the altimeter sea level trend. Figure 13 (left) shows the mean differences between altimeter and Argo data. With half of the Argo float, the trend of the sea level differences is not affected over the period Jan. 2004 / Aug.2012 and the standard deviation of the differences is also unchanged.

With a quarter of the floats, the trend is relatively weakly modified by ± 0.2 mm/yr according to the subsampling considered. When the mass contribution is also withdrawn (figure 13, right), the trend is also not modified with half of the floats but the impact is slightly higher with a quarter of the floats (up to 0.4 mm/yr). Thus, the subsampling of the Argo dataset has a relatively reduced impact on the trend of the sea level differences.

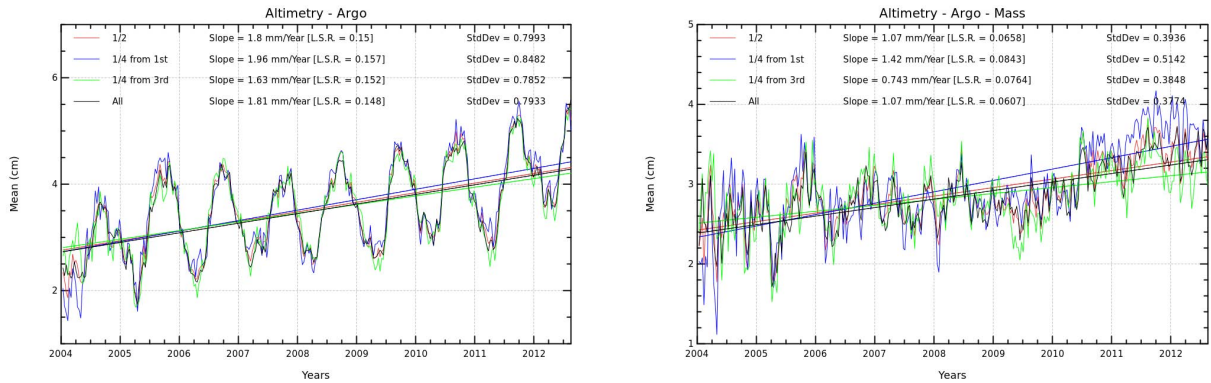


Figure 13: Global mean differences (with different subsampling of the list of Argo floats) between altimetry (AVISO DUACS merged product) and Argo measurements (left) and between altimetry and Argo+GRACE (GRGS V2) data (right).

The coherence between altimetry and in-situ measurements is now analyzed and figure 14 (left) displays the Argo+mass time series (bottom curves) for different subsampling of the Argo floats and the corresponding colocated altimetry (top curves). All time series are slightly modified according to the in-situ subsampling and in particular, the phase and amplitude of the annual signal does not appear to be strongly modified. The Taylor distance figure 14 (right) between altimetry (gray reference dot) and the Argo+mass time series is computed for different subsampling of the Argo floats. The greater Taylor distance is obtained with the total Argo dataset (red square) and the subsampling of the number of Argo floats clearly deteriorates the coherence between the altimeter signal and Argo + mass contributions. It is thus clearly recommended to maintain the spatial coverage of the Argo network.

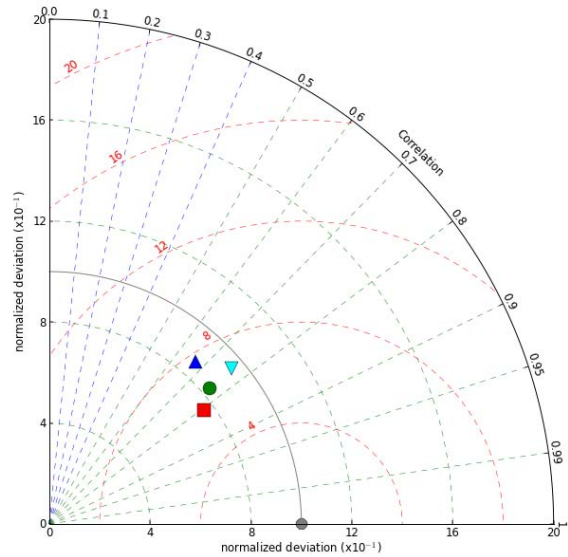
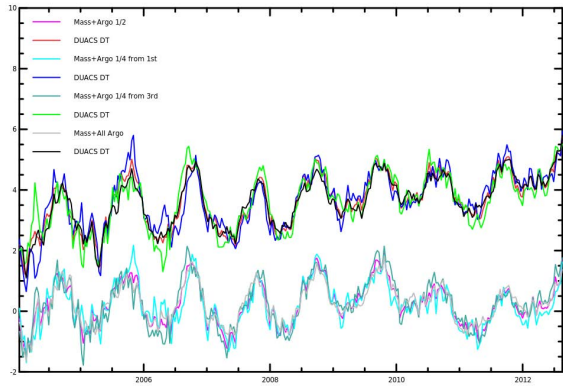


Figure 14: *Left: mean of Argo + GRACE (GRGS V2) sea level measurements with different sub-sampling of the Argo floats (bottom curves) and mean of the corresponding colocated DUACS merged altimeter data. Right: Taylor diagram (correlation and standard deviation) of these time series: the gray dot is the altimeter DUACS merged sea level product and statistics obtained with Argo+mass values are represented for different sampling of the Argo floats: all (red square), half (green circle), 1/4 (blue and cyan triangles). Trends and periodic signals are included.*

3.4.4. Argo steric dynamic heights: impact of the reference depth on the comparison with altimetry

The Argo network of in-situ profiling floats provides Temperature and salinity (T/S) measurements through the water column every 10 days. Dynamic heights are derived from the Argo T/S profiles as the integration of the T/S measurements through the water column. This integration requires a reference level (pressure) and:

- The deeper the reference level, the more information from the T/S profiles is taken into account,
- But the more T/S profiles are not used (those who do not reach the reference level)

Thus, we first aim at determining the impacts of a given reference depth of integration on the global Argo sampling but also on the regional Argo distribution. Secondly, it should be determined how much steric signal is missed with the choice of a given reference depth.

These two issues have been analyzed in the framework of the Sea Level Climate Change Initiative and E-AIMS projects. The sea level closure budget is analyzed through the comparison of various contributions to the sea level, the steric sea level being one of these contributions (associated with the thermohaline expansion of the water column). The impact of the choice of the reference level on the global Argo sampling and the regional Argo distribution has been first analyzed. Then, three time series of monthly maps of steric sea level have been computed with a 900 dbar, 1200 dbar and 1900 dbar reference depth in order to estimate how much steric signal is missed between these products. Then, the physical contents of these products are analyzed and compared with other datasets (altimetry minus mass contribution from GRACE) and the differences are discussed. An estimation of the error of the method used to compute global maps of steric sea level has been provided. The report summarizing the results is appended to the present document as an annex (see Annex 8.2. page 42).

As a summary, in the context of the quality assessment of the altimeter MSL, it turns out that the choice of a reference depth to compute Argo steric dynamic heights is not clear:

- The steric MSL referenced to 1900 dbar will be preferred in case of assessing the altimeter MSL trend and discuss the altimeter sea level closure budget.
- However, when removing the effect of the trend, the standard deviation of altimetry is closer to the steric + mass signals with a 900 dbar reference and the correlation between altimetry and Argo + mass is slightly increased with the 900dbar time series. In addition, steric MSL trends are more homogeneously distributed compared with altimetry at 900dbar rather than with deeper references. Thus, in case of assessing the impact of a new altimeter standard in terms of variance, the 900 dbar steric signal may be preferred.

4. Analyses of the altimeter sea level differences with the external reference

In this section, we discuss the global mean sea level trend of several altimeter missions compared with Argo+GRACE measurements, the inter-annual signals, the regional mean differences and the major differences observed between different missions.

4.1. Global altimeter drifts and inter annual variability

Figure 15 (left) presents the mean differences between altimetry and Argo+mass (GRGS V2) for Jason-1 (red), Envisat (blue) and Jason-2 (green) missions. As mentioned in the former section, a GIA correction is applied on these trends. A 0.7 mm/yr drift is observed for Jason-1 and 2.2 mm/yr for Envisat over 2005-2012.5 period. Concerning Jason-2, a 1.9 mm/yr drift is observed over its shorter period. When using SSALTO/DUACS altimeter merged products, a 1.1 mm/yr drift is observed over the 2005-2012.5 period (see figure 13, right but also figure 6 in annex 8.2.). The 1 mm/yr remaining drift of altimetry compared with Argo and GRACE measurements could have several origins:

- The reference level of integration used to compute steric dynamic heights. Indeed, as discussed in the previous section (sensitivity analysis of the steric heights to the reference level) and detailed in annex 8.2., this residual trend is affected by a change of reference depth of the steric heights.
- A leakage effect of the GRACE data around areas of strong continental ice loss (mainly Greenland but also Patagonia and Antarctic peninsula). A selection of data only at coastal distance greater than 500 km or with a maximum threshold on the GRACE trends could help to assess whether this leakage effect has an impact on the residual altimeter drift.

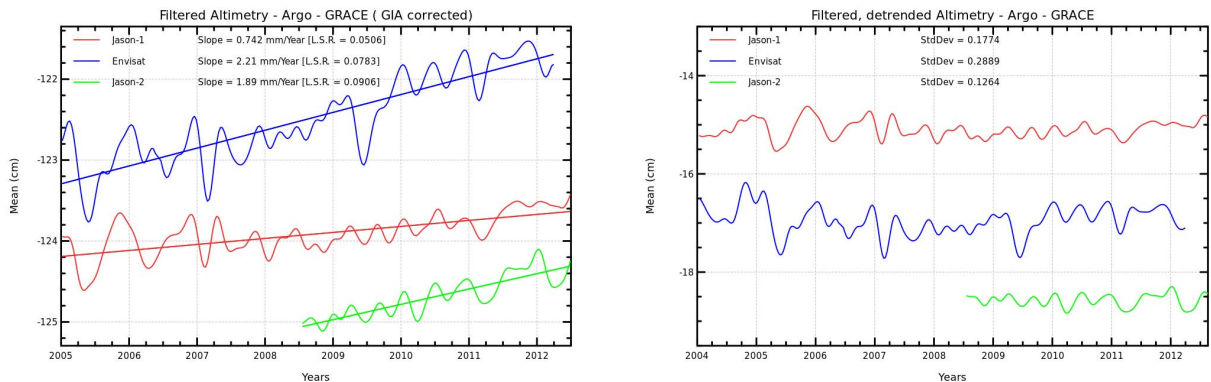


Figure 15: *Left: 3-months filtered mean differences between altimetry and Argo+mass (GRGS V2) for Jason-1 (red), Envisat (blue) and Jason-2 (green) missions with the GIA effects included. Right: idem after removing the trend.*

The analysis of the inter annual signals is made thanks to the detrended time series of the mean differences (figure 15, right). Over the total period, the standard deviation of the filtered time series is significantly higher for the Envisat mission than for Jason-1 (0.29 cm and 0.18 cm respectively). The difference of altimeter standards contributes to this difference. The value associated

with Jason-2 over its shorter period (0.13 cm) is slightly reduced compared with Jason-1. At inter annual time scales, higher variability is observed both for Jason-1 (red) and Envisat (green) in 2005 and at the beginning of 2007. A drop of the Envisat signal is observed in 2009 but it is not detected with other altimeter missions.

4.2. Regional mean differences

The regional mean differences between Jason-1 sea level and Argo data only are shown on figure 16 (left). These differences are of the order of less than 1 cm, except in areas of high ocean variability where the error associated with the collocation of altimetry with Argo profiles is higher. As mentioned when describing the datasets, the GRACE GRGS V2 measurements can be used to compute global altimeter absolute drift but as the data are not filtered, stripes are clearly observed (see figure 4) and it has a strong impact on the regional distribution of the mean differences between altimetry, Argo and GRACE data, as illustrated on figure 16 (right). Thus, regional analyses can not be performed in terms of absolute differences compared with Argo and GRACE, but the use of this dataset will not affect relative regional differences between two missions for instance.

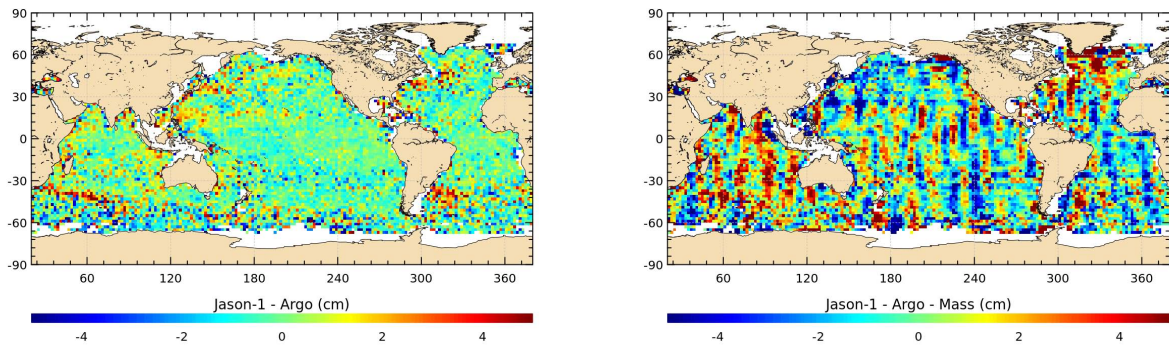


Figure 16: *Regional mean differences between Jason-1 sea level and Argo (left) or Argo+mass (GRGS V2) (right).*

This is illustrated on figure 17 (left) which shows the discrepancies between Jason-1 and Envisat of the mean differences between altimetry and Argo+GRACE. The stripes of the GRACE dataset have cancelled in the comparison and an East/West hemispheric bias is clearly observed. This well-known anomaly is related with the GDR-C orbit solution and is also observed when the sea level of both missions are directly compared. The discrepancies between Jason-1 and Jason-2 of the mean sea level differences computed over Jason-2 period (see figure 17, right) show a slight East/West bias together with a North/South hemispheric bias. This first one is related with the GDR-C orbit solution used for Jason-1 at the beginning of the studied period and the second one is associated with the GDR-D orbit solution which is affected by the South Atlantic Anomaly (SAA). This anomaly will be discussed in details in the next section.

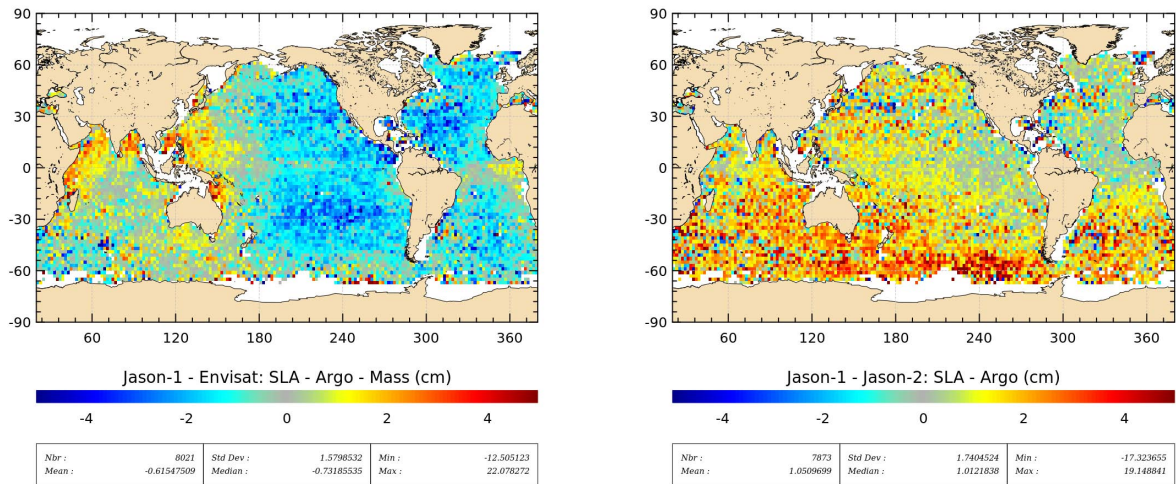


Figure 17: *Left: regional differences between Jason-1 and Envisat of the mean differences between altimetry and Argo+mass (GRGS V2) over 2004.5-2012.5. Right: regional differences between Jason-1 and Jason-2 of the mean differences between altimetry and Argo data over 2008.5-2012.*

5. Evaluation of new altimeter standards

5.1. Overview

The impact of a new altimeter standard (orbit solution, geophysical or instrumental correction, re-tracking algorithm) on the sea level computed from altimetry may be estimated by comparison with in-situ measurements using successively the old and new version of the altimeter standard. This approach also helps us to better characterize the uncertainty associated with our method. Indeed, the more analyses of impacts are performed, the more it will be possible to a priori determine in which situation the impact of a new standard can be detected or not.

Various analyses of impact have been performed over the previous years concerning updated or reprocessed altimeter data for Jason-1, Jason-2 and Envisat, the use of a new MSS, the modelled or radiometric wet troposphere correction but also the quality assessment of new orbit solutions (GDR-C/D, GSFC) and so on (see previous annual reports of the activity). The criteria of improvement used for these analyses are based on the consistency (variance difference) between the updated altimeter data and the in-situ reference but also on the evolution of the correlation and of the sea level trends. According to the studied altimeter standard and the expected impact, one of these criteria will be preferred. Concerning the impact of a new orbit solution, the Argo dynamic heights are the only external reference that can be used to assess its impact. As no hemispheric bias is expected in the trend of the Argo dynamic heights, the coherence of the trend differences between two hemispheres is a strong criterion to estimate the performance of a new orbit solution (see Valladeau and Legeais 2012, [14]).

As already mention, altimeter regional sea level trends are little correlated with the regional trends of the mass contribution to the sea level and relatively high uncertainty is associated with the regional trends of this latter contribution, so the mass contribution to the sea level is not systematically used to detect the impact of new altimeter standards.

Other diagnoses should be used to estimate the impact of new altimeter standards. For instance, data could be first filtered out in the frequency band where the impact of the new standard is expected to be maximal. The regional impact could be better characterized with the maps of the correlation and rms of the differences obtained with the former and the new standards. All these diagnoses have not been used yet in the studies performed in 2013, which are synthetized below. Efforts have been made to better determine the uncertainty of the method associated with the detection of trends differences. This has been done in the context of the impact estimation of new orbit solutions. Other analyses have concerned the impact of a new wet troposphere correction for TOPEX/Poseidon mission, the assessment of the ESA CCI sea level dataset and of the reprocessed SSALTO/DUACS 2014 merged product.

5.2. Uncertainty of the method for the detection of trends difference

5.2.1. Impact of the weighting of DORIS stations in the South Atlantic Anomaly region on the Jason-1 orbit solution

The mean sea level differences between Jason-1 and Jason-2 over its verification phase display a North/South hemispheric bias with the GDR-D orbit solution. This solution includes for Jason-1 an under-weighting of some DORIS stations (Lemoine and Capedeville, 2006, [8]) in the South Atlantic Anomaly (SAA) region (see the right panel of figure 17, for an illustration of this hemispheric bias over all the Jason-2 period) to get around an instrumental sensitivity of the mission to the SAA. Without under-weighting these stations for the Jason-1 mission, it reduces the regional bias but it also has an impact on the Jason-1 regional MSL trends: a ± 0.5 mm/yr North/South hemispheric bias is observed (see 2013 Jason-1 annual report: [13]).

As no hemispheric bias is expected in the trend of Argo dynamic heights, we compute the trend of the differences between Jason-1 SLA and Argo data for both orbit solutions and separating the North and South hemispheres (for $|lat| \geq 20^\circ$). However, the order of magnitude of the searched trend differences is of ± 0.5 mm/yr. This is very small compared with the ± 3.0 mm/yr which has been detected with the GDR-C orbit solution (Valladeau and Legeais 2012, [14]). The orbit solution without under-weighting of SAA DORIS stations for Jason-1 is expected to be better since more in agreement with Jason-2 which is not sensitive to the SAA. Thus, if the impact on the trend is detected with our method, this analysis will provides an estimation of the uncertainty on the trends obtained with our method of in-situ comparison.

Figure 18 indicates that the Jason-1 orbit with and without under-weighting of DORIS SAA stations leads to N/S MSL trends difference of 0.0 mm/yr and 0.6 mm/yr respectively. If the uncertainty was null, this would suggest that the new orbit solution is worse. But the use of a Monte-Carlo statistic method to estimate the uncertainty of the trends difference associated with the method of comparison provides values of 1.2 and 1.3 mm/yr respectively. This means that the difference of 0.6 mm/yr observed between both solutions can not be distinguished given the uncertainty of the method and we can not conclude which orbit solution is the best.

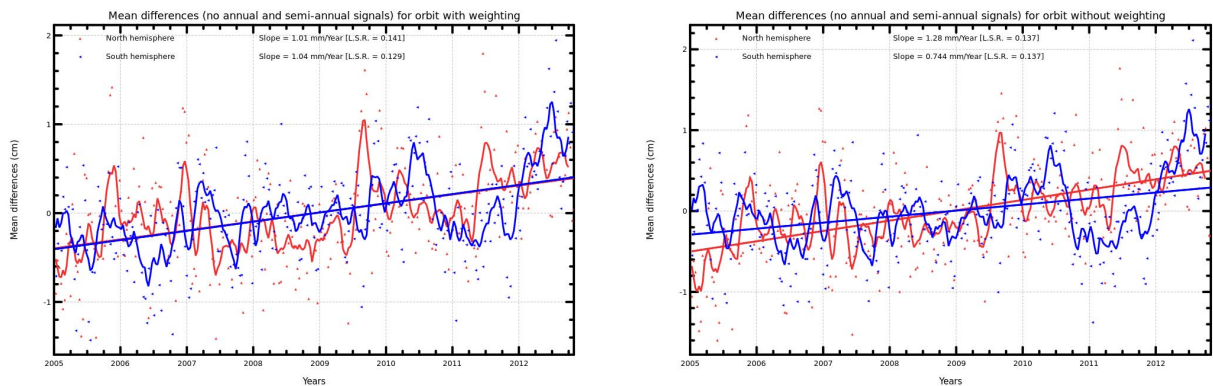


Figure 18: Trends of the differences between Jason-1 SLA and Argo data separating the North and South hemispheres ($|lat| \geq 20^\circ$) with (left) and without (right) under-weighting of the DORIS stations in the SAA. The hemispheric trend differences are of 0.0 mm/yr and 0.6 mm/yr respectively.

5.2.2. Comparison of GFZ and GDR-D orbit solutions for Envisat

The GFZ orbit solution has been compared with the GDR-D solution for the Envisat sea level estimation and the mean sea level trends difference displays an hemispheric East / West difference of ± 0.5 mm/yr (figure 19). As for previous studies, the Envisat sea level is compared with Argo dynamic heights in order to detect which orbit solution is responsible for this hemispheric bias.

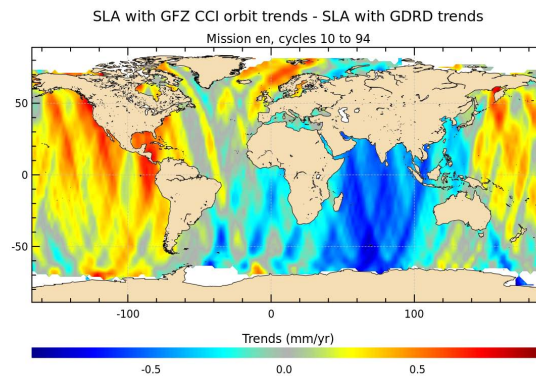


Figure 19: *Difference of maps of sea level trends from Envisat derived with the GFZ and GDR-D orbit solutions.*

Figure 20 indicates that the hemispheric trends difference is the same (0.8 mm/yr) with both orbit solutions. As previously discussed, the uncertainty of the in-situ method of comparison do not allow us to distinguish sea level trends difference of the order of ± 0.5 mm/yr. Thus, the method of comparison should be improved (colocation of the altimeter / in-situ data, etc) in order to reduce the associated trend uncertainty.

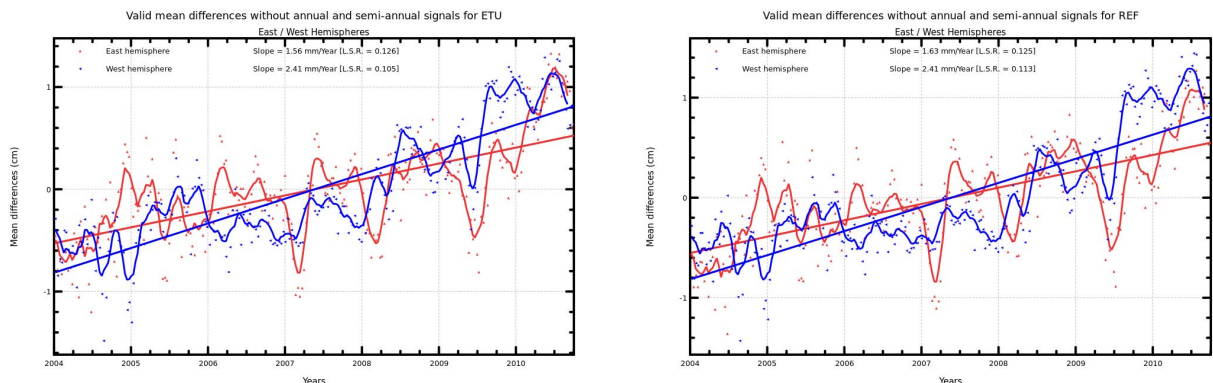


Figure 20: *Trends of the differences between Envisat SLA and Argo data separating the Western ($180^\circ - 0^\circ$) and Eastern hemispheres ($0^\circ - 180^\circ$) with the GFZ (left) and GDR-D (right) orbit solution. The hemispheric trend differences are of 0.8 mm/yr with both solutions.*

5.3. Assessment of the GPD wet troposphere correction on TP

In the framework of the ESA Sea Level Climate Change Initiative (SL-CCI), University of Porto (Portugal) has produced a new wet troposphere correction for all altimeter mission based on a combination of radiometer data and modelled data with GNSS Path Delay (GPD) measurements. The use of this GPD correction for the TOPEX/Poseidon mission has a strong impact on the sea level trends (more than 1 mm/yr) in the Indian ocean compared with the use of the radiometer correction (figure 21).

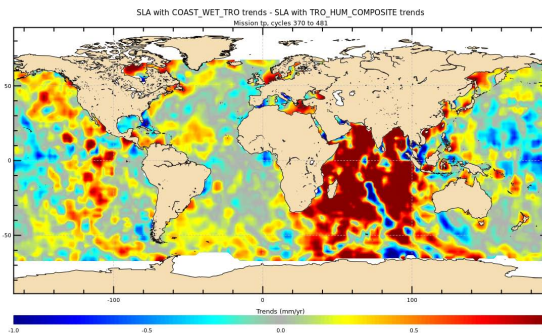


Figure 21: *Regional sea level trend differences for the TOPEX sea level measurements computed with the GPD versus the radiometer wet troposphere correction over TOPEX cycles 370 to 481.*

In terms of trends, Argo measurements are used to estimate which altimeter standard provides the best results. The North Pacific ocean is used as a neutral reference region where the trend differences are small. As no systematic bias is expected between these two regions in the Argo sea level trends, we compute the trend of the differences between altimetry and in-situ data in these regions in order to detect the best standard. Figure 22 shows regional differences of 2.2 mm/yr with the radiometer correction and 0.8 mm/yr with the GPD correction. This would suggest that the GPD correction improves the TOPEX sea level trends in the Indian ocean but the rather short period of analysis (Jan. 2004 - Oct. 2005) leads to a very high uncertainty on the trends with a low confidence in this result.

As the period is very short for a good trend estimation, the impact is also analyzed in term of variance. Figure 23 shows that both tide gauges and Argo data indicate that TOPEX measurements are more homogeneous with in-situ data when using the GPD wet troposphere correction. Thus, the new correction is estimated to be an improvement.

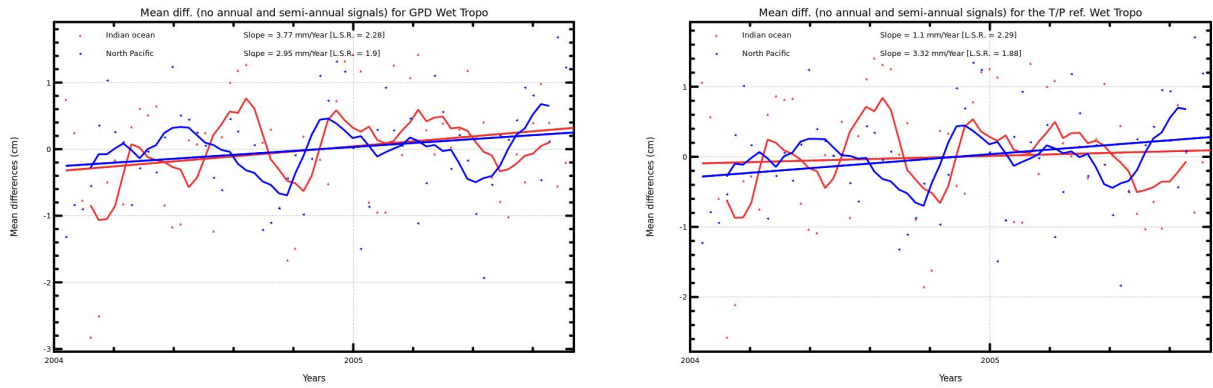


Figure 22: Trends of the differences between TOPEX SLA and Argo data separating the Indian ocean and the North Pacific ocean with the GPD (left) and the radiometer (right) wet troposphere correction.

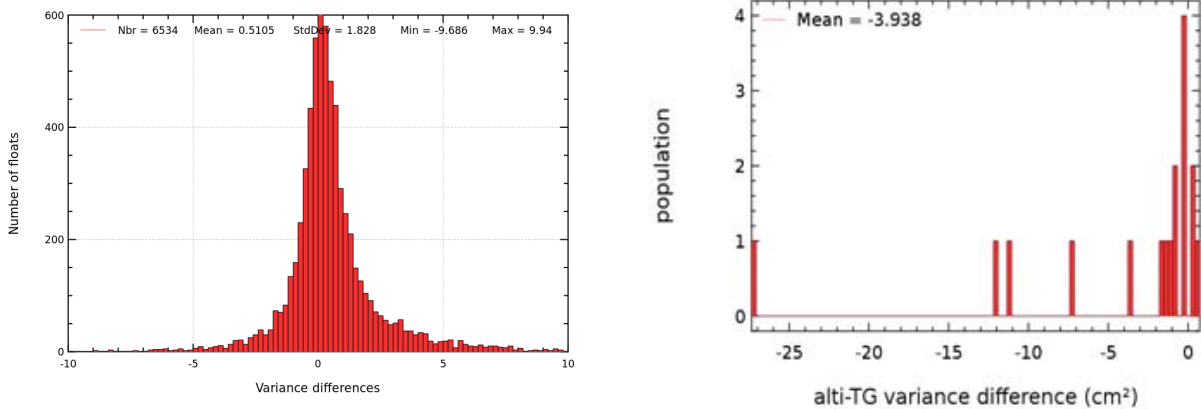


Figure 23: Histogram of the variance differences between altimetry and Argo data (left) and tide gauges (right) using successively the GPD and the radiometer wet troposphere correction for the TOPEX mission. Negative values traduce a more homogeneous altimeter sea level with in-situ data when using the GPD correction.

5.4. Quality assessment of the DUACS DT 2014 reprocessing

Twenty years of SSALTO/DUACS AVISO sea level altimeter data have been reprocessed and will be released in 2014. The quality of this new dataset has been estimated by comparison with Argo in-situ data and compared with the performances of the current version of the product available from AVISO (2010 reprocessing). The differences between both altimeter time series consist in different altimeter standards for the different missions but also in new parametrisation of the processing of the level 2 measurements and their mapping technique. An important evolution is the change of reference period for the computation of the sea level anomalies: 20 years versus 7 years for the former version.

Global statistics are computed over all colocated altimeter / Argo profiles over 2004-2012 and the global correlation between each altimeter dataset and in-situ measurements is unchanged (0.87). This statistic includes all temporal and spatial scales and it shows that detailed analysis is required to distinguish the performances of each product.

The global mean differences with Argo measurements does not show significant evolution between both altimeter versions (figure 24, left) and the trend of the differences is globally unchanged (1.6 mm/yr, figure 24, right).

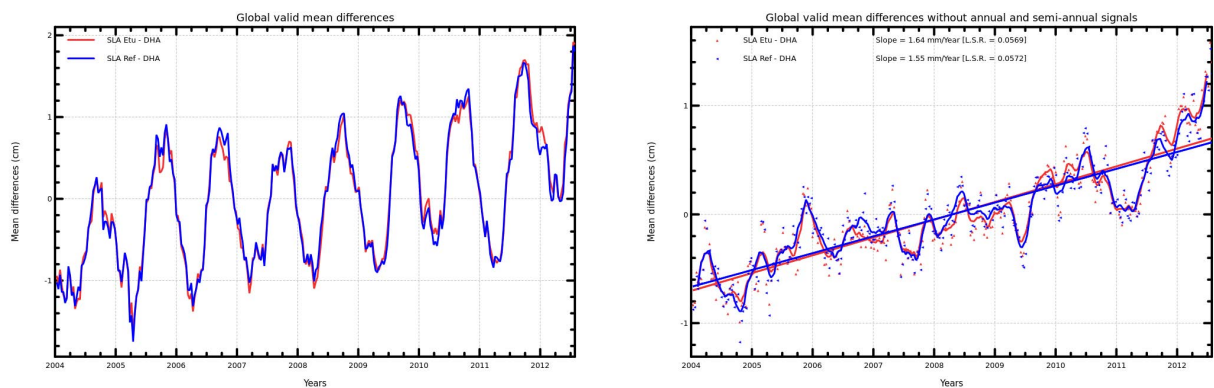


Figure 24: *Global mean differences between altimetry (AVISO 2014 in red and AVISO 2010 in blue) and Argo measurements with (left) and without (right) annual and semi-annual signals.*

At regional scales, the sea level trend differences between AVISO V2010 and V2014 display an hemispheric East/West bias directly associated with the evolution of the orbit solution (GDR-D standard). This impact can also be detected with the regional mean differences (colocated with Argo floats positions). The trend of the differences between altimetry and Argo measurements are computed separating each hemisphere in order to detect which orbit solution provides the best regional coherence of the sea level trends, as observed by the Argo dataset. Hemispheric sea level trends differences are of +0.9 mm/yr with AVISO 2010 and -0.1 mm/yr with AVISO 2014. This is in line with the impact of the GRD-D orbit solution compared with the GDR-C standard on the Jason-1 sea level measurements (see Valladeau and Legeais 2012, [14]) which indicated hemispheric sea level trend differences of +0.9 mm/yr with GDR-C and -0.7 mm/yr with GDR-D. Thus the comparison with in-situ measurements indicates an improvement of the AVISO 2014 with the new orbit standard in terms of regional consistency of the sea level trends.

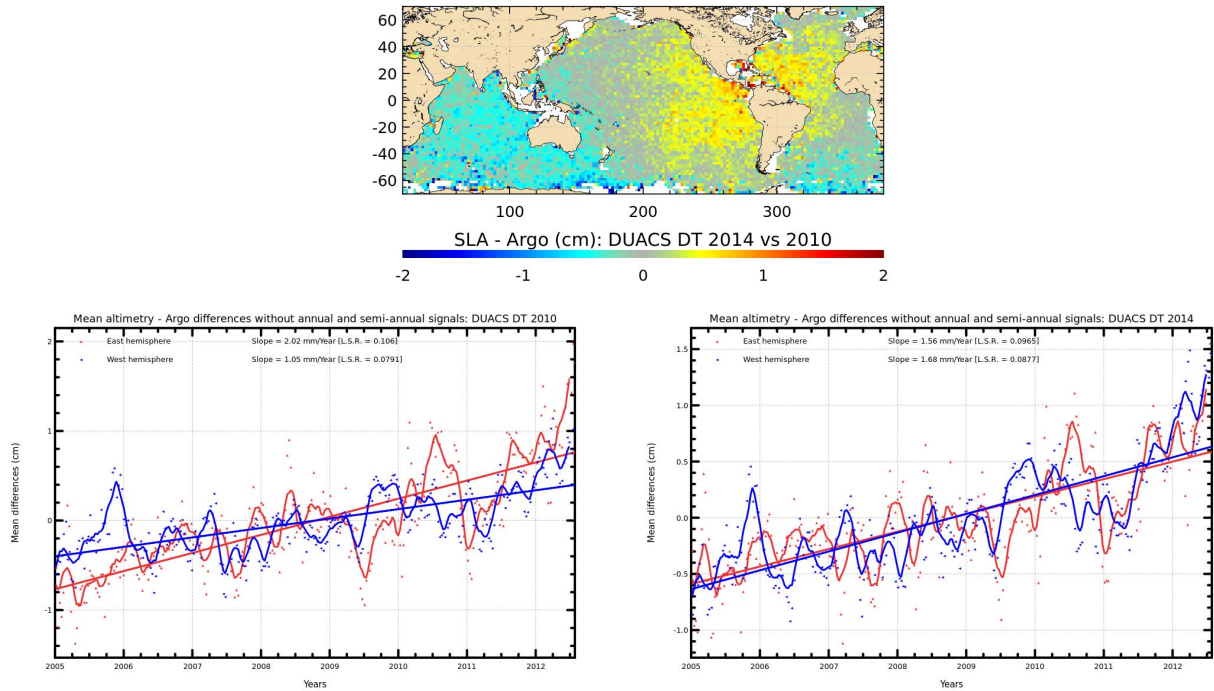


Figure 25: *Top: Regional mean differences between AVISO 2014 and 2010 (colocated with Argo profiles) over 2004-2012. Bottom: trends of the differences between altimetry and Argo data separating the Western ($180^\circ - 0^\circ$) and Eastern hemispheres ($0^\circ - 180^\circ$) with the AVISO 2010 (left) and AVISO 2014 (right) versions.*

As the physical content of altimetry and Argo measurements are different (cf figure 24 which shows strong amplitude of the annual signal of their difference), we use the mass contribution (GRACE GRGS V2) to perform absolute comparisons in terms of amplitude of the periodic signals and concerning the evolution of the coherence between altimetry and Argo + mass.

Figure 26 (left) indicates that when comparing altimetry with Argo and the mass contribution, the annual signal of the differences almost disappears, which is confirmed by figure 26 (right), showing that the amplitude of the annual signal is reduced from 1.1 mm (AVISO 2010) to 0.7 mm (AVISO 2014).

Figure 27 (left) shows the sea level time series of the global mean of altimetry (blue and red) and Argo + mass contributions (green) and we analyze the evolution of their correlation and standard deviation of the signals (Taylor diagram on the right panel), separating different temporal scales for AVISO V2010 (circles) and V2014 (triangles):

- As for the detrended global time series (black), the correlation with Argo+mass is not changed (0.92) and the altimeter standard deviation is very slightly closer to the one of the in-situ reference with the 2014 reprocessed altimeter dataset (black triangle).
- When considering the annual signal only (green), the correlation with Argo+mass is very high (0.99), illustrating that the correlation is mainly associated with this signal.
- At high frequencies (≤ 1 year, in red), the correlation is unchanged and the standard deviation

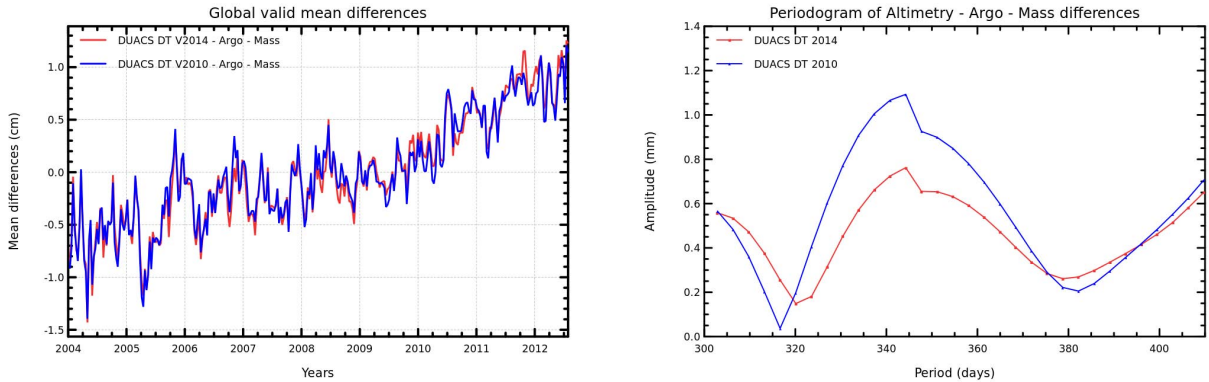


Figure 26: Global mean differences between altimetry (AVISO 2014 in red and AVISO 2010 in blue) and summed Argo + mass (GRACE GRGS V2) measurements (left) and periodogram of the annual signal of the differences (right).

of the altimeter time series is slightly closer with the one of the reference with the former V2010 dataset.

- At low frequencies (≥ 1 year, in blue), the correlation with Argo+mass is increased with V2014 and the altimeter variability is slightly closer to the one of the reference with the reprocessed AVISO product.

However the sensitivity analysis performed on the Taylor distance (see paragraph 3.4) suggests that the differences observed here are rather small and this Taylor diagram mainly indicates that no major error has been introduced in the 2014 reprocessed altimeter dataset.

In terms of variance, the temporal variance of the differences between altimeter sea level and Argo measurements computed for each Argo floats time series does not reveal any significant evolution with both altimeter datasets (figure 28, top). Thus, the datasets are restricted to the region of strong ocean variability of the Antarctic Circumpolar Current (ACC, 35S/60S) (figure 28, left) where the error of the method is higher (colocation of altimetry with Argo profiles) but the difference between both altimeter dataset is expected to be higher in terms of variance. The Taylor diagram (right panel) shows that the AVISO 2014 time series (triangle) has a standard deviation slightly closer to the one of the reference and an unchanged correlation with Argo+mass (gray dot).

Thus, the comparison of altimetry with in-situ Argo measurements has shown that the impact of the 2014 reprocessed dataset varies according to the temporal frequencies considered (trend, annual signal, low and high frequencies) and the AVISO 2014 shows globally slightly better coherence with the in-situ dataset.

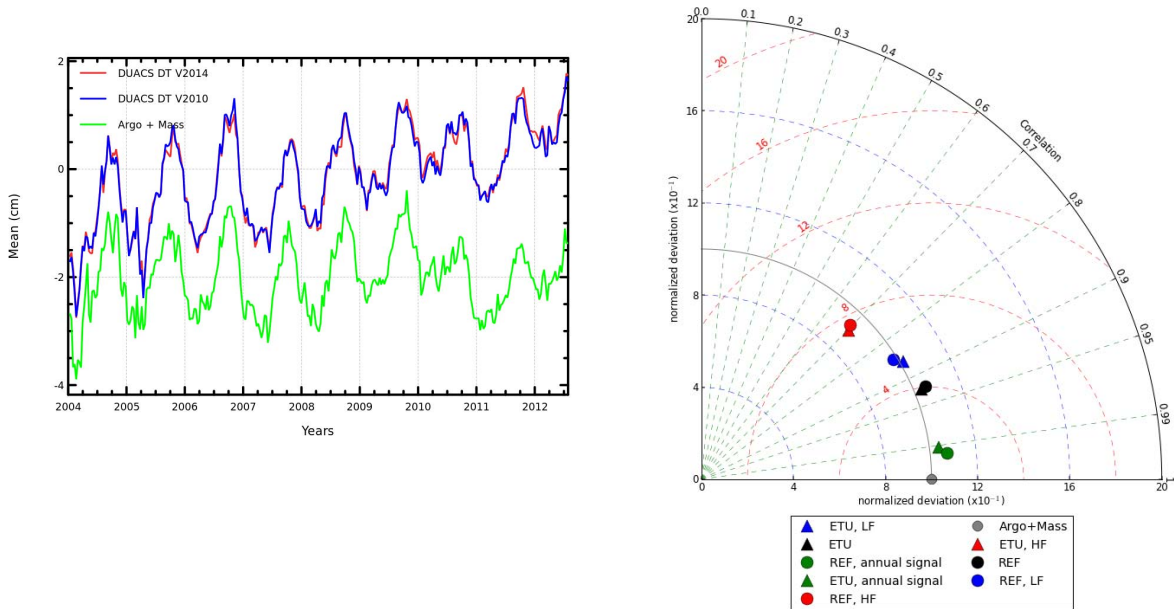


Figure 27: *Time series of altimetry (AVISO 2014 in red and AVISO 2010 in blue) and summed Argo + mass (GRACE GRGS V2) measurements (left) and associated Taylor diagram (correlation and standard deviation) of these time series: the gray dot is the Argo+mass reference value and statistics obtained with AVISO 2014 (AVISO 2010) are represented by triangles (circles), separating different temporal scales: detrended (black), annual cycle (green), high frequencies ($\leq 1y.$, red) and low frequencies ($\geq 1y.$, blue).*

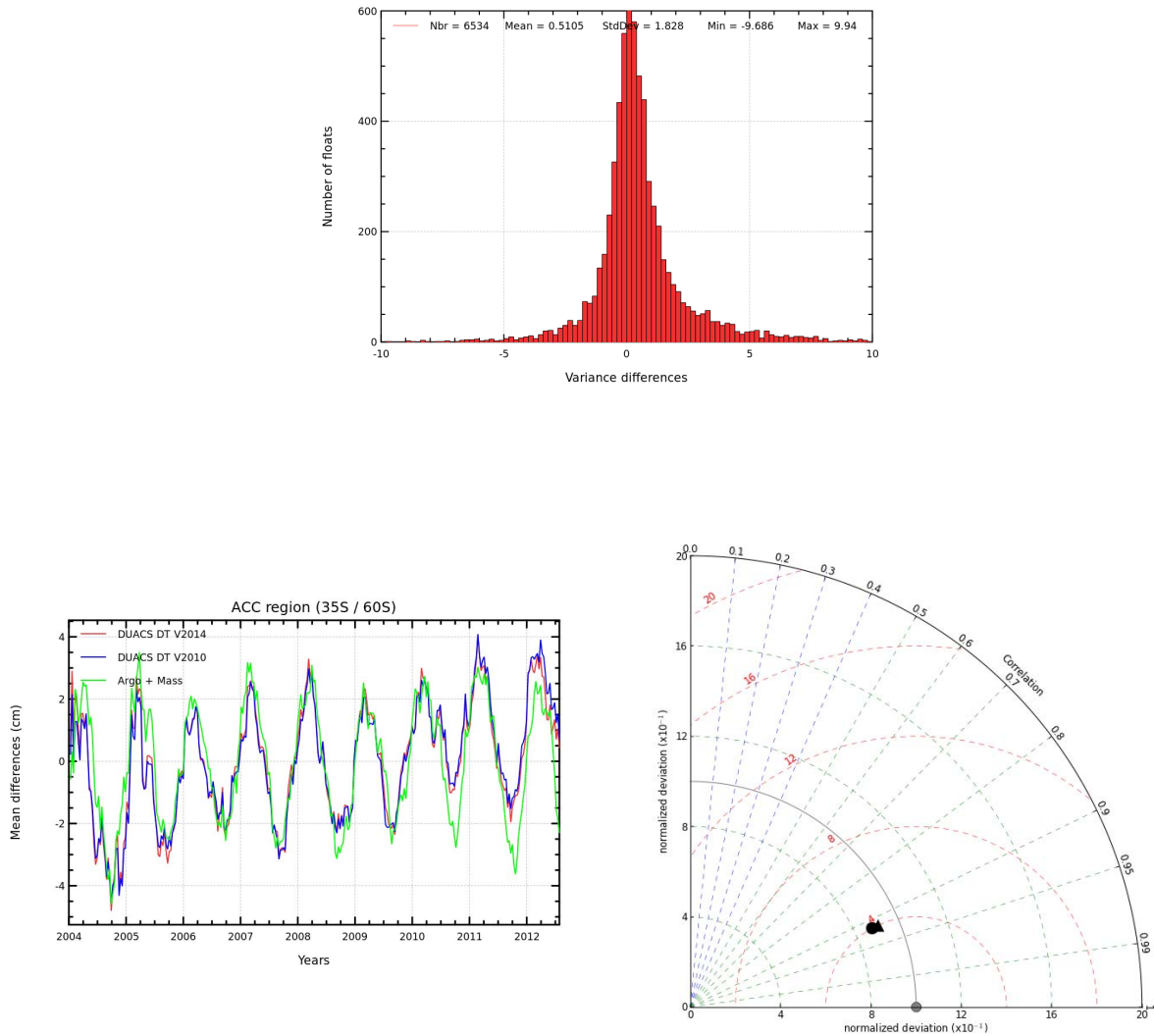


Figure 28: Top: histogram of the variance differences for all time series of each Argo floats: $Var(AVISO\ 2014 - Argo) - Var(AVISO\ 2010 - Argo)$. Bottom: time series of altimetry (AVISO 2014 in red and AVISO 2010 in blue) and summed Argo + mass (GRACE GRGS V2) measurements restricted to the Antarctic Circumpolar Current (left) and associated Taylor diagram (correlation and standard deviation) of these time series (right): the gray dot is the Argo+mass reference value and statistics obtained in the ACC with detrended AVISO 2014 (AVISO 2010) are represented by a triangle (circle).

5.5. Assessment of the ESA Sea Level Climate Change Initiative product

In 2013 has been performed a complete evaluation of the sea level grids computed within the framework of ESA's Climate Change Initiative (CCI) project with respect to in-situ data, both tide gauges and Argo profiles. For this evaluation, a new approach has been used and the signals observed by satellite altimeters have been compared to in-situ sensors separating different time and space scales. The report summarizing the results is appended to the present document as an annex (see Annex 8.3. page 63).

6. Conclusions and futures

Major improvements have been achieved in 2013 in order to improve the validation of altimeter measurements and to better characterize the sensitivity of the method of comparison to various parameters. The GRGS (V2) GRACE dataset of the mass contribution to the sea level is adapted to the global comparison with altimeter measurements (after being colocated with each Argo profile). Together with the steric in-situ dynamic heights from Argo, it provides sea level estimations with the same physical content as the altimeter measurements. The use of this GRACE dataset has required a correction of the Glacial Isostatic Adjustment to take into account the response of the solid Earth to the last deglaciation and thus compare altimetry and GRACE homogeneously. As for the data processing, the reference period used to compute sea level anomalies has been increased to the 2003-2011 period and a new version of the processing chain has been developed so that it is more efficient and it automatically provides diagnoses in the context of systematic Cal/Val analyses. This work is performed in an operational framework which is essential to make this activity durable.

In addition, the estimation of the uncertainty of the method has been improved with the development of a new tool providing statistical estimations of the uncertainty of the trend of the sea level differences. New diagnoses have also been integrated such as the Taylor diagram for the analyses of different wavelengths at global scales and maps of statistics of the differences at regional scales. At last, significant efforts have been made to estimate the sensibility of the method to the pre processing of altimeter data, to the length of the time series, to the spatial sampling of Argo data and also to the reference depth of integration of the in-situ steric dynamic heights. This choice is not clear since the steric MSL referenced to a deep level (1900 dbar) will be preferred in case of assessing the altimeter MSL trend and discuss the altimeter sea level closure budget. However the standard deviation of altimetry is closer to the steric + mass signals with a shallower reference (900 dbar) and the correlation between altimetry and Argo + mass is slightly increased with the 900 dbar time series. In addition, steric MSL trends are more homogeneously distributed compared with altimetry at 900 dbar rather than with deeper references. Thus, in case of assessing the impact of a new altimeter standard in terms of variance, the 900 dbar steric signal may be preferred.

All these evolutions have contributed to better characterize the uncertainty of the method and improve the confidence in the results. The main objectives of the activity have benefited from these improvements: first, the uncertainty associated with the altimeter MSL drift has been reduced and thus, the detection of relative differences is improved and more confidence is attributed in the absolute altimeter MSL drift estimation. Secondly, new altimeter standards are used to improve altimeter products for end-users and the previously mentioned evolutions provide a better detection of their impact. Note that the mass contribution is not systematically used since its trends are little correlated with the altimeter MSL trends at regional scales and the associated uncertainty is relatively high. The analyses performed this year concern several aspects: the impact estimation of new orbit solutions has been used to better determine the uncertainty of the method associated with the detection of trends differences. Other analyses have concerned the impact of a new wet troposphere correction for TOPEX/Poseidon mission, the assessment of the ESA CCI sea level dataset and of the reprocessed SSALTO/DUACS 2014 merged product. The third goal is to detect anomalies in in-situ measurements and thus qualify these data, which is supported by a Coriolis project and not performed in the context of this study (Guinehut et al., 2009 [3]). Our results are strongly dependent of this validation phase since it provides reliable datasets of in-situ measurements.

This work has been presented this year at the OSTST meeting in Boulder ([9]), at the ESA living

.....

planet symposium in Edimburgh and at the Envisat Quality Working Group workshop. In addition, meetings have been organized in May and December 2013 with users and scientific experts of altimetry and in-situ data (CLS, CNES, LEGOS, Noveltis) in order to share the points of view and discuss the methods and the results. These meetings aim at increasing the synergy on the activity. A collaboration has been implemented with orbitography experts from CNES (A. Couhert) aiming at describing in which extent Argo in-situ data can be used to detect orbit errors in the regional mean sea level (publication in preparation).

Major part of the discussed results would not have been obtained with the same confidence without comparison with the results derived from global altimeter internal analyses and from the comparison with tide gauges. The synergy between these approaches is a key element to provide more and more reliable and accurate results, globally as well as regionally. However, the comparison with Argo data could benefit from some improvements which could contribute to reduce the remaining uncertainty and whose integration is planned in 2014. Among them, the use of the new GRACE GRGS V3 dataset of the mass contribution could increase the coherence with altimeter sea level and also reduce the formal error adjustment of the MSL trends. Concerning the computation of these trends, the use of a regional estimation of the GIA correction could be better than a global estimation. Altimetry is currently corrected from the high frequencies of the Dynamical Atmospheric Correction (DAC) and the impact of correcting also the low frequencies should be analyzed. Moreover the development of new diagnoses of comparison will contribute to better characterize the differences at inter-annual and annual frequencies at global and regional scales and better estimate the impact of new altimeter standards. At last, these techniques will be adapted to perform quality assessment of new missions (AltiKa, Sentinel 3) and it will be interesting to determine whether the method can contribute to validate SAR measurements.

7. References

References

- [1] Ablain M., G. Larnicol, Y. Faugere, A. Cazenave, B. Meyssignac, N. Picot, J. Benveniste. Error Characterization of altimetry measurements at Climate Scales. OSTST 2012, Venice.
- [2] Chen J.L., C.R. Wilson, D.P. Chambers, R.S. Nerem, B.D. Tapley. Seasonal global water mass budget and mean sea level variations. *Geophys. Res. Letters*. Vol. 25; No. 19; pp 3555-3558, 1998.
- [3] Guinehut S., C. Coatanoan, A.-L. Dhomps, P.-Y. Le Traon and G. Larnicol: On the use of satellite altimeter data in Argo quality control, *J. Atmos. Oceanic. Technol.*, Vol. 26 No 2. pp 395-402, 2009.
- [4] Johnson and Chambers 2013, *Jour. Of Geophys. Res.: Oceans*, Vol. 118, 1-13, doi:10.1002/jgrc.20307.
- [5] Labroue, S., 2007 : RA2 ocean and MWR measurement long term monitoring, 2007 report for WP3, Task 2 - SSB estimation for RA2 altimeter. Contract 17293/03/I-OL. CLS-DOS-NT-07-198, 53pp. CLS Ramonville St. Agne.
- [6] Legeais J.F., Ablain M. 2011: CalVal altimetry / Argo annual report. Validation of altimeter data by comparison with in-situ T/S Argo profiles. Ref. CLS/DOS/NT/10-305. Contrat SALP-RP-MA-EA-22045-CLS.
- [7] Legeais J.F., Ablain M. 2012: CalVal altimetry / Argo annual report. Validation of altimeter data by comparison with in-situ T/S Argo profiles. Ref. CLS/DOS/NT/12-261. Contrat SALP-RP-MA-EA-22176-CLS.
- [8] Lemoine J.-M. and H. Capedeville. A corrective model for Jason-1 DORIS Doppler data in relation to the South Atlantic Anomaly. *J. Geod.* (2006) 80: 507-523. DOI 10.1007/s00190-006-0068-2.
- [9] Prandi P, G. Valladeau, M. Ablain, J.F. Legeais, N. Picot, 2013: Analysis of altimetry errors using in-situ measurements: tide gauges and Argo profiles. Oral presentation, OSTST, Boulder.
- [10] Roemmich, D. and J. Gilson, 2009: The 2004-2008 mean and annual cycle of temperature, salinity, and steric height in the global ocean from the Argo Program. *Progress in Oceanography*, 82, 81-100.
- [11] Schaeffer P., Y. Faugère, JF Legeais, A. Ollivier, T. Guinle and N. Picot. The CNES-CLS11 Global Mean Sea Surface computed from 16 years of satellite altimeter data. *Marine Geodesy* 2012, volume35. Suppl. issue on OSTM/Jason-2 applications.
- [12] Tamisiea M. and J. Mitrovica, 2011. The Moving Boundaries of Sea Level Change. *Understanding the Origins og Geographic Variability. Oceanography*, Vol. 24, No 2.
- [13] Roinard H., and Philips S.: Jason-1 validation and cross calibration activities (annual report 2013). Ref. CLS/DOS/NT/13-226. Contrat SALP-RP-MA-EA-22269-CLS.

- [14] Valladeau G., J.-F. Legeais, M. Ablain, S. Guinehut and N. Picot, 2012: Comparing altimetry with tide gauges and Argo profiling floats for data quality assessment and Mean Sea Level studies. *Marine Geodesy* 2012, volume35. Suppl. issue on OSTM/Jason-2 applications.

8. Annexes

8.1. Annex: Corrections applied for altimeter SSH computation

All the corrections applied on SSH for TOPEX/Poseidon, Jason-1, Jason-2 and Envisat space altimetric missions are summarized in the following table:

Orbits and corrections	TOPEX/Poseidon	Jason-1	Jason-2	Envisat
Orbit	GSFC POE (09/2008), ITRF2005+Grace	CNES POE (GDR-C standards until cycle 374, GDR-D standards from cycle 500 onwards)	CNES POE (GDR-D standards)	CNES POE (GDR-C standards)
Mean Sea Surface (MSS)	MSS CNES/CLS 2011	MSS CNES/CLS 2011	MSS CNES/CLS 2011	MSS CNES/CLS 2011
Dry troposphere	ECMWF model computed	ECMWF model computed	ECMWF model computed	ECMWF model computed
Wet troposphere	TMR with drift correction [Scharroo et al. 2004] and empirical correction of yaw maneuvers [2005 annual validation report]	Jason-1 radiometer (JMR)	Jason-2 radiometer (AMR)	MWR (corrected from side lobes) + new corrected files
Ionosphere	Filtered dual-frequency altimeter range measurements (for TOPEX) and Doris (for Poseidon)	Filtered dual-frequency altimeter range measurements	Filtered dual-frequency altimeter range measurements	Dual-Frequency updated with S-Band SSB (< cycle 65) GIM model + global bias of 8 mm (>= cycle 65)
Sea State Bias	Non parametric SSB (for TOPEX), BM4 formula (for Poseidon)	Non parametric SSB (GDR product)	Non parametric SSB (GDR product)	Updated homogeneous to GDR-C (Labroue, 2007 [5])
Ocean and loading tides	GOT4.7 (S1 parameter is included)	GOT4.7 (S1 parameter is included)	GOT4.8	GOT4.7 (S1 parameter is included)
Solid Earth tide	Elastic response to tidal potential [Cartwright and Tayler, 1971] [Cartwright and Edden, 1973]	Elastic response to tidal potential [Cartwright and Tayler, 1971] [Cartwright and Edden, 1973]	Elastic response to tidal potential [Cartwright and Tayler, 1971] [Cartwright and Edden, 1973]	Elastic response to tidal potential [Cartwright and Tayler, 1971] [Cartwright and Edden, 1973]
				.../...

Orbits and corrections	TOPEX/Poseidon	Jason-1	Jason-2	Envisat
Pole tide	[Wahr,1985]	[Wahr,1985]	[Wahr,1985]	[Wahr,1985]
Combined atmospheric correction	High Resolution Mog2D Model [Carrère and Lyard, 2003] + inverse barometer computed from ECMWF model (rectangular grids)	High Resolution Mog2D Model [Carrère and Lyard, 2003] + inverse barometer computed from ECMWF model (rectangular grids)	High Resolution Mog2D Model [Carrère and Lyard, 2003] + inverse barometer computed from ECMWF model (rectangular grids)	High Resolution Mog2D Model [Carrère and Lyard, 2003] + inverse barometer computed from ECMWF model (rectangular grids)
Specific corrections	Doris/Altimeter ionospheric bias, TOPEX-A/TOPEX-B bias and TOPEX/Poseidon bias	Jason-1 / T/P global MSL bias	Jason-2 / T/P global MSL bias	USO correction included in the range after V2.1 reprocessing + PTR ¹

Table 1: *Corrections applied for altimetric SSH calculation*¹External corrections available on ESA website near V2.1 GDR products

8.2. A contribution to the sea level closure budget: global steric sea level estimation from Argo



ESA Sea Level CCI

WP4300: A contribution to the sea level closure budget: global Steric Sea level estimation from Argo

Reference: Cliquez ici pour taper du texte.

Nomenclature: Cliquez ici pour taper du texte.

Issue: 1. 0

Date: Nov. 8, 13





Chronology Issues:			
Issue:	Date:	Reason for change:	Author
1.0	2013-11-08	Initialization	JF Legeais

People involved in this issue:		
Written by (*):	JF Legeais	Date + Initials:(visa or ref)
Checked by (*):	M. Ablain	Date + Initial:(visa ou ref)
Approved by (*):		Date + Initial:(visa ou ref)
Application authorized by (*):		Date + Initial:(visa ou ref)

**In the opposite box: Last and First name of the person + company if different from CLS*

Index Sheet:	
Context:	
Keywords:	Oceanography, sea level
Hyperlink:	

Distribution:		
Company	Means of distribution	Names
CLS	Notification	



List of tables and figures

List of tables:

Aucune entrée de table d'illustration n'a été trouvée.

List of figures:

Figure 1: Number of floats according to their mean maximum pressure over their lifetime2

Figure 2: Percentage of the floats whose mean maximum pressure is smaller than a given threshold2

Figure 3: Argo floats whose mean max depth is at least (deeper) the labelled reference depth (left) and Argo floats whose mean max depth is shallower than the labelled reference depth (right). For a given reference depth, the left map display the floats taken into account and the associated right map show the floats which will not be used.4

Figure 4: Steric global mean sea level trends over 2005-2012 with the altimeter mean sea level (AVISO SSALTO/DUACS) which is masked, filtered and interpolated at monthly intervals as for in-situ maps. An arbitrary bias is used. The Glacial Isostatic Adjustment (GIA) is not taken into account in this altimeter time series.....6

Figure 5: Global mean sea level trends over Jan. 2005 - Aug. 2012 of the steric + mass (GRACE GRGS V2) contributions with various reference depth of integration of the steric heights. The added altimeter mean sea level (AVISO SSALTO/DUACS) is masked, filtered and interpolated at monthly intervals as for in-situ maps.7

Figure 6: Global mean sea level trends over Jan. 2005 - Aug. 2012 of the differences between the altimeter mean sea level (AVISO SSALTO/DUACS) and the steric + mass (GRACE GRGS V2) contributions with various reference depth of integration of the steric heights. The altimeter data is masked, filtered and interpolated at monthly intervals as for in-situ maps. A -0.3 mm/yr and -0.9 mm/yr GIA effect is applied on the altimetry and mass contribution respectively.8

Figure 7: Detrended steric + mass (GRACE GRGS V2) contributions and altimeter (AVISO SSALTO/DUACS) mean sea level time series over Jan. 2005 - Aug. 2012 with various reference depth of integration of the steric heights. Altimetry is masked, filtered and interpolated at monthly intervals as for in-situ maps.9

Figure 8: Taylor diagram of the detrended steric + mass (GRACE GRGS V2) contributions compared with the altimeter (AVISO SSALTO/DUACS) mean sea level time series over Jan. 2005 - Aug. 2012 with various reference depth of integration of the steric heights. Altimetry is masked, filtered and interpolated at monthly intervals as for in-situ maps.9

Figure 9: Regional steric and altimeter (AVISO SSALTO/DUACS, bottom left) mean sea level trends over Jan. 2005 -Dec. 2012 with various reference depths of integration of the steric heights. Altimetry is masked and filtered as for in-situ maps. 10

Figure 10: Regional mean sea level trend differences between the steric sea level and altimetry (AVISO SSALTO/DUACS) over Jan. 2005 -Dec. 2012 with various reference depths of integration of the steric heights. Altimetry is masked and filtered as for in-situ maps. Maps are centered. 11

Figure 11: Global weekly (red) and monthly (magenta) altimeter MSL from AVISO SSALTO/DUACS products (DUACS Delayed Time, DDT) and associated MSL masked and filtered as for in-situ steric maps at weekly (blue) and monthly (cyan) intervals. 12

Figure 12: Regional altimeter MSL trends over 2005-2012 (right) and regional altimeter trends masked and filtered as for in-situ steric maps (left) 12

Figure 13: Map of the Dec. 17, 2008 mean sea level from DUACS (top left) and reconstructed mean sea level from the Dec. 15, 2008 (top right) and their difference (bottom)..... 13



Figure 14: Global altimeter (AVISO SSALTO/DUACS referenced over the Argo in-situ temporal reference: 2003-2011) and reconstructed altimeter mean sea level over the Jan. 2005 - Jun. 2012 period. 13

Figure 15: Taylor diagram of the detrended reconstructed altimeter MSL time series compared with original detrended altimeter MSL over Jan. 2005 - Jun. 2012 period. Altimetry is masked, filtered and interpolated at monthly intervals as for the reconstructed dataset. 14

Figure 16: Altimeter MSL trends masked and filtered as for in-situ maps, based on weekly maps with the same inter annual reference as Argo maps (2003-2011) (top left). Reconstructed altimeter MSL trends based on monthly maps (top right). Difference between the original and reconstructed altimeter MSL trends..... 15

List of items to be confirmed or to be defined

Lists of TBC:

Aucune entrée de table des matières n'a été trouvée.

Lists of TBD:

Aucune entrée de table des matières n'a été trouvée.

Applicable documents

AD 1 Sea level CCI project Management Plan
CLS-DOS-NT-10-013

Reference documents

RD 1 Manuel du processus Documentation
CLS-DOC



List of Contents

1. Introduction.....	1
2. Data and methodology.....	1
2.1. Data description.....	1
2.2. Methodology.....	1
3. Impact of the reference depth of the Argo dynamic heights.....	1
3.1. Introduction.....	1
3.2. Impact on the global Argo sampling.....	2
3.3. Impact on the regional Argo distribution.....	2
4. Computation of a steric sea level product from Argo.....	5
4.1. Introduction.....	5
4.2. Monthly maps of the steric mean sea level.....	5
5. Assessment of the steric mean sea level.....	5
5.1. Global analyses.....	5
5.1.1. Global steric mean sea level.....	5
5.1.2. Annual signal.....	6
5.1.3. Comparison with altimetry and mass contribution.....	7
5.2. Regional steric mean sea level trends.....	10
5.3. Error of the method.....	11
5.3.1. Impact of the spatial mask and filtering.....	11
5.3.2. Impact of the mapping method.....	12
6. Conclusion.....	15



1. Introduction

In the framework of the SL-CCI WP4000 task, the sea level closure budget is analyzed through the comparison of various contributions to the sea level. One of these contributions is the steric sea level associated with the thermohaline expansion of the water column.

In this document, the computation of a steric sea level is described based on the Argo dataset. The physical content of this product is analyzed and compared with other datasets (altimetry minus mass contribution from GRACE).

2. Data and methodology

2.1. Data description

Temperature and Salinity profiles measured by Argo floats are retrieved from the Coriolis GDAC database (<http://www.coriolis.eu.org/>) as in March 2013. Then a global quality control is performed for each profile by comparison with the altimeter AVISO SSALTO/DUACS sea level products. 45 floats are listed as floats to be checked (feedback to the Coriolis GDAC) and are thus not used in this study and it remains 8189 floats.

The steric mean sea level products computed in this study are then compared with other datasets and we use the mass contribution to the sea level derived from the GRACE GRGS V2 dataset.

2.2. Methodology

For each Argo T/S profile, a steric Dynamic Height Anomaly (DHA) is computed using a specific reference depth. The impact of the choice of this reference depth on the Argo sampling is first analyzed. Then monthly maps of the steric sea level are computed with different reference depths in order to estimate how much steric signal is missed with the choice of a given reference depth. The results and the differences between the different steric datasets are then discussed.

3. Impact of the reference depth of the Argo dynamic heights

3.1. Introduction

The Argo network of in-situ profiling floats provides Temperature and salinity (T/S) measurements through the water column which are widespread over almost the global open ocean since 2004. Each float acquires T/S profiles every 10 days. Dynamic heights are derived from the Argo T/S profiles as the integration of the T/S measurements through the water column.

This integration requires a reference level (pressure) and,

- The deeper the reference level, the more information from the T/S profiles is taken into account
- But the more T/S profiles are not used (those who don't reach the reference level)

Thus, we first aim at determining the impacts of a given reference depth of integration on the global Argo sampling and on the regional Argo distribution.



3.2. Impact on the global Argo sampling

Figure 1 indicates that among the 8189 floats, most of them (3506 or 43%) have a mean maximum pressure between 1900 dbar and 2000 dbar.

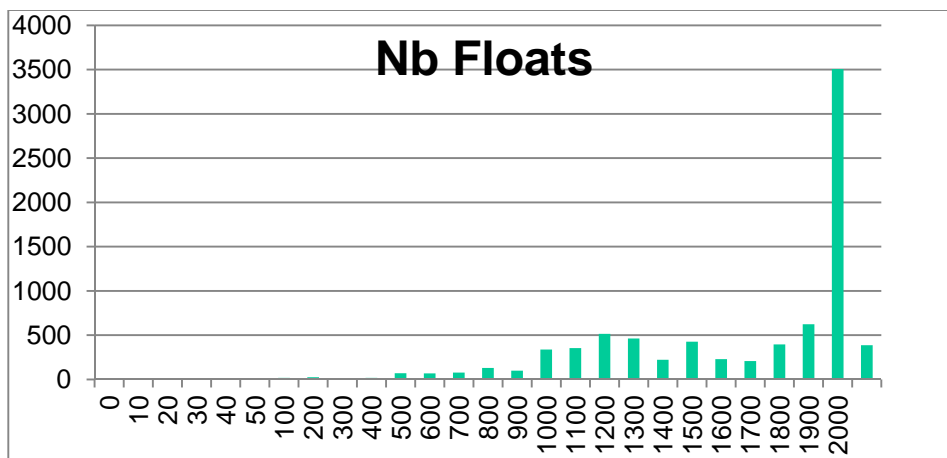


Figure 1: Number of floats according to their mean maximum pressure over their lifetime

All the floats whose mean maximum pressure does not reach the chosen reference level will not be used. Thus, Figure 2 shows that:

- 6% of the floats are missed with a reference level at 900 dbar
- 21% of the floats are missed with a reference level at 1200 dbar
- 29% of the floats are missed with a reference level at 1400 dbar
- 52% of the floats are missed with a reference level at 1900 dbar

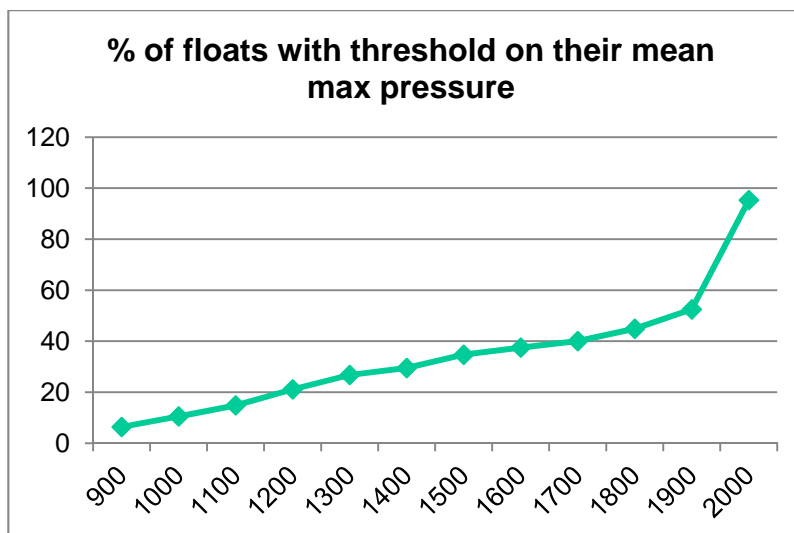


Figure 2: Percentage of the floats whose mean maximum pressure is smaller than a given threshold

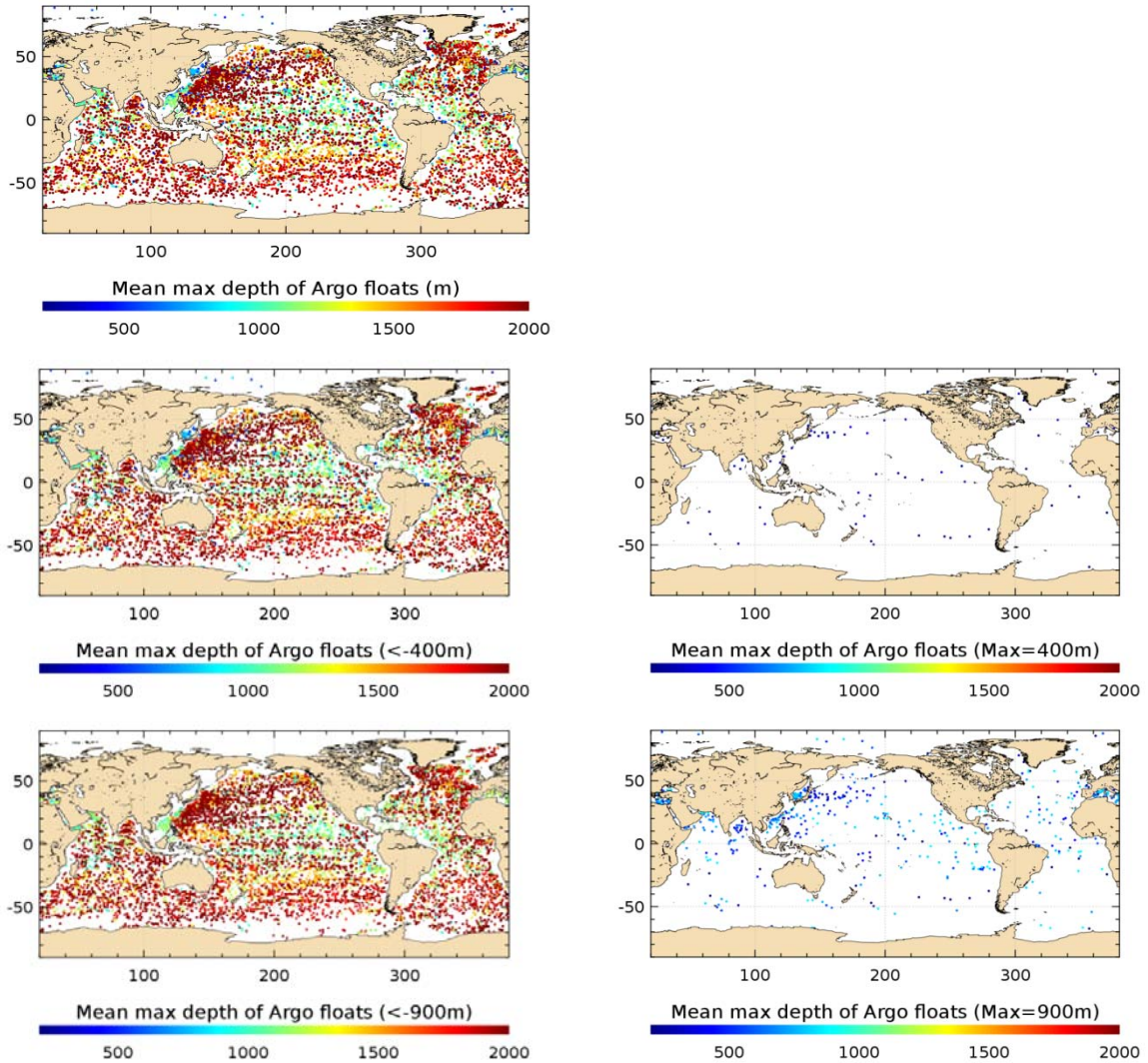
3.3. Impact on the regional Argo distribution

We want to determine how the spatial distribution of the floats is affected by the choice of the reference level. For a given reference depth, Figure 3 displays on the left maps the floats taken into account and the associated maps on the right show the floats which will not be used (mean max depth shallower than the reference).



Floats with a mean maximum pressure less than 900 dbar are mainly located in the Pacific western boundary current (Kuroshio) and in the Mediterranean Sea.

Floats with a mean maximum pressure between 900 dbar and 1400 dbar are mainly located at equatorial latitudes of all ocean basins. In these areas, the water column is very stratified and the steric signal is thus confined in the upper layer. Thus, with a reference depth of 1400 dbar compared with 900 dbar, the water column will be better sampled over the global ocean (which improves the retrieved steric signal) but we will miss a significant part of this steric signal at equatorial latitudes.



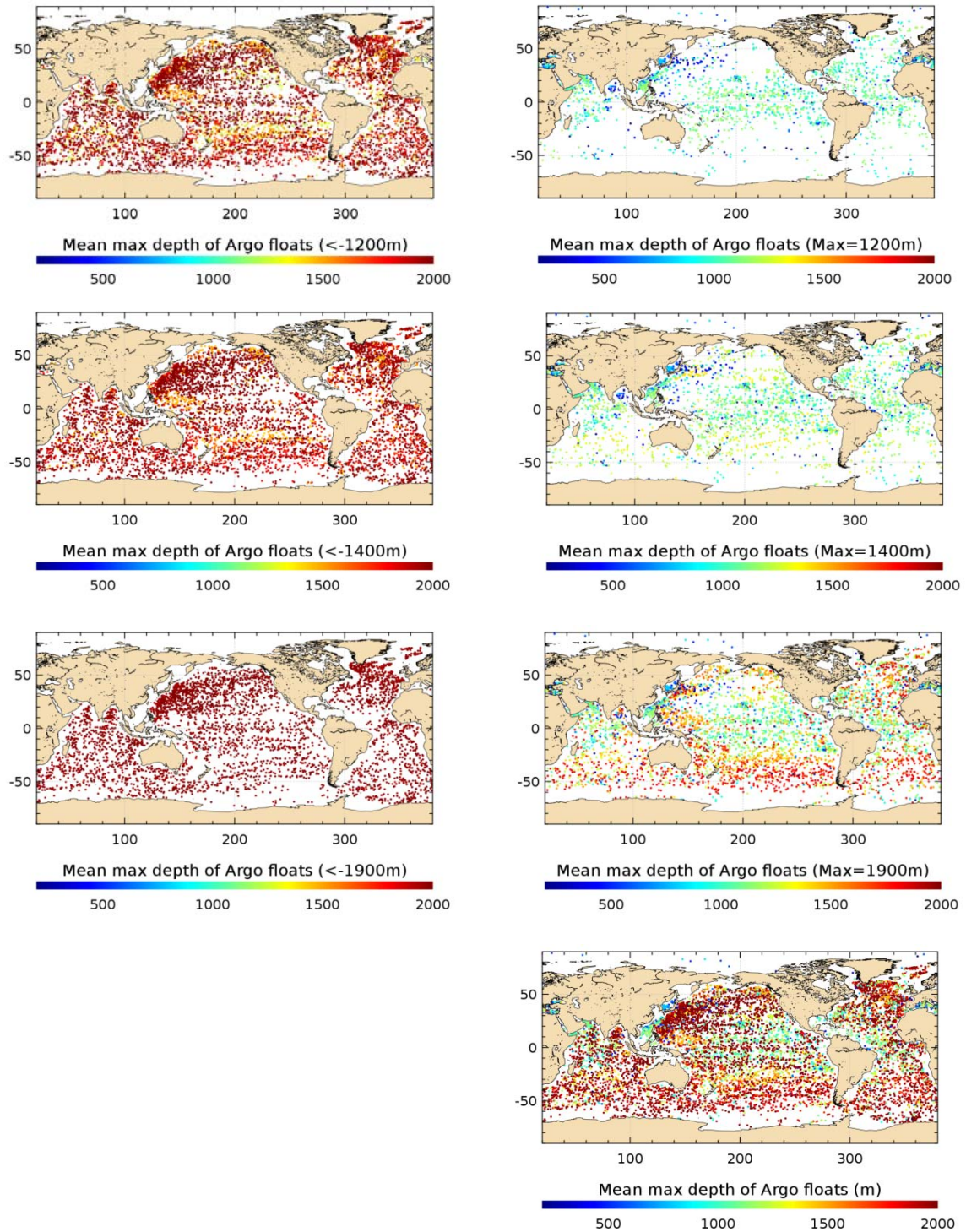


Figure 3: Argo floats whose mean max depth is at least (deeper) the labelled reference depth (left) and Argo floats whose mean max depth is shallower than the labelled reference depth (right). For a given reference depth, the left map display the floats taken into account and the associated right map show the floats which will not be used.



4. Computation of a steric sea level product from Argo

4.1. Introduction

The former section provides statistical information on the global and regional sampling of the Argo floats according to the choice of a reference level of integration. But it has to be determined how much steric signal is affected. Thus, maps of the Argo steric dynamic heights are computed with different reference levels. We choose to compute steric MSL with three different reference levels: 900 dbar, 1200 dbar and 1900 dbar. This choice is based on the previous impact analysis of the Argo sampling and it also takes into account the mean dynamic heights already available for a few different reference depths.

4.2. Monthly maps of the steric mean sea level

Three datasets of Argo steric dynamic heights are computed from the T/S profiles. For each profile, a steric Dynamic Height Anomaly (DHA) is computed using the reference level and a contemporaneous mean dynamic height (also called synthetic climatology).

Then monthly maps of the Argo steric MSL are computed with the three different reference levels via optimal interpolation of the in-situ observations, including:

- Spatial mask of the data based on the same spatial coverage of the steric MSL products derived from the SCRIPPS institution (about $\pm 66^\circ$ without coastal and enclosed areas such as the Indonesian through flow, the Gulf of Mexico, the Mediterranean Sea)
- Correlation scales used in the optimal interpolation are 45 days and latitudinally varying spatial scales: 780-1250km (meridional) and 780-1750km (zonal)
- A priori error = 50% of the altimeter variability

5. Assessment of the steric mean sea level

5.1. Global analyses

5.1.1. Global steric mean sea level

Figure 4 shows the global steric MSL time series and their trends for the 3 different reference depths. An arbitrary bias is used.

- The contribution of the 1200 / 1900 dbar layer has a very small impact on the steric MSL trend. This suggests that this layer does not contribute to the temporal increase of the steric sea level. However, we have previously shown that a great part of the floats within this layer depth are located at equatorial latitudes where the water column is very stratified and the steric signal is thus confined in the upper layer. This could explain this small trend difference between 1200 dbar and 1900 dbar.
- Looking at the different curves, the annual signal is getting deteriorated:
 - As time goes backwards before 2007,
 - As the reference depth is getting deeper

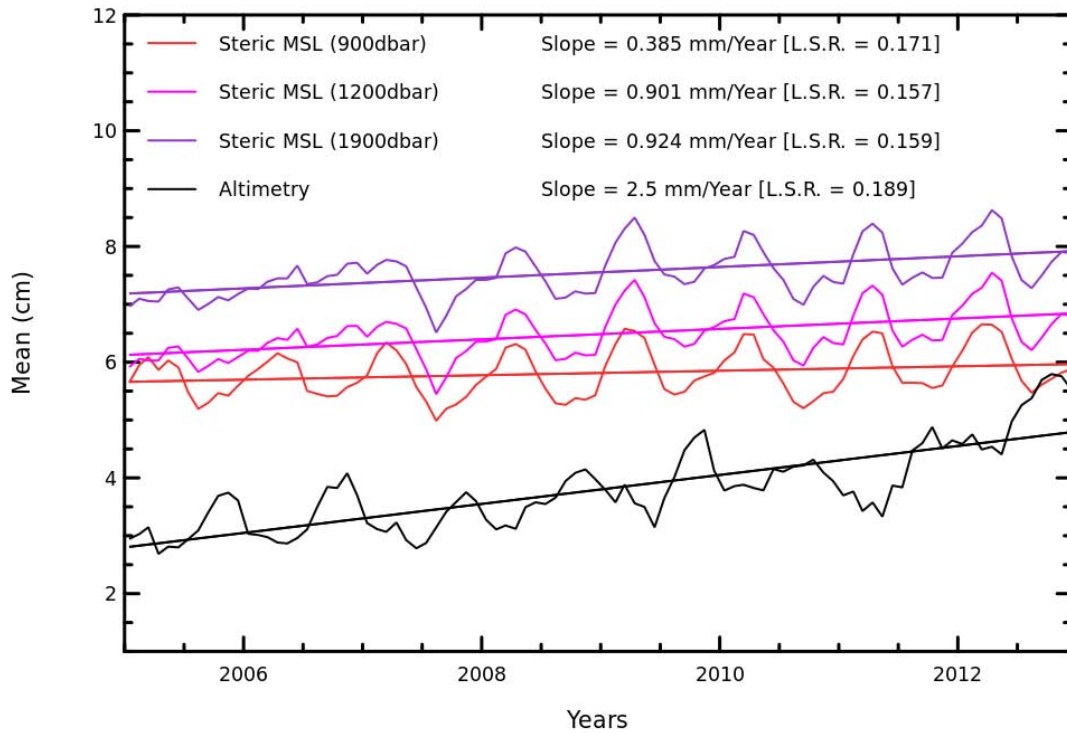


Figure 4: Steric global mean sea level trends over 2005-2012 with the altimeter mean sea level (AVISO SSALTO/DUACS) which is masked, filtered and interpolated at monthly intervals as for in-situ maps. An arbitrary bias is used. The Glacial Isostatic Adjustment (GIA) is not taken into account in this altimeter time series.

5.1.2. Annual signal

The amplitude and phase of the annual steric signal is compared between our products and the bibliography over different periods and with different reference depths.

Steric annual signal	Amplitude (mm)	Phase (deg) (ref Jan. 1st)
This study 900 dbar (2005-2012)	4.9	84
This study 1200 dbar (2005-2012)	3.4	81
This study 1900 dbar (2005-2012)	3.3	81
This study 900 dbar (2004-2008)	4.0	91
Llovel/Guinehut 2010 (CLS version 900 dbar, 2004-2008)	3.5	95
Llovel/Guinehut 2010 (SCRIPPS version, 2004-2008)	4.5	100
Llovel/Guinehut 2010 (IPRC version, 2004-2008)	4.7	98



This study 900 dbar (2004-2007)	3.8	90
Leuliette & Miller 09 (900 dbar, 2004-2007)	3.9	90
Lombard et al. 2007 (J1 - GRGS, 08-2002 / 04-2006)	5.6	70

Table 1: Comparison of the amplitude and phase of the annual signal of the steric mean sea level with various studies over different period and with different reference depths

5.1.3. Comparison with altimetry and mass contribution

Altimeter and steric sea levels are different since altimetry includes the mass contribution to the sea level whereas the steric signal only includes the thermohaline expansion of the water column. Thus we compare altimetry with the sum of our steric products with the mass contribution derived from the GRACE GRGS V2 products.

Contrary to Figure 4, Figure 5 shows that the signals are now in phase and the time series are very similar to each other.

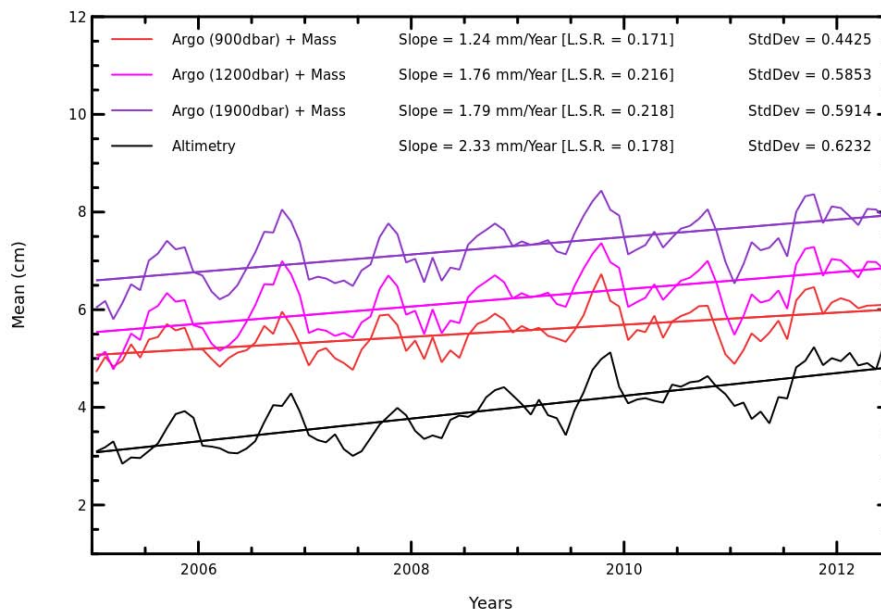


Figure 5: Global mean sea level trends over Jan. 2005 - Aug. 2012 of the steric + mass (GRACE GRGS V2) contributions with various reference depth of integration of the steric heights. The added altimeter mean sea level (AVISO SSALTO/DUACS) is masked, filtered and interpolated at monthly intervals as for in-situ maps.

Figure 6 shows the time series of the differences between altimetry and steric plus mass signals. The Glacial Isostatic Adjustment (GIA) effects are taken into account for altimetry (-0.3 mm/yr) and for the mass contribution (-0.9 mm/yr).

The trend of the differences is smaller with the deeper steric contributions (0.5 mm/yr with a 1900 dbar reference and 1.1 mm/yr with a 900 dbar reference).



In the context of using these steric products to assess the quality of altimeter products, the steric MSL referenced to 1900 dbar will be preferred in case of assessing the altimeter MSL trend and discuss the altimeter sea level closure budget.

In addition, in spite of a greater standard deviation with a 900dbar reference, the formal error adjustment of the trend of the differences is smaller with the 900 dbar reference (0.12 mm/yr) than with a deeper reference (0.15 mm/yr with a 1900 dbar reference). This suggests that the variability of the altimeter MSL is better reproduced with the steric signal referenced at 900 dbar. Thus, in case of assessing the impact of a new altimeter standard in terms of variance, the 900 dbar steric signal may be preferred.

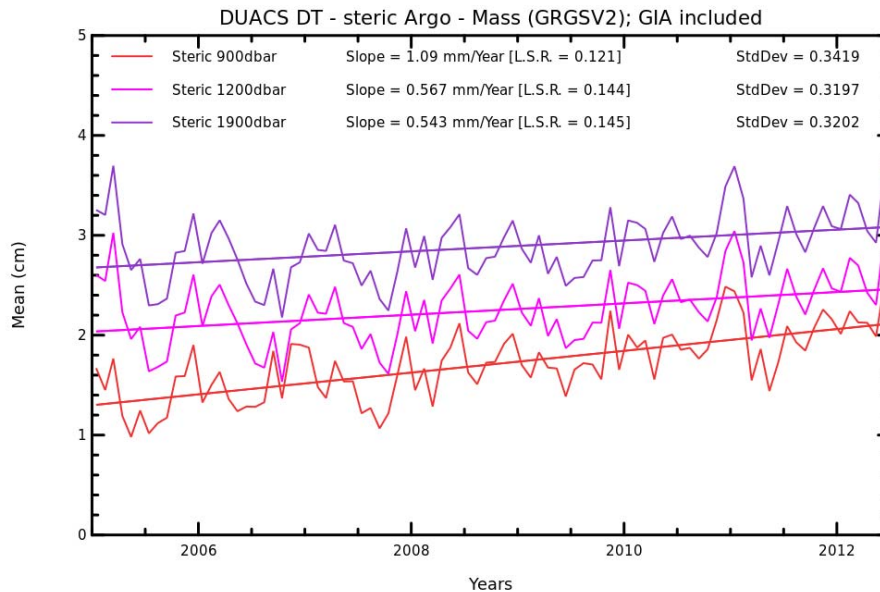


Figure 6: Global mean sea level trends over Jan. 2005 - Aug. 2012 of the differences between the altimeter mean sea level (AVISO SSALTO/DUACS) and the steric + mass (GRACE GRGS V2) contributions with various reference depth of integration of the steric heights. The altimeter data is masked, filtered and interpolated at monthly intervals as for in-situ maps. A -0.3 mm/yr and -0.9 mm/yr GIA effect is applied on the altimetry and mass contribution respectively.

To confirm this impact on the variance, the comparison with the altimeter MSL is now performed in terms of the Taylor distance (correlation and standard deviation of the time series) after removing the trend of the time series in order to estimate the impact of the reference depth on the correlation only in terms of variance and without the impact of the long-term evolution.

Figure 7 indicates that the standard deviation of the steric + mass signals is closer to the one of altimetry with the 900 dbar reference, which confirms the asset of this dataset in terms of variance.

The Taylor distance is computed (Figure 8) between these detrended steric + mass time series and the altimeter MSL, showing that the standard deviation of altimetry is closer to the 900dbar steric MSL and the correlation between altimetry and Argo + Mass is slightly increased with the 900dbar time series.

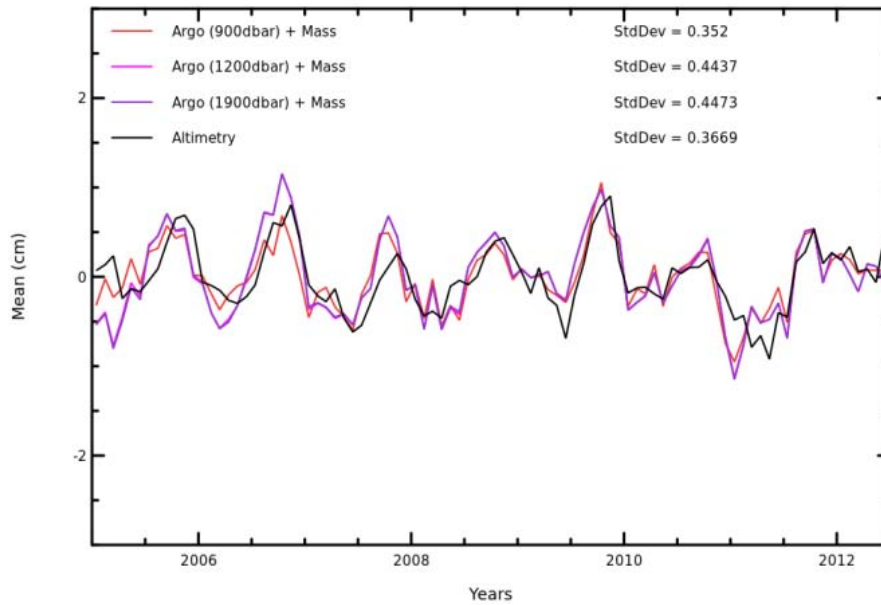


Figure 7: Detrended steric + mass (GRACE GRGS V2) contributions and altimeter (AVISO SSALTO/DUACS) mean sea level time series over Jan. 2005 - Aug. 2012 with various reference depth of integration of the steric heights. Altimetry is masked, filtered and interpolated at monthly intervals as for in-situ maps.

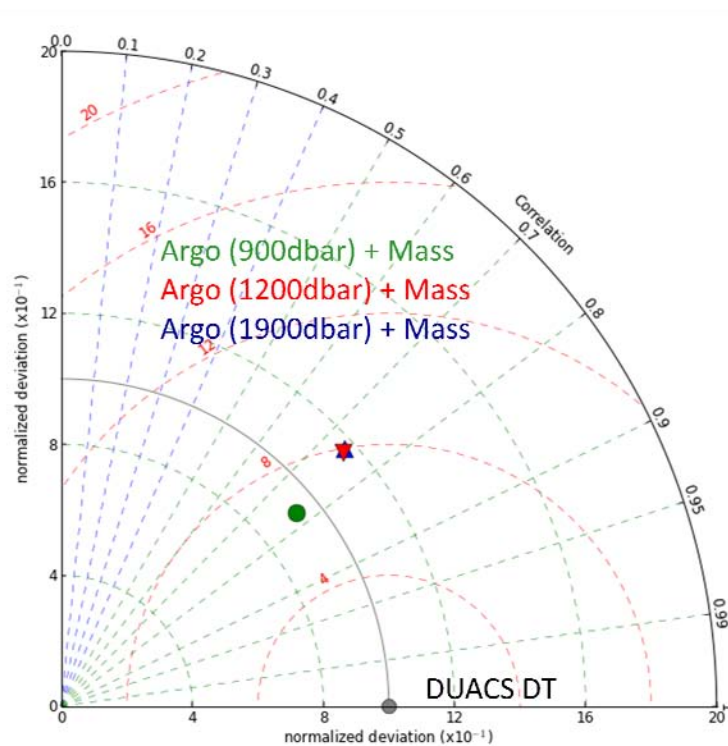


Figure 8: Taylor diagram of the detrended steric + mass (GRACE GRGS V2) contributions compared with the altimeter (AVISO SSALTO/DUACS) mean sea level time series over Jan. 2005 - Aug. 2012 with various reference depth of integration of the steric heights. Altimetry is masked, filtered and interpolated at monthly intervals as for in-situ maps.



5.2. Regional steric mean sea level trends

Figure 9 shows that the regional steric mean sea level trends are globally very similar to the altimeter mean sea level trends.

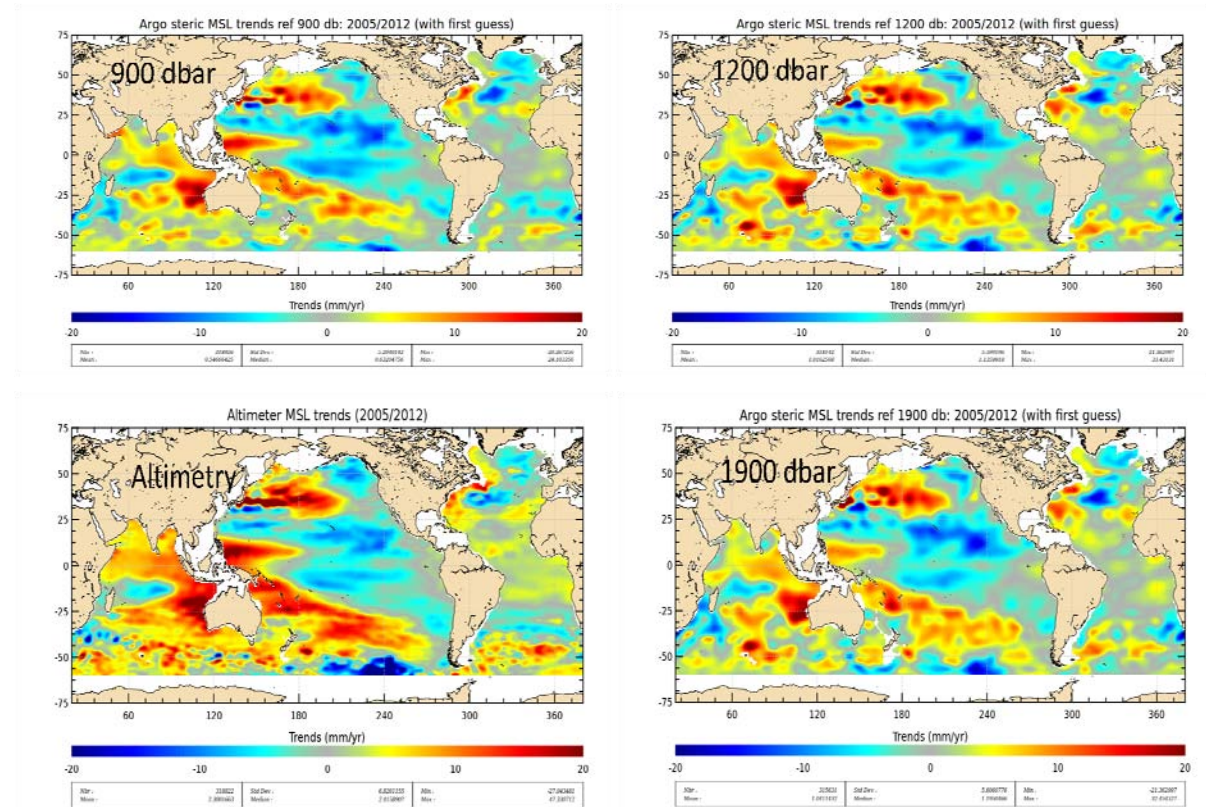


Figure 9: Regional steric and altimeter (AVISO SSALTO/DUACS, bottom left) mean sea level trends over Jan. 2005 -Dec. 2012 with various reference depths of integration of the steric heights. Altimetry is masked and filtered as for in-situ maps.

The centered maps of the differences between steric and altimeter MSL trends are shown on Figure 10. As already shown on global analyses, the regional steric - altimeter differences are very close to each other with the use of the 1200 dbar and 1900 dbar reference level.

Some differences are observed between these both similar maps and the one with the 900 dbar reference. As indicated by black ellipses, main differences are observed in the western Pacific ocean, in the South-East Pacific ocean, in the North-West and South-West Atlantic ocean.

The global standard deviation of these maps of trend differences are:

- 1.21 mm/yr with the 900 dbar reference
- 1.38 mm/yr with the 1200 dbar reference
- 1.39 mm/yr with the 1900 dbar reference

Thus, in addition to what has been shown for the global analysis (see previous section), the steric MSL trends are more homogeneously distributed compared with altimetry at 900dbar rather than with deeper references.

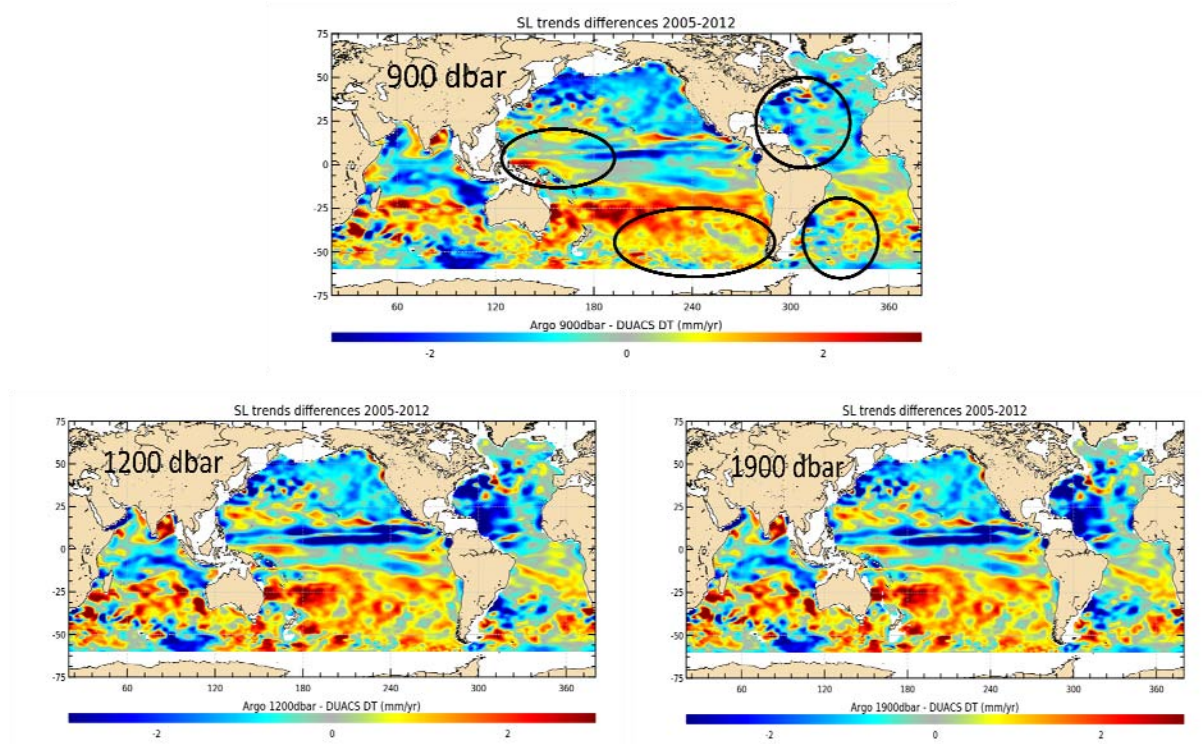


Figure 10: Regional mean sea level trend differences between the steric sea level and altimetry (AVISO SSALTO/DUACS) over Jan. 2005 -Dec. 2012 with various reference depths of integration of the steric heights. Altimetry is masked and filtered as for in-situ maps. Maps are centered.

5.3. Error of the method

5.3.1. Impact of the spatial mask and filtering

Figure 11 and Figure 12 show the impact of the regional mask and the filtering of the MSL as it is performed for the steric maps. The amplitude of the annual signal is slightly affected but the phase remains unchanged. Small geographical structures are filtered and it only remains signals with wavelengths higher than a few hundreds of kms.

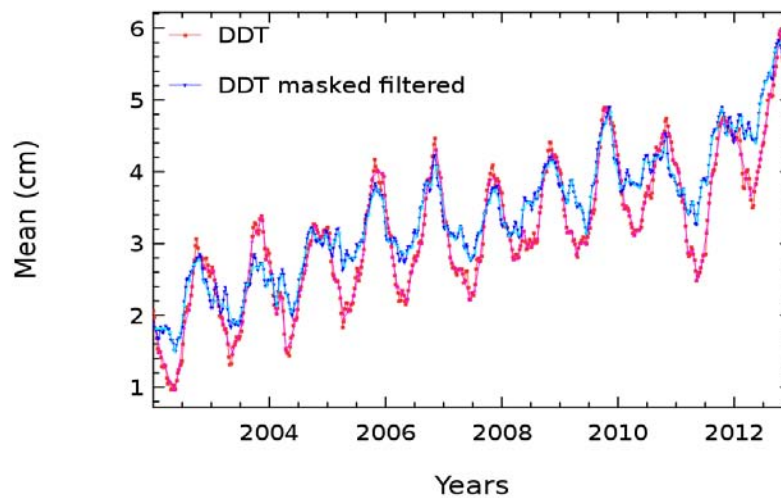




Figure 11: Global weekly (red) and monthly (magenta) altimeter MSL from AVISO SSALTO/DUACS products (DUACS Delayed Time, DDT) and associated MSL masked and filtered as for in-situ steric maps at weekly (blue) and monthly (cyan) intervals.

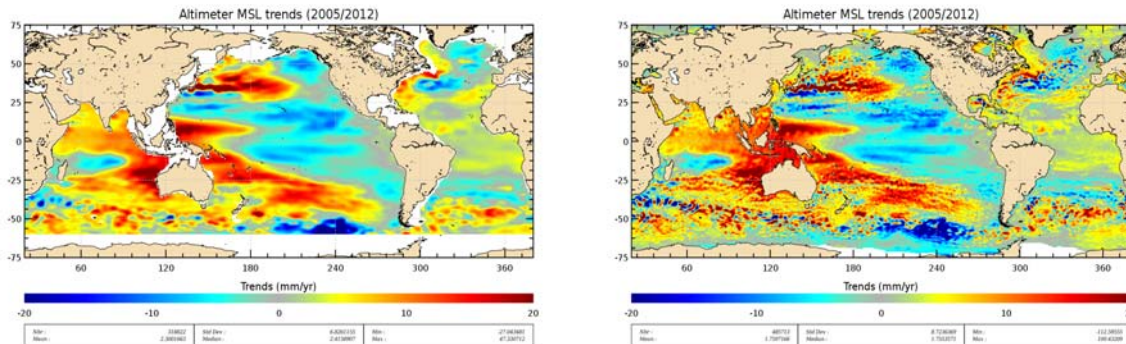


Figure 12: Regional altimeter MSL trends over 2005-2012 (right) and regional altimeter trends masked and filtered as for in-situ steric maps (left)

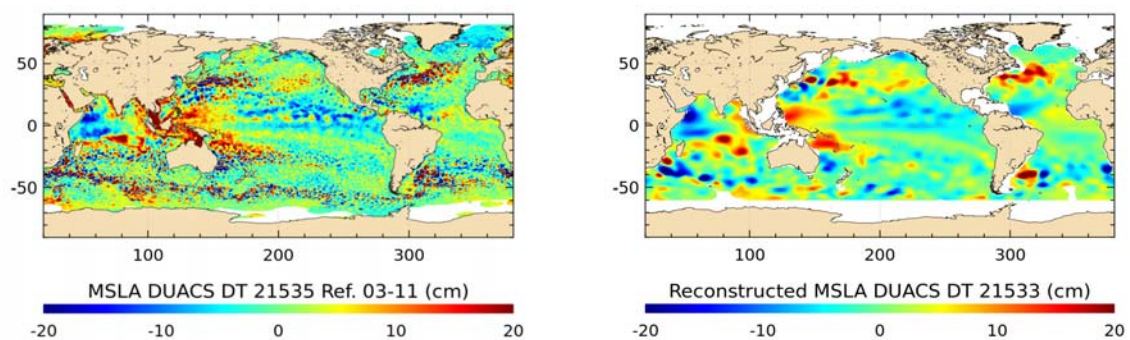
5.3.2. Impact of the mapping method

In order to quantify the error associated with the mapping method (and the related impact of the coverage of the Argo in-situ profiles which is not global), the following steps are followed:

1. Maps of altimeter SLA are collocated at the position and time of each Argo profiles. The altimeter SLA is the AVISO SSALTO/DUACS products with the same temporal reference as the Argo dynamic heights anomalies (2003-2011).
2. Reconstructed maps of altimeter SLA are computed with the same method applied for in-situ steric measurements, based on these « pseudo » observations.

Figure 13 show the impact for a single global estimation of the MSL. Original altimeter SLA from Dec. 17, 2008 is compared with the reconstructed map from the Dec. 15, 2008 (the original dataset is weekly maps and the reconstructed dataset is monthly maps).

As shown by the map of their differences, the discrepancies are mainly observed at small scales, due to the filtering of the reconstructed maps.



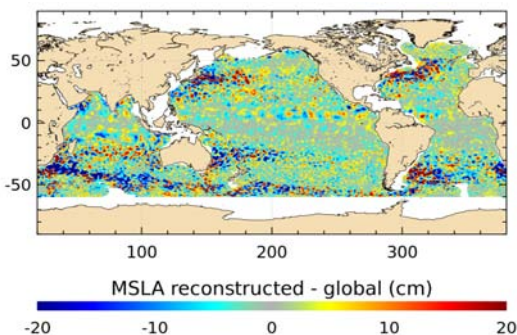


Figure 13: Map of the Dec. 17, 2008 mean sea level from DUACS (top left) and reconstructed mean sea level from the Dec. 15, 2008 (top right) and their difference (bottom).

Reconstructed altimeter maps are computed over the 2005 - 2012.5 period and the global MSL trends are compared between:

- The original altimeter MSL:
 - geographically masked and filtered as for in-situ maps
 - weekly timeseries interpolated at monthly intervals
 - with the same inter annual reference as Argo maps
- And the reconstructed MSL. Note that for the Argo in-situ steric maps, potential holes have been filled thanks to the use of a global synthetic climatology. But it is not used in the case of this reconstructed altimeter dataset. Thus only a few monthly maps from the year 2005 have small holes in SE Pacific and S Atl. oceans due to the Argo deteriorated sampling at this period. We consider that it does not affect the reconstructed MSL trend.

Indeed, as shown on Figure 14, MSL trends are identical. A slightly higher formal error adjustment (0.20 mm/yr vs 0.18 mm/yr) and standard deviation (0.60 mm/yr vs 0.57 mm/yr) are found for the reconstructed time series.

Thus, our mapping method has a non significant impact on the global MSL trend (0.01 mm/yr).

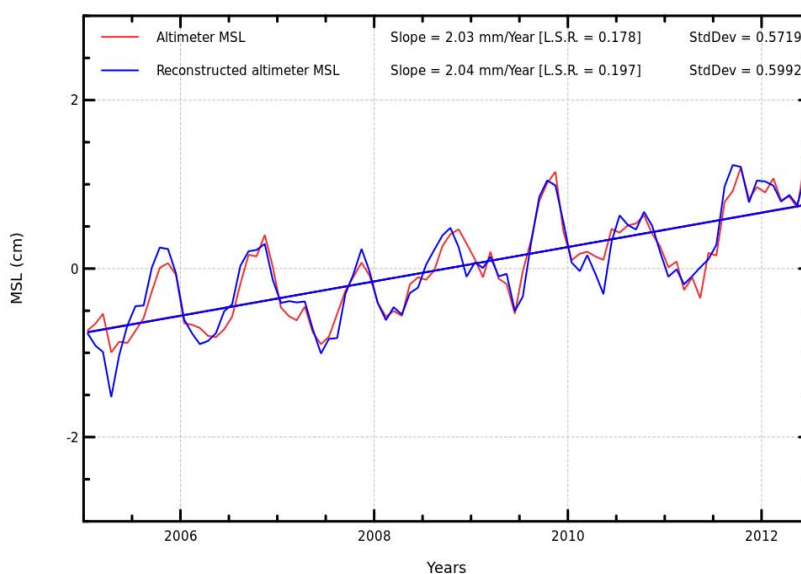


Figure 14: Global altimeter (AVISO SSALTO/DUACS referenced over the Argo in-situ temporal reference: 2003-2011) and reconstructed altimeter mean sea level over the Jan. 2005 - Jun. 2012 period.



The Taylor distance is computed between the detrended times series of the original and reconstructed altimeter MSL (Figure 15).

- ⇒ Very good correlation between the two datasets (0.91)
- ⇒ Slightly higher standard deviation of the reconstructed time series (0.60 cm vs 0.57 cm, cf Figure 14)

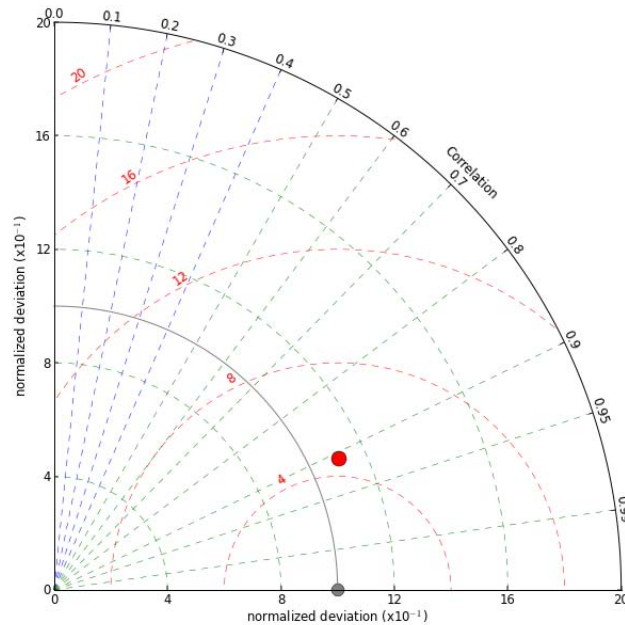


Figure 15: Taylor diagram of the detrended reconstructed altimeter MSL time series compared with original detrended altimeter MSL over Jan. 2005 - Jun. 2012 period. Altimetry is masked, filtered and interpolated at monthly intervals as for the reconstructed dataset.

The maps of the altimeter MSL trends are computed (Figure 16) over the 2005 -2012.5 period with:

- The original altimeter MSL:
 - geographically masked and filtered as for in-situ maps
 - weekly timeseries
 - with the same inter annual reference as Argo maps
- The reconstructed altimeter MSL:
 - monthly timeseries

Very similar geographical patterns are observed and some systematic regional biases are observed such as along the western equatorial Pacific ocean (+/- 1mm/yr) and in regions of high ocean variability (+/- 3 mm/yr).

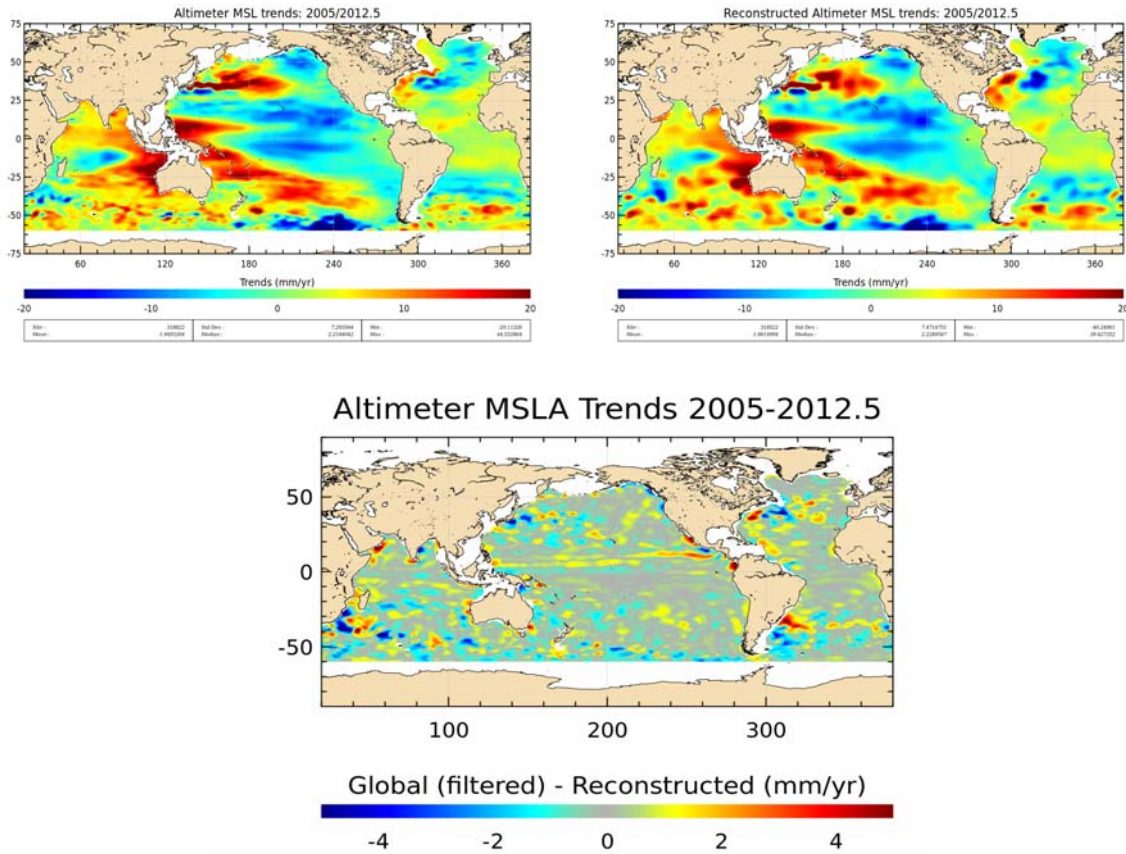


Figure 16: Altimeter MSL trends masked and filtered as for in-situ maps, based on weekly maps with the same inter annual reference as Argo maps (2003-2011) (top left). Reconstructed altimeter MSL trends based on monthly maps (top right). Difference between the original and reconstructed altimeter MSL trends.

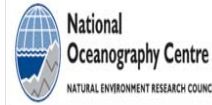
6. Conclusion

In the framework of the SL-CCI project (WP4300), this work intended to provide datasets of monthly maps of the steric mean sea level in order to contribute to the estimation of the altimeter sea level closure budget. Three datasets has been provided associated with three different reference depth of integration of the Argo dynamic heights (900 dbar, 1200 dbar and 1900 dbar).

In addition, in the context of the quality assessment of the altimeter MSL, this study contributes to determine which reference level is better adapted to compute steric dynamic height. It turns out that the choice of this reference depth is not clear:

- The steric MSL referenced to 1900 dbar will be preferred in case of assessing the altimeter MSL trend and discuss the altimeter sea level closure budget.
- However, when removing the effect of the trend, the standard deviation of altimetry is closer to the steric + mass signals with a 900 dbar reference and the correlation between altimetry and Argo + mass is slightly increased with the 900dbar time series. In addition, steric MSL trends are more homogeneously distributed compared with altimetry at 900dbar rather than with deeper references. Thus, in case of assessing the impact of a new altimeter standard in terms of variance, the 900 dbar steric signal may be preferred.

8.3. Evaluation of the Sea Level CCI dataset with respect to in-situ data



ESA Sea Level CCI

Validation Report: WP4XXX Altimetry validation with respect to in-situ data

Reference: CLS-DOS-NT-12-59

Nomenclature: SLCCI-VR-57

Issue: 1. 2

Date: Nov. 26, 12





Chronology Issues:			
Issue:	Date:	Reason for change:	Author
1.0	Nov. 26 11	Initialization	P. Prandi

People involved in this issue:		
Written by (*):	P. Prandi, V. Pignot	Date + Initials:(visa or ref)
Checked by (*):		Date + Initial:(visa ou ref)
Approved by (*):		Date + Initial:(visa ou ref)
Application authorized by (*):	ESA	Date + Initial:(visa ou ref)

**In the opposite box: Last and First name of the person + company if different from CLS*

Index Sheet:	
Context:	Baghera tool, project ACT-OCEAN
Keywords:	Oceanography, sea level
Hyperlink:	

Distribution:		
Company	Means of distribution	Names
CLS	Notification	



List of tables and figures

List of tables:

Table 1 : Global Mean Sea Level trends evaluated from altimetry data and in-situ measurements (all trends are expressed in $\text{mm}\cdot\text{yr}^{-1}$)	4
Table 2: SLA trend differences (mm/yr) between altimetry and in-situ estimated over different oceanic basins.....	7

List of figures:

Figure 1: Time series of the global mean SLA from tide gauges and collocated altimetry (left) and from altimetry and Argo profiles (right), the differences time series are artificially translated vertically.	3
Figure 2: Coherence diagram between altimetry and tide gauges (left), and between altimetry and Argo floats (right) for the global mean SLA time series	3
Figure 3: Time series of the inter-annual variability of the global mean SLA from tide gauges (left) and Argo profiles (right), and the corresponding co-located altimetry.....	5
Figure 4: Global mean SLA annual cycle estimated from tide gauges and Argo T/S data, and the corresponding co-located satellite altimetry (95% confidence levels for the monthly mean are overlaid as thin grey lines for the in-situ estimates)	5
Figure 5: Time series of the high frequencies of the SLA from tide gauges (left) and Argo profiles (right), and the corresponding co-located altimetry. The time series of the differences are represented in black with an artificial vertical shift.	6
Figure 6: Taylor diagram comparing altimetry (grey dot), tide gauges (triangles) and Argo profiles (circles) for the raw signal(black), the inter-annual signal (red) and the annual cycle (blue) and the high frequencies of the SLA (green)	7
Figure 7: Taylor diagram comparing tide gauges (triangles) and Argo profiles (circles) for the inter-annual signal of the ocean-basin wide averages of SLA over the Pacific Ocean (red), the Atlantic Ocean (blue) and the Indian Ocean (green). The global mean is represented in black.....	8
Figure 8: Basin-wide average SLA annual cycle for altimetry and tide gauge data for the Pacific Ocean (left), the Atlantic Ocean (center) and the Indian Ocean (right)	9
Figure 9: Basin-wide average SLA annual cycle for altimetry and Argo data for the Pacific Ocean (left), the Atlantic Ocean (center) and the Indian Ocean (right)	9
Figure 10: Taylor diagram comparing tide gauges (triangles) and Argo profiles (circles) for the high frequencies of the basin-wide mean SLA over the Pacific Ocean (black), the Atlantic Ocean (red) and the Indian Ocean (blue)	10
Figure 11: Coherence diagram between tide gauges and co-located altimetry (left) and Argo profiles and co-located altimetry (right) data for the high frequencies of the Pacific (red), Atlantic (blue) and Indian (green) oceans.....	10
Figure 12: Map of the SLA differences trends between altimetry and tide gauges (left) and between altimetry and Argo profiles (right).....	11
Figure 13: Histograms of the trend differences (in mm/yr) between tide gauges and co-located altimetry (left) and Argo profiles and co-located altimetry (right)	11
Figure 14: Map of the inter-annual SLA variance differences between altimetry and tide gauges (left) and between altimetry and Argo profiles (right)	12



Figure 15: Maps of the annual cycle amplitude (left) and phase (right) differences between SLCCI altimetry and tide gauges..... 12

Figure 16: Maps of the annual cycle amplitude (left) and phase (right) differences between SLCCI altimetry and Argo profiles 13

Figure 17: Map of the SLA variance differences between altimetry and tide gauges records (left) and between altimetry and Argo profiles (right) for the high frequency part of the signal 13

Figure 18: Time series of the global mean SLA estimated from the SLCCI (blue) and PVA (red) satellite altimetry datasets..... 14

Figure 19: Maps of the SLA trend differences between CCI and SALTO/DUACS datasets, estimated over the 1993-2010 (left) and 2003.5-2010 (right) periods 16

Figure 20: Map differences between trend differences between altimetry and Argo profiles evaluated with CCI and SALTO/DUACS altimetry datasets..... 16

Figure 21: Time series of hemispheric SLA (west left and east right) from Argo profiles (red) and co-located altimetry from CCI (red) and SALTO/DUACS (blue) 16

List of items to be confirmed or to be defined

Lists of TBC:

Aucune entrée de table des matières n'a été trouvée.

Lists of TBD:

Aucune entrée de table des matières n'a été trouvée.

Applicable documents

AD 1 Sea level CCI project Management Plan
CLS-DOS-NT-10-013

Reference documents

RD 1 Manuel du processus Documentation
CLS-DOC



List of Contents

1. Introduction	1
1.1. Data description	1
1.2. Data comparison methods	1
1.2.1. Tide gauges	1
1.2.2. Argo profiles	2
1.3. Description of work	2
2. SLCCI altimetry product assessment	2
2.1. Global Mean Sea Level	2
2.1.1. Long term trends	4
2.1.2. Inter-annual variability	4
2.1.3. Annual Cycle	5
2.1.4. High Frequency Signals	6
2.1.5. Summarizing global average performance	6
2.2. Regional Mean Sea Level	7
2.2.1. Long term trends	7
2.2.2. Inter-annual signals	8
2.2.3. Annual cycle	8
2.2.4. High Frequency signals	9
2.3. Local Mean Sea Level	11
2.3.1. Long term trends	11
2.3.2. Inter-annual variability	12
2.3.3. Annual Cycle	12
2.3.4. High Frequency signals	13
3. Comparison between SLCCI and DUACS products with respect to in-situ data	13
3.1. Global Mean Sea Level	14
3.2. Regional mean sea level	15
3.2.1. Long term trends	15
4. Conclusions and recommendations	17
5. References	17
Appendix A - List of acronyms	19



1. Introduction

The purpose of this report is to present the results of the altimetry/in-situ comparisons performed within the framework of the ESA Sea Level CCI project. In-situ data are used as an external and independent source of comparison.

The first and major goal of this work is to assess and describe the consistency between two independent measurements of the physical quantity of interest: the Sea Level Anomaly (hereinafter noted SLA).

A secondary goal of this document is to attempt to demonstrate the improvements achieved by the new satellite altimetry sea level dataset generated within the project with respect to previously existing datasets.

1.1. Data description

Three types of sea level measurements are used here, satellite altimetry, tide gauge measurements and dynamic height anomalies derived from Argo temperature and salinity profiles.

Two satellite altimetry datasets are considered in this work:

- The Sea Level CCI dataset (hereinafter noted SLCCI) which was generated during the ESA Sea Level project after a careful selection of algorithms in order to achieve the highest climate-oriented performance levels. The dataset consists in weekly SLA grids spanning 18 years from 1993 to 2010,
- A dataset directly derived from the SALTO/DUACS processing but generated at the same spatial and temporal resolution than the SLCCI product to ensure consistency of the SLA estimations,
- Monthly tide gauge records are downloaded from the PSMSL database and corrected for the glacial isostatic adjustment using the ICE5G-VM4 model (Peltier, 2004) and for atmospheric effects using ERA model outputs,
- Temperature and Salinity profiles measured by Argo floats are retrieved from the Coriolis GDAC database (<http://www.coriolis.eu.org/>). For each profile, a steric Dynamic Height Anomaly (DHA) is computed using a reference level at 900 dbar and a contemporaneous mean dynamic height (also called synthetic climatology). Grace observations from the JPL are also used to constraint the mass component that is missing in the Argo observations (<http://grace.jpl.nasa.gov>; Chambers 2006). Altimeter SLA and GRACE are collocated to Argo in-situ DHA to perform the comparison. Hereinafter, the term "Argo profiles" refers to the sum of the steric height calculated from the Argo temperature and salinity measurements and mass component derived from GRACE gravity measurements.

1.2. Data comparison methods

The methodology used to compare satellite altimetry and in-situ measurements (Tide gauges and Argo profiles) is extensively described in the annual reports dedicated to these activities (reference) the interest of such comparisons is further demonstrated by Valladeau et al. (2012). Here we give only a brief overview of the methods.

1.2.1. Tide gauges

For every available station in the PSMSL database, we compute the correlation coefficients between altimetry and the tide gauges record within a 100 km radius area from the station's position. The matching satellite altimetry time series is extracted at the position of the maximum of correlation, given that:

- Correlation coefficient is higher than 0.3,



- Differences between the two records do not exceed 12 cm with standard deviation lower than 30 cm,

This procedure leads to a subset of PSMSL database with a matching altimetry time series for each tide gauge station. To limit the impact of gaps in the tide gauges series, only the tide gauge time series which are at least 80% complete (and the matching satellite altimetry time series) are considered in this work. The dataset used to estimate statistics consists in 475 pairs of tide gauges and corresponding altimetry time series.

Tide gauge time series should be commonly referenced before estimating ensemble averages. In the standard procedure the bias (estimated as the mean of the differences) between altimetry and tide gauge is removed from the tide gauge record. This method prevents any determination of regional biases between the two types of observations, but can deal with large gaps in tide gauge time series. Here, as we consider only almost complete tide gauge records, we rather removed the mean from each tide gauge time series, a method already used for global average comparisons between altimetry and tide gauges (Prandi et al., 2009).

It should be noted that the spatial sampling achieved by the tide gauges is far from even along the global ocean coasts, with a strong bias towards the northern hemisphere. The purpose of this work is not to extrapolate global average sea level from these data. When comparing to altimetry data, we apply the tide gauge spatial sampling to the altimetry data in order to perform a spatially consistent comparison.

1.2.2. Argo profiles

For each Argo profile data, the gridded satellite altimetry SLA is interpolated bilinearly at the time and position of the profile. Whenever the difference between altimeter SLA and the steric Argo dynamic height exceeds 20 cm, the data point is removed from further analysis. Satellite altimetry and in-situ SLA pairs are then used to estimate statistics on a $2^\circ \times 2^\circ$ grid with a temporal resolution of 10 days.

1.3. Description of work

This work benefits from the Round Robin Data Package (RRDP) framework developed within the Sea Level CCI project to assess the quality of two equivalent terms of the satellite altimetry equation. Following this framework, in this work, differences between in-situ and satellite altimetry estimates of SLA variability are separated into different temporal (long-term trends, inter-annual variability, annual signal, high frequency signal) and spatial (global mean, basin-wide averages, local phenomena) scales.

The major advantage of such approach is to allow an independent assessment of the agreement between satellite altimetry and in-situ measurements for the different scales of the climate signals the Sea Level CCI is dedicated to, at the cost though of a certain level of complexity.

2. SLCCI altimetry product assessment

In this section we assess the performance of the satellite altimetry SLA grids calculated within the framework of the SLCCI project by comparing them to independent measurements of the SLA by two types of in-situ probes: tide gauges and Argo floats.

The comparisons performed are classified by spatial and temporal scales of the signal considered.

2.1. Global Mean Sea Level

First we consider global average SLA as the raw result, without any post-processing, of the comparison procedure. The global average SLA time series estimated from altimetry, tide gauges



and in-situ profiles with the adequate collocation methods are presented on Figure 1. Satellite altimetry time series are represented in red while in-situ estimates are represented in blue on both graphs.

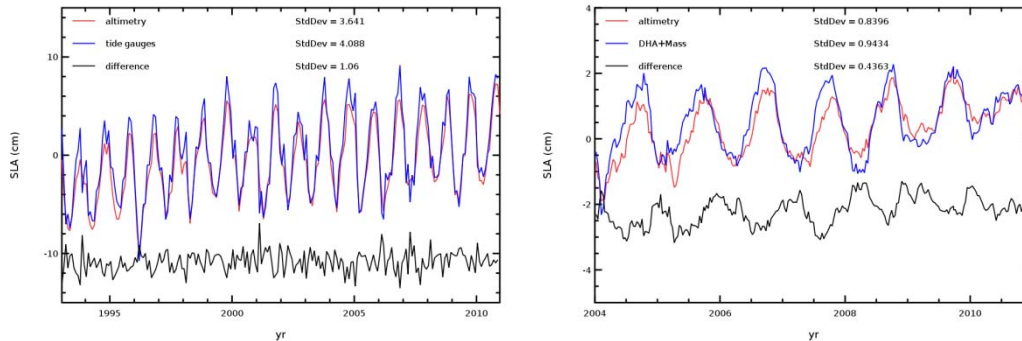


Figure 1: Time series of the global mean SLA from tide gauges and collocated altimetry (left) and from altimetry and Argo profiles (right), the differences time series are artificially translated vertically.

Regarding the global mean SLA, SLCCI and in-situ data show a good agreement:

- correlation coefficients are 0.96 and 0.84 when comparing altimetry to tide gauges and Argo profiles, respectively (correlations drop to 0.85 and 0.68 when annual and semi-annual signals are removed)
- the RMS differences are 1.2 cm and 0.6 cm when comparing altimetry to tide gauges and Argo profiles, respectively

However the time series are marked by an important annual cycle which may be masking the other temporal scales of the SLA variability. A first way to separate temporal scales is to look at the coherence between altimetry and in-situ data. Figure 2 shows the coherence between the global mean SLA time series of Figure 1. Coherence levels at low frequencies (long periods) should be viewed with caution given the relatively short time span available, and Figure 2 thus is focused on periods shorter the 900 days. The annual signal is clearly the most coherent signal between altimetry and tide gauges (wide peak around $T=365$ days). For the comparison to Argo profiles the peak is shifted towards shorter periods, probably as a result of the small phase shift between altimetry and in-situ annual signals visible on Figure 1. Coherence is also important at higher frequencies, with significant levels for the semi-annual signal, and two months signal, which is a lower limit considering monthly PSMSL tide gauges comparisons.

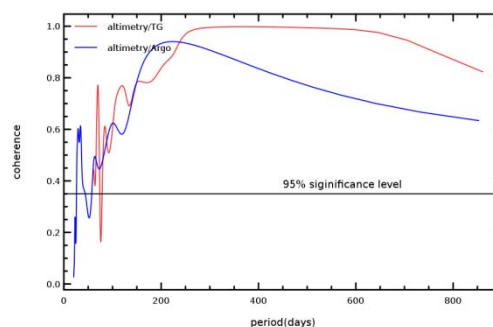


Figure 2: Coherence diagram between altimetry and tide gauges (red), and between altimetry and Argo floats (blue) for the global mean SLA time series



2.1.1. Long term trends

Considering global mean sea level, long term trend is arguably the figure which catches most attention. Table 1 summarizes the global mean sea level trend evaluated from in-situ data and collocated altimetry.

It should be noted that the SLCCI/TG comparison is performed over the whole altimetry period (1993-2010). However Argo T/S profiles are only available after 2004 and the comparison is therefore limited to the end of the period. Given the uncertainties on the comparison method (-0.7 mm.yr^{-1} for the tide gauge comparison and $\sim 1 \text{ mm/yr}$ for the Argo profiles comparison) between altimetry and in-situ data, there is almost no drift of the altimetry with respect to tide gauges. However, Argo profiles see a slightly lower sea level rise than the altimetry.

	Tide gauges (1993-2010)	Argo profiles (2004-2010)
Altimetry	2.9	2.0
In-Situ	2.7	0.9
difference	0.2	1.1

Table 1 : Global Mean Sea Level trends evaluated from altimetry data and in-situ measurements (all trends are expressed in mm.yr^{-1})

2.1.2. Inter-annual variability

The inter-annual variability considered here corresponds to signals with periods larger than two years but without the long-term trends. Despite its low amplitude (compared to the annual signal for example), this frequency domain of the SLA signal variability is of climatic importance, as it depends on low-frequency oscillations of the climate system.

To obtain the inter-annual time series, we apply a low-pass filter to the detrended time series of Figure 1, in order to remove all signals with periods lower than two years. The time series of the global mean SLA inter-annual variability are displayed on Figure 3, for the tide gauge and Argo profiles comparison.

For the altimetry/tide-gauges comparison however, there is a very good agreement between in-situ and altimetry records, both for the amplitude and the phasing of the inter-annual variability, as suggested by the coherence diagram of Figure 2. The correlation between the time series of Figure 3 is very high at 0.94, but tide gauges still record a higher level than the altimetry does.

It should be noted that for the Argo comparison, the inter-annual variability is small with about 0.5 cm maximum amplitude. The short period available (only 7 years) is an important limit for this type of low-frequency signals comparison, and uncertainty levels are high. If the two time series show a consistent behavior ($r=0.68$), there appears to be a shift in the phasing of the signals, resulting in a standard deviation of the differences almost as large as the altimetry or Argo time series. The satellite altimetry time series displays a larger inter-annual variability levels than the Argo time series.

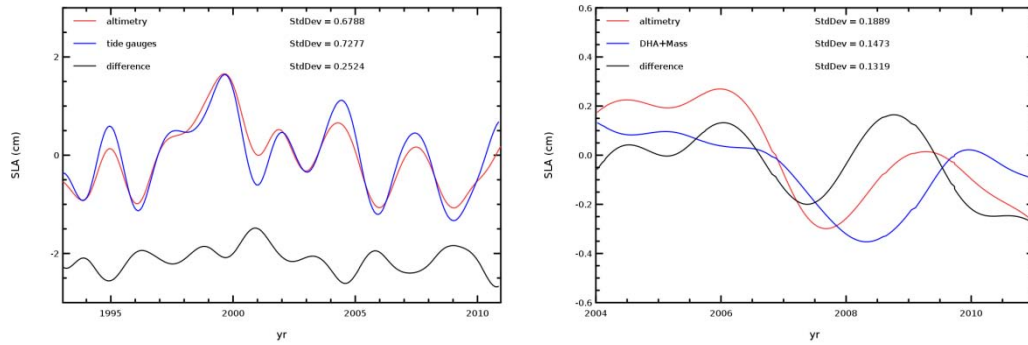


Figure 3: Time series of the inter-annual variability of the global mean SLA from tide gauges (left) and Argo profiles (right), and the corresponding co-located altimetry.

Regarding global average inter-annual variability, the comparison to tide gauges records shows that the SLCCI altimetry dataset performs well in reproducing the observed sea level variability. Performance is somewhat lower when comparing it to Argo profiles but given the short period available, inter-annual signals should be viewed with caution.

2.1.3. Annual Cycle

From Figure 1, it is apparent that the annual cycle explains an important part of the variability of the global mean SLA, either observed by satellite altimetry or by in-situ data. The seasonal cycles derived from the time series of Figure 1 are represented on Figure 4.

Considering the altimetry/tide gauges comparison, there is an excellent agreement between annual cycles, both in term of amplitudes (altimetry amplitude is about 1 cm lower than the tide gauges one) and phasing of the signal (the minimum is reached in March while the maximum is reached in September for both datasets).

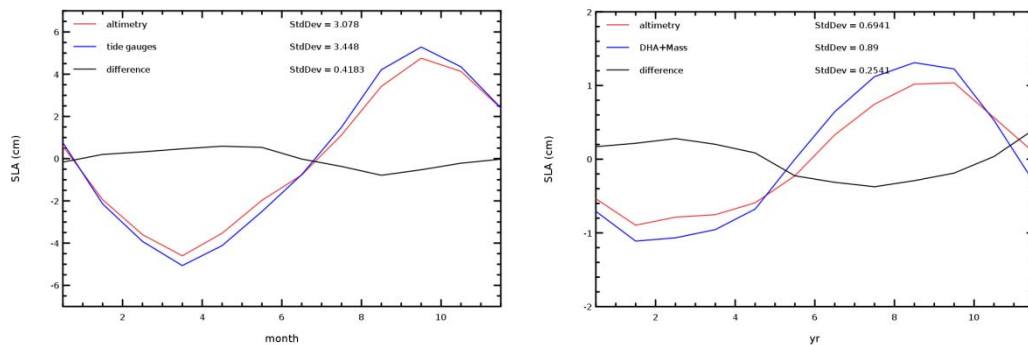


Figure 4: Global mean SLA annual cycle estimated from tide gauges and Argo T/S data, and the corresponding co-located satellite altimetry (95% confidence levels for the monthly mean are overlaid as thin grey lines for the in-situ estimates)

When comparing altimetry to Argo profiles, the altimetry amplitude is lower than the Argo one, and the two seasonal cycles seem shifted by one month (altimetry being delayed) for the position of the maximum. It should however be noted that the amplitude of the seasonal cycle measured by Argo is much lower than the one measured by tide gauges, one possible cause for this is that, as Argo samples a much broader part of the ocean than tide gauges, out of phase signals in the Northern and Southern hemispheres are averaged out.

On a global scale, the SLCCI satellite altimetry dataset is in very good agreement with in-situ data regarding the seasonal cycle, which is an important part of the total SLA variability.



2.1.4. High Frequency Signals

The previous sections of this report were dedicated to long-term trends, inter-annual variability and the seasonal cycle. After these signals have been removed from the total SLA time series, only the high-frequency variability remains. Figure 5 shows the high frequency variability of the global average SLA time series of in-situ and collocated satellite altimetry. Here we consider signals with a period shorter than six months.

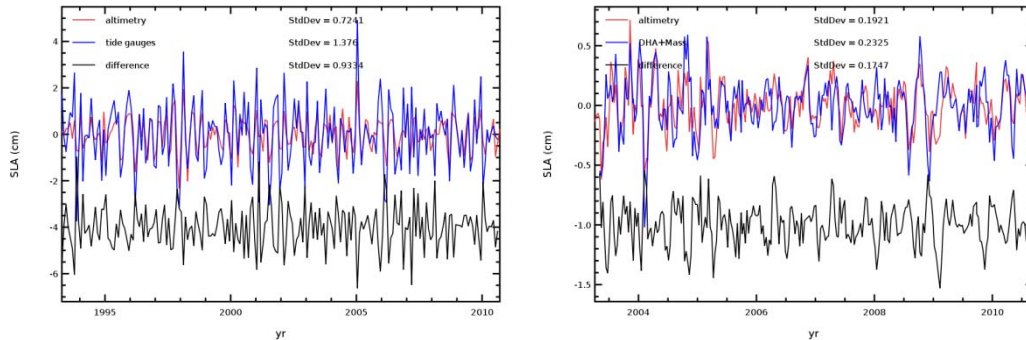


Figure 5: Time series of the high frequencies of the SLA from tide gauges (left) and Argo profiles (right), and the corresponding co-located altimetry. The time series of the differences are represented in black with an artificial vertical shift.

The high frequencies represent an important part of the total SLA variability with standard deviations of 1.4 cm and 0.7 cm for the tide gauge and collocated altimetry data (standard deviations are 4.1 cm and 3.6 cm for the total SLA content (high and low frequencies)) for example. For both comparisons, correlations are high between altimetry and in-situ ($r=0.78$ for tide gauges and $r=0.68$ for Argo profiles), though satellite altimetry records show lower levels of high frequency variability than in-situ records, and the standard deviation of the differences has the same magnitude than altimetry or in-situ records alone.

2.1.5. Summarizing global average performance

In order to provide a synthetic look on the comparisons between global mean SLA estimated from altimetry and in-situ data for the different temporal scales considered in this study, Figure 6 displays a Taylor diagram summarizing these different aspects. In this figure, all standard deviations are normalized by the corresponding altimetry standard deviation for convenience purposes, and the RMS of the difference therefore can't be read directly from the graph.

For the altimetry/tide gauges comparison, the annual and inter-annual signals are in very good agreement with correlations higher than 0.9 and comparable variability levels resulting in low RMS of the differences (0.58 and 0.24 cm respectively). The performance is much lower for the high frequency part of the signal, due to very difference standard deviations.

It is interesting to note that generally, the performance of the Argo profiles comparison is slightly lower, regardless of the period of the signal considered except for the high frequencies of the signal. For inter-annual variability, the correlation between altimetry and Argo profiles is low ($r=0.68$, red dot on Figure 6) resulting in a high RMS difference, even if the two techniques show comparable variability levels.

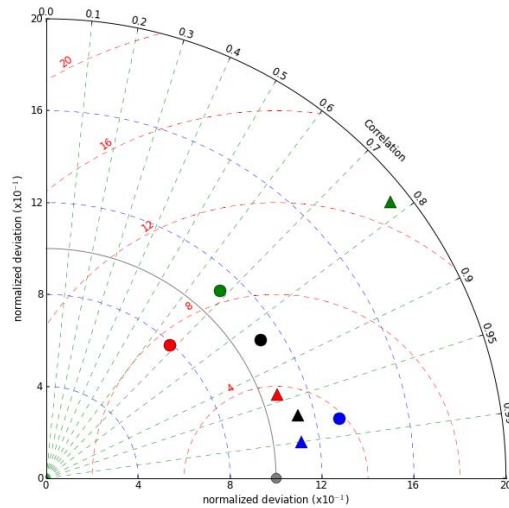


Figure 6: Taylor diagram comparing altimetry (grey dot), tide gauges (triangles) and Argo profiles (circles) for the raw signal (black), the inter-annual signal (red) and the annual cycle (blue) and the high frequencies of the SLA (green)

For both the altimetry/tide gauges and altimetry/Argo profiles comparisons, the seasonal cycle, which is a dominant signal in the global average variability, is in good agreement between altimetry and in-situ data.

2.2. Regional Mean Sea Level

After considering the global mean SLA, in this section we consider smaller spatial scales and investigate the comparison between altimetry and in-situ for basin-wide averages. When moving from global average to basin-wide (or regional) average the SLA variability should increase, at least in some areas. In this study we consider three major ocean basins: the Pacific, Atlantic and Indian Oceans. As in the previous section, the SLA variability is separated by time scales.

2.2.1. Long term trends

The basin average SLA trends, estimated from in-situ data and co-located SLCCI altimetry, are summarized in Table 2.

		Pacific Ocean	Atlantic Ocean	Indian Ocean
1993-2010	altimetry	2.1	2.7	4.0
	tide gauges	1.7	2.1	4.2
	difference	0.4	0.6	-0.2
2004-2010	altimetry	0.6	2.1	5.1
	Argo profiles	0.0	0.4	4.4
	difference	0.6	1.7	0.7

Table 2: SLA trend differences (mm/yr) between altimetry and in-situ estimated over different oceanic basins

For the altimetry/tide gauges comparisons, trend differences are evenly distributed for the three oceanic domains considered in this study. The largest trend difference is observed in the Atlantic



Ocean with 0.6 mm.yr^{-1} drift between the two techniques. Such a difference is below the uncertainty of the method (-0.7 mm.yr^{-1} for the global average, and certainly higher for a regional average) and therefore not significant. The Indian Ocean is poorly sampled and uncertainties are much larger in this area, despite the good agreement between the two techniques.

Trend differences are larger for the altimetry/Argo profiles comparison, and all positive, reflecting a larger and spatially consistent global mean drift of the SLCCI altimetry dataset compared to Argo floats, altimetry always measuring a higher rate of sea level rise than Argo floats. The largest trend difference is again observed in the Atlantic Ocean with a 1.7 mm/yr trend difference, larger than the methodology uncertainty.

2.2.2. Inter-annual signals

In order to summarize the inter-annual variability comparisons for basin-wide SLA averages, the corresponding Taylor diagram is represented on Figure 7.

High values of the correlation coefficients are found for the altimetry/tide gauges comparisons over all three oceans ($r > 0.75$), but with higher levels of variability for the tide gauge records than the altimetry. Such feature is observed on all temporal and spatial scales. Performances of the altimetry versus tide gauge are fairly similar in the Atlantic and Pacific Oceans.

Regarding the comparison to Argo floats, and unlike the comparison to tide gauges, the different basins show different behaviors. In the Pacific and Atlantic Oceans, the altimetry variability is higher than the in-situ one. The opposite is observed in the Indian Ocean.

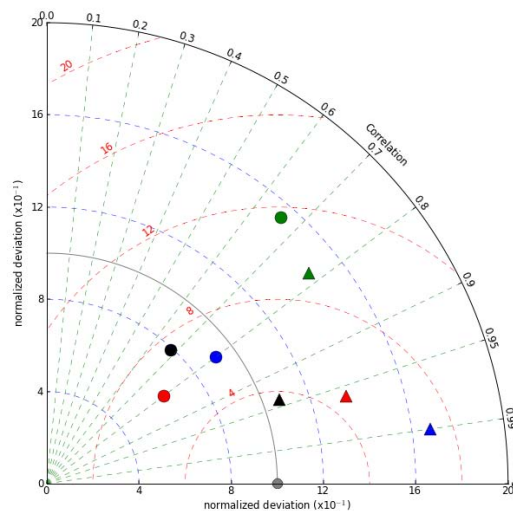


Figure 7: Taylor diagram comparing tide gauges (triangles) and Argo profiles (circles) for the inter-annual signal of the ocean-basin wide averages of SLA over the Pacific Ocean (red), the Atlantic Ocean (blue) and the Indian Ocean (green). The global mean is represented in black

For both the altimetry/tide gauges and altimetry/Argo profiles comparison, the performance is lower in the Indian Ocean than in other basins, but with a consistent behavior of both tide gauges and Argo comparisons. The low tide gauge sampling along the coasts of the basin might explain part of the observed differences, but more investigations are required regarding the altimetry/Argo comparison.

2.2.3. Annual cycle

For the global mean SLA, annual cycles estimated from in-situ records and collocated SLCCI altimetry show a good agreement, despite the one month shift observed between Argo profiles and collocated altimetry.



Figure 8 displays the SLA seasonal cycle estimated from tide gauge and collocated altimetry records over the Pacific, Atlantic and Indian oceans. Over the three basins considered, the SLCCI altimetry dataset observes a seasonal cycle very close to the one observed by tide gauges.

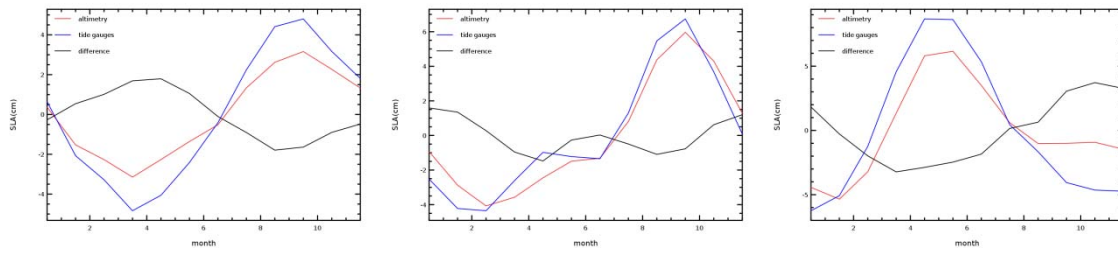


Figure 8: Basin-wide average SLA annual cycle for altimetry and tide gauge data for the Pacific Ocean (left), the Atlantic Ocean (center) and the Indian Ocean (right)

Figure 9 is similar to Figure 8 but for the SLA derived from Argo profiles and collocated altimetry. The seasonal cycles in the Pacific and Atlantic Oceans observed by Argo profiles and collocated altimetry are very similar: amplitudes differences are small and there is no phase shift. The agreement is much poorer in the Indian Ocean where seasonal cycles observed by the two techniques are very different, both in term of amplitude and phase.

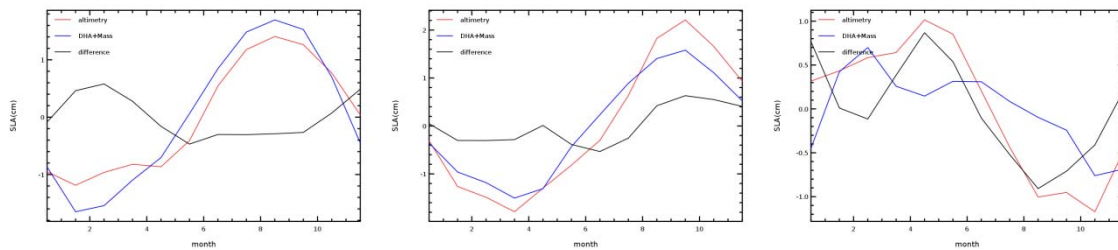


Figure 9: Basin-wide average SLA annual cycle for altimetry and Argo data for the Pacific Ocean (left), the Atlantic Ocean (center) and the Indian Ocean (right)

2.2.4. High Frequency signals

The performance of in-situ records with respect to collocated altimetry regarding the high frequency part of the regional average SLA over the Pacific, Atlantic and Indian Oceans is summarized on the Taylor diagram of Figure 10.

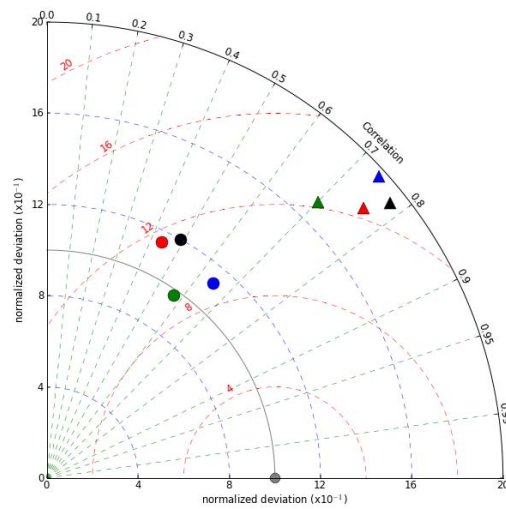


Figure 10: Taylor diagram comparing tide gauges (triangles) and Argo profiles (circles) for the high frequencies of the basin-wide mean SLA over the Pacific Ocean (black), the Atlantic Ocean (red) and the Indian Ocean (blue)

At this spatial and temporal scale of the SLA signal, some of the features already observed still hold true: tide gauges SLA variability is higher than collocated altimetry SLA variability, although correlations remain high ($r > 0.7$). The high frequency variability of the Argo profiles' SLA is close to the collocated altimetry one, but correlations are generally lower than for the comparison to tide gauges. For both in-situ data comparisons, the three basin averages considered display similar performances with respect to altimetry data.

Figure 10 does not separate the different scales present in the high frequencies of the signal as we consider them here. In order to investigate those smaller scales, we calculate the coherence diagram between the high frequencies of the basin-wide average SLA estimated from in-situ records and co-located altimetry. The corresponding coherence diagrams are presented on Figure 11. The monthly sampling of the tide gauge data limits the resolution achievable by the analysis. The comparison between altimetry and Argo profiles is performed with a ten day temporal sampling so higher frequency behaviours are observable: coherence values are high for very short periods (20-30 days), and again around 70 days, especially in the Indian and Atlantic Oceans. In the Indian Ocean, coherence around a one year period is lower than in other basins, in agreement with larger seasonal cycle differences between altimetry and in-situ in this basin than in the others.

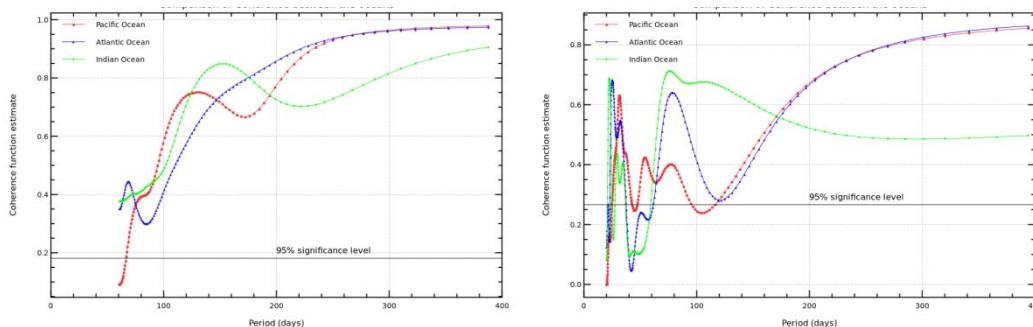


Figure 11: Coherence diagram between tide gauges and co-located altimetry (left) and Argo profiles and co-located altimetry (right) data for the high frequencies of the Pacific (red), Atlantic (blue) and Indian (green) oceans



2.3. Local Mean Sea Level

In this section, in order to get a hint of the spatial distribution of the differences between altimetry and in-situ records, we map these differences after separating the total SLA signal into temporal scales. When considering local averages (2° box average for the Argo comparison and individual time series for the tide gauge comparison), uncertainties are much larger than when considering the global average and therefore estimates of the differences should be viewed with caution.

2.3.1. Long term trends

First we investigate long term trends. The maps of trend differences between in-situ records and collocated SLCCI satellite altimetry are displayed on Figure 12. The left panel referring to the altimetry/tide gauges comparison shows the spatial distribution of the stations used in this study. Some regions seem to have coherent drifts: along the coast of Norway or in the north-western Atlantic Ocean for example. This could indicate an error in the altimetry data, or in tide gauges data (for example subsidence of the earth's crust that would affect all tide gauges stations in a region). The Argo profiles/altimetry comparison maps shows trends that seem evenly spatially distributed, no large coherent spatial patterns are found.

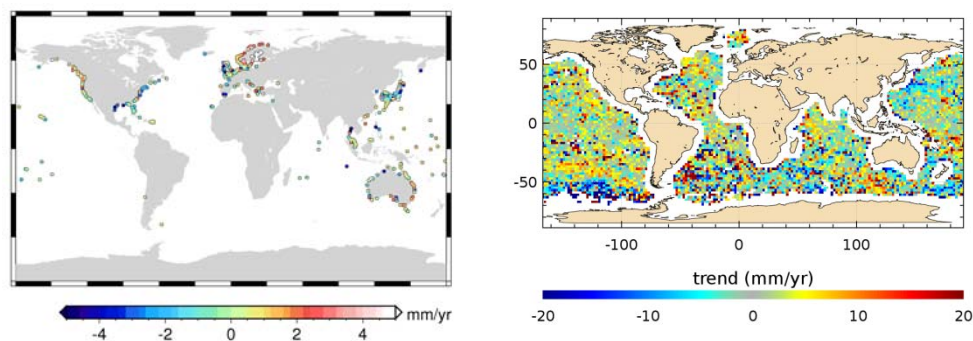


Figure 12: Map of the SLA differences trends between altimetry and tide gauges (left) and between altimetry and Argo profiles (right)

For both the tide gauges/altimetry and Argo profiles/altimetry comparisons, the low drifts observed when considering global or basin-wide averages appear on the map of Figure 12 to hide a wide distribution of the individual stations' trends.

The distribution of the trend differences between altimetry and in-situ records is further investigated by the means of the histograms displayed on Figure 13, illustrating the wide spread of the trend differences.

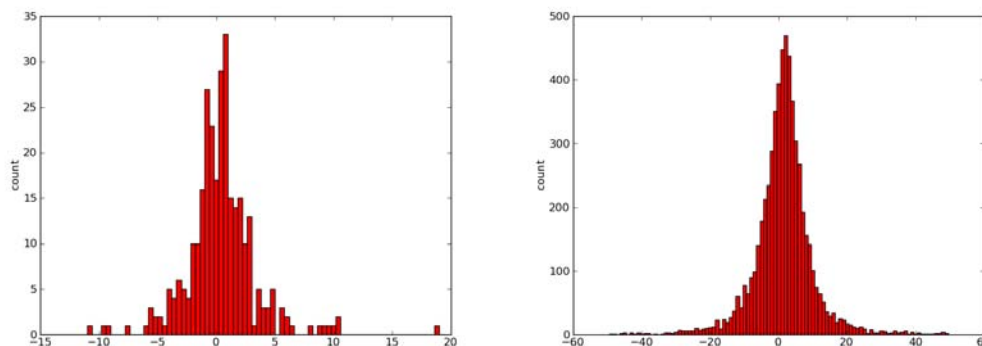


Figure 13: Histograms of the trend differences (in mm/yr) between tide gauges and co-located altimetry (left) and Argo profiles and co-located altimetry (right)



2.3.2. Inter-annual variability

Figure 14 displays the maps of SLA variance differences between altimetry and in-situ data estimated from the low-frequency (i.e. inter-annual variability) of the signal.

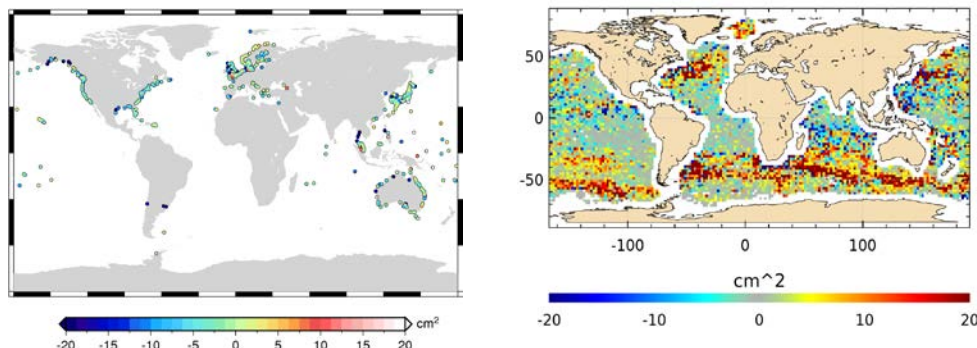


Figure 14: Map of the inter-annual SLA variance differences between altimetry and tide gauges (left) and between altimetry and Argo profiles (right)

On the comparison between SLCCI altimetry dataset and Argo profiles (right panel) high oceanic variability areas (ACC, western boundary currents) stand out with positive values, meaning that in these areas, altimetry records observe higher SLA variances than the Argo profiles.

The SLCCI altimetry/tide gauges comparison shows a good performance, with most of the variance differences ranging between -5 and 5 cm^2 despite some extreme values.

2.3.3. Annual Cycle

As was demonstrated on global or regional averages, the annual cycle is an important part of the total SLA variability, especially when considering the comparison between altimetry and tide gauges. When considering global or basin-wide averages, there is generally a good agreement between altimetry and in-situ data (excepted in the Indian Ocean). In order to investigate the spatial distribution of the annual signal differences, we computed maps of the annual signals differences between altimetry and in-situ records.

Figure 15 represents the spatial distribution of annual cycle amplitude and phase differences between tide gauge and collocated satellite altimetry data. Phase differences appear to be evenly distributed with low differences (15 degrees represents half a month shift in the phasing of the annual cycle) observed at all stations. The map of amplitudes differences displays a different behavior: differences are low in the Atlantic Ocean but much higher for the coastal stations of the Pacific Ocean (differences remain low for island stations).

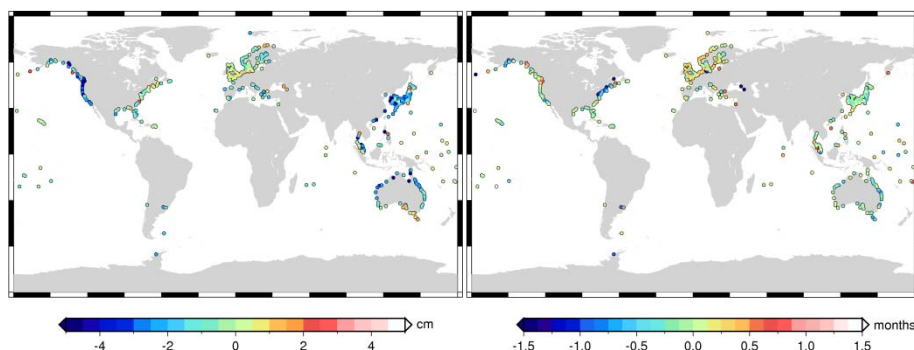


Figure 15: Maps of the annual cycle amplitude (left) and phase (right) differences between SLCCI altimetry and tide gauges

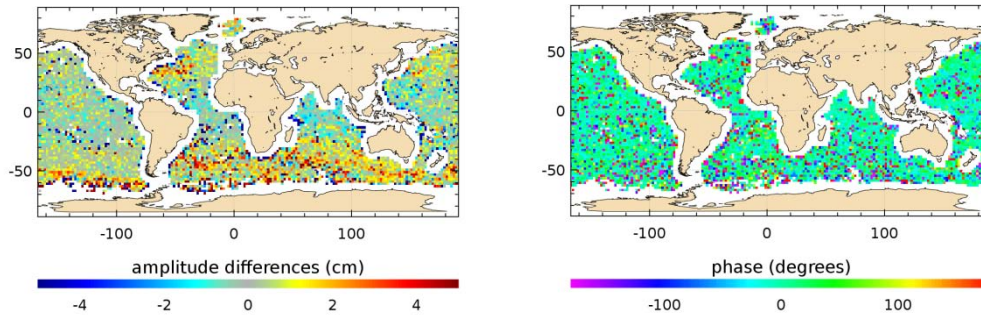


Figure 16: Maps of the annual cycle amplitude (left) and phase (right) differences between SLCCI altimetry and Argo profiles

Figure 16 shows the maps of the differences between altimetry and Argo profiles for the amplitude and phase of the annual signal. The phase differences appear to be very noisy but with an evenly distributed spatial pattern. The map of the amplitudes differences displays a latitude dependant pattern with negative differences in the tropical band where Argo profiles are seeing a larger amplitude than the altimetry and positive differences at lower latitudes (especially in the southern hemisphere) where altimetry amplitudes are larger than Argo ones. Again, in high oceanic variability areas such as the Gulf Stream, the differences are large.

2.3.4. High Frequency signals

The maps on Figure 16 display the variance differences between altimetry and in-situ collocated records for the high frequency part of the SLA variability. Tide gauges stations generally observe higher variability levels for this frequency band than the corresponding altimetry. However, island stations seem to show a better agreement with altimetry than continental coastal ones.

The altimetry versus Argo profiles comparison map displays a latitude dependant pattern: in the tropical band of all oceanic basins, variance differences are negative indicating higher variability levels in the in-situ records than in the altimetry data. In areas of high oceanic variability (ACC, Gulf Stream and Kuroshio) variability levels measured by Argo floats are lower than the altimetry ones.

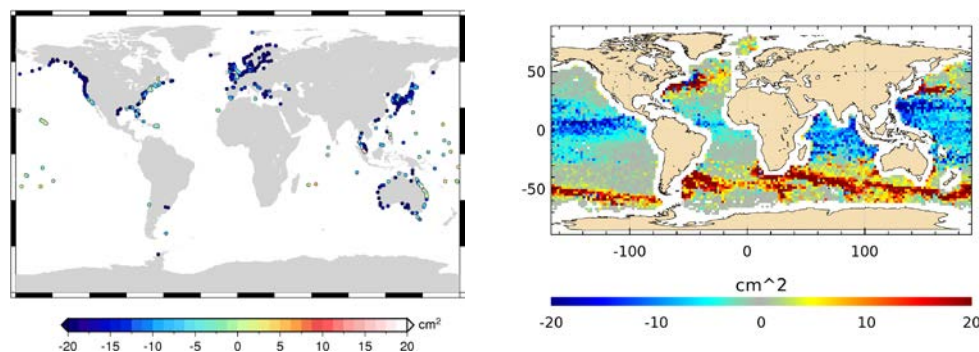


Figure 17: Map of the differences of SLA variances between altimetry and tide gauges records (left) and between altimetry and Argo profiles (right) for the high frequency part of the signal

3. Comparison between SLCCI and DUACS products with respect to in-situ data

The previous section of this report was dedicated to the comparison of the satellite altimetry SLA gridded dataset generated within the SLCCI project. One secondary objective of the study,



presented in this section, is to compare two satellite altimetry products with respect to available in-situ data (both tide gauges and Argo profiles).

For this purpose, we considered the SLCCI dataset and compared it to a reference dataset based on SALTO/DUACS processing, adapted to match the monthly temporal resolution of the SLCCI grids. Different spatial and temporal scales of the signal are studied, with the objective of determining which dataset fits the in-situ data (considered here as the "truth") best.

The spatial and temporal scales of the signal at which comparisons with in-situ data are investigated depend on a first evaluation of the differences between the two altimetry datasets. We focused on scales where the largest differences between the two altimetry datasets were found.

3.1. Global Mean Sea Level

When considering SLA time series averaged globally, the differences between the two datasets are very small. As an example, Figure 17 displays the global mean SLA time series estimated from the SLCCI and SALTO/DUACS datasets. Apart from years 1994 and 1995, the differences between the two time series are very low. As a result, the long term trends differ only by 0.02 mm/yr, a value which is not statistically significant (Ablain et al, 2009 estimated that the uncertainty on the global mean sea level trend is about 0.5 mm/yr). The same results are found for the other temporal scales of the global mean SLA considered in this study (inter-annual, seasonal and high-frequency variability).

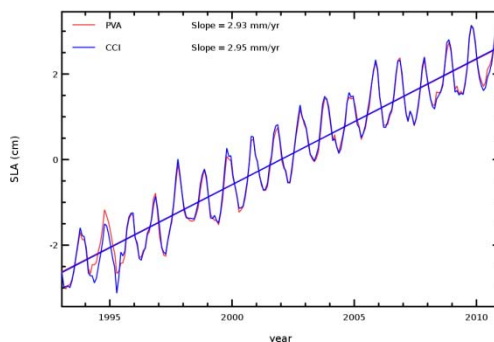


Figure 18: Time series of the global mean SLA estimated from the SLCCI (blue) and PVA (red) satellite altimetry datasets

Given the uncertainty levels of the altimetry/in-situ comparison method (about 0.5 mm/yr for the global mean SLA trend for example) it is hard to discriminate the two altimetry products when considering global averages. However, Figure 19 displays the differences observed between altimetry and in-situ for the different temporal scales of the global average signal for both the CCI/in-situ and DUACS/in-situ comparisons. For almost all time scales considered here, the in-situ data seems to be closer to the CCI data (triangles) than the DUACS data (circles). This results suggests that there is a better agreement between CCI altimetry and in-situ data than between DUACS altimetry and in-situ.

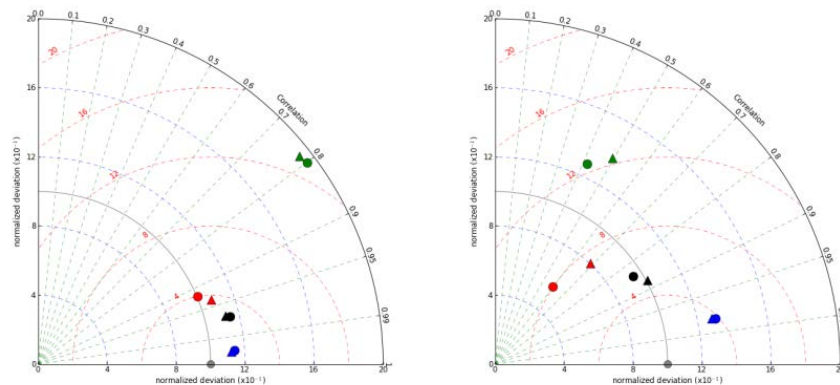


Figure 19: Taylor diagrams comparing altimetry and in-situ data (left: tide gauges, right: Argo profiles) for CCI (triangles) and DUACS (circles) data. Global averages are considered for the total signal (black), the annual cycle (blue), the inter-annual variability (red) and the high frequencies (green)

3.2. Regional mean sea level

We showed that differences between satellite altimetry datasets were too low on the global average to be separated by the comparison to in-situ data. When moving from global to regional averages, and depending on the region used to calculate spatial averages, one can expect the differences between the two satellite altimetry datasets to become larger, and therefore to be able to discriminate those two datasets by means of the comparison to in-situ data.

Of course what “regional” means may well vary, and choosing the suitable region for averaging results from a compromise: the smaller the averaging region, the larger the differences at the cost of increased noise and errors. In this study, we considered large regional averages, typically basin-wide.

3.2.1. Long term trends

Figure 18 displays the maps of SLA trend differences between SLCCI and SALTO/DUACS altimetry datasets for the whole altimetry period and for the last part of the period, over which Argo profiles are available. The very low difference observed on global means appears to be unevenly distributed over the globe and large areas are experiencing trend differences larger than 1 mm/yr.

Over the longest period, the trend differences map exhibits a North/South hemispheric pattern, over the Argo period; there remains a hemispheric pattern in the trend differences, but with an East/West spatial repartition. Differences are larger over the Argo period and we therefore focus on this time span (i.e. 2003.5-2010). We consider East/West hemispheric averages, for latitudes between 66°S and 66°N (thus excluding the very large trend differences observed in the Arctic Ocean).

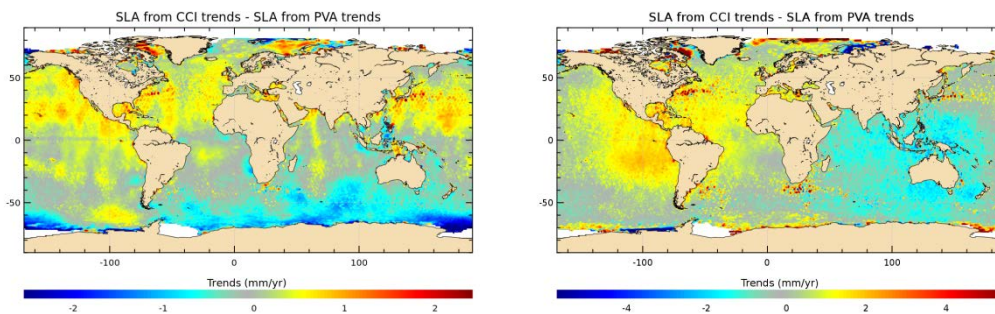


Figure 20: Maps of the SLA trend differences between CCI and SALTO/DUACS datasets, estimated over the 1993-2010 (left) and 2003.5-2010 (right) periods

The map of the drift differences between CCI and SALTO/DUACS satellite altimetry products with respect to Argo profiles (i.e. $(T_{CCI} - T_{Argo}) - (T_{PVA} - T_{Argo})$) is presented on Figure 21. This figure displays a hemispheric pattern somewhat similar to Figure 20's one, demonstrating that despite the spatial and temporal sub-sampling inherent to the altimetry/Argo comparison the technique is able to observe such trend differences.

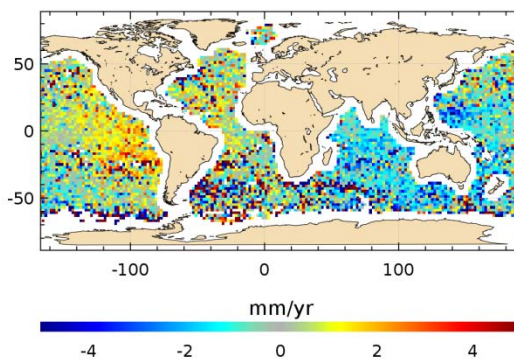


Figure 21: Map differences between trend differences between altimetry and Argo profiles evaluated with CCI and SALTO/DUACS altimetry datasets

Once the drift differences map of Figure 21 has been evaluated, there remains to investigate if the comparison to Argo profiles is useful to find the "best" altimetry dataset. We estimate East/West hemispheric SLA time series from Argo profiles, collocated SSALTO/DUACS altimetry, and collocated SLCCI altimetry. The corresponding time series are displayed on Figure 22, with the annual and semi-annual signals removed.

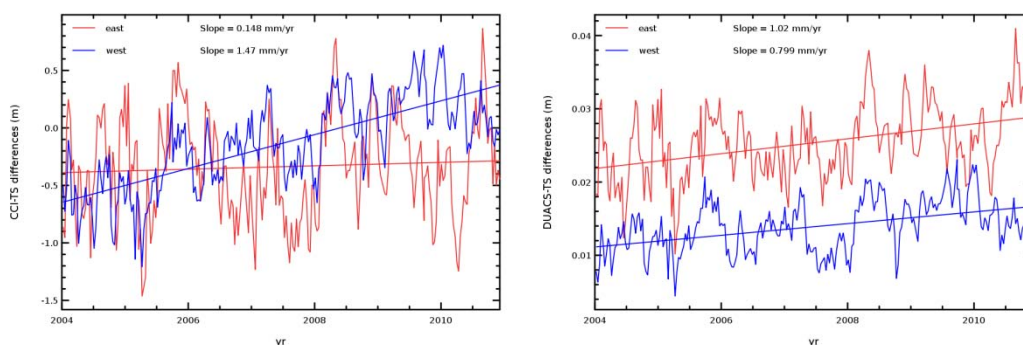


Figure 22: Time series of hemispheric SLA (west blue and east red) from Argo profiles and co-located altimetry from CCI (left) and SALTO/DUACS (right)

For the DUACS altimetry dataset, the drift respective to Argo floats is almost the same in both hemispheres. This situation is changed when considering CCI altimetry where the east/west drift



difference amounts to 1.3 mm/yr. This is expected due to the use of GDR-D orbits in the CCI products versus GDR-C orbits in DUACS. This standard change has demonstrated its relevance on Envisat data, which does not appear here because the generation process of SLCCI (and DUACS) data includes an empirical orbit error reduction step to fit Envisat data on Jason-1 over the period considered here.

4. Conclusions and recommendations

The main goal of this report was to compare the SLCCI altimetry dataset to in-situ records. Satellite altimetry was compared to two independent in-situ datasets: monthly tide gauge records from the PSMSL database and in-situ SLA derived from the combination of Argo temperature and salinity profiles and GRACE gravity data. In order to investigate the agreement between SLCCI satellite altimetry and in-situ data the different temporal and spatial scales of the SLA variability were separated: long-term trends, inter-annual variability, seasonal cycles and high-frequency variability are considered for global and basin-wide averages as well as local comparisons.

In general, tide gauge records observe higher level of variability than the collocated altimetry data, on the contrary, SLA records derived from Argo profiles and GRACE ocean mass show lower levels of variability than satellite altimetry.

The seasonal cycle is dominating the SLA variability, for both in-situ datasets and the corresponding collocated satellite altimetry. On global and regional scales, seasonal cycles agree well between in-situ and satellite altimetry records. The agreement is slightly better for the tide gauge/altimetry comparison than for the Argo profiles/altimetry one. However, these low regional differences hide a large dispersion when considering local comparisons (station or grid point wise).

The long term evolution of sea level is a main interest in climate studies. Comparing long term trends estimated over 18 years of tide gauge and collocated satellite altimetry data, we found a difference between the two techniques of only 0.2 mm/yr, and therefore a good agreement between the two records. Argo profiles are not available over the whole period, and the trend difference over the 2004-2009 period with respect to collocated satellite altimetry is higher at 1.1 mm/yr. It should be noted that this trend is heavily dependent on the GRACE mass fields used to estimate the ocean mass component added to the steric sea level estimated from the Argo temperature and salinity profiles.

A secondary goal of this report was to use in-situ data to compare the quality of two satellite altimetry datasets: the SLCCI and SALTO/DUACS grids. For this purpose we first evaluated the differences between the two satellite altimetry datasets, looking for signals large enough which could be separated by the in-situ comparison. The differences are low but suggest a better agreement to in-situ data when using SLCCI dataset rather than SALTO/DUACS. The east/west difference observed when comparing to Argo floats is expected due to the orbit changes.

5. References

Ablain, M., A. Cazenave, G. Valladeau, and S. Guinehut, 2009: A New Assessment of the error budget of global mean sea level rate estimated by satellite altimetry over 1993-2008, *Ocean Sci.*, 5:193-201.

Chambers, D.P., 2006: Evaluation of New GRACE Time-Variable Gravity Data over the Ocean. *Geophys. Res. Lett.*, 33(17), L17603.

Legouis J.F., Ablain M. 2012: CalVal altimetry / Argo annual report. Validation of altimeter data by comparison with in-situ T/S Argo profiles. Ref. CLS/DOS/NT/12-261.

Peltier, W.R., 2004: Global Glacial Isostasy and the Surface of the Ice-Age Earth: The ICE-5G (VM2) Model and GRACE, *Annual Review of Earth and Planetary Science*, 32, 111-149, 2004



Prandi, P., A. Cazenave, and M. Becker, 2009: Is coastal mean sea level rising faster than the global mean? A comparison between tide gauges and satellite altimetry over 1993–2007, *Geophys. Res. Lett.*, 36, L05602, doi:10.1029/2008GL036564.

Valladeau, G., J.-F. Legeais, M. Ablain, S. Guinehut and N. Picot, 2012, Comparing Altimetry with Tide Gauges and Argo Profiling Floats for Data Quality Assessment and Mean Sea Level Studies, *Marine Geodesy*, 35, supp. 1, pp.42-60



Appendix A - List of acronyms

TBC	To be confirmed
TBD	To be defined
AD	Applicable Document
RD	Reference Document